Shear Wave Velocity Measurements

June 2025
Final Report

Project number TR202403
MoDOT Research Report number cmr 25-009

PREPARED BY:

Evgeniy "Eugene" Torgashov, Ph.D.

Neil Anderson, Ph.D.

Thomas J. Casey, P.E.

SCI Engineering, Inc.

PREPARED FOR:

Missouri Department of Transportation

Construction and Materials Division, Research Section

Shear Wave Velocity Measurements

By
Evgeniy “Eugene” Torgashov, Ph.D.
Neil Anderson, Ph.D.
Thomas J. Casey, P.E.
SCI Engineering, Inc.

Prepared for
Missouri Department of Transportation

June 2025

Final Report

Technical Report Documentation Page

1. Report No. cmr 25-009	2. Government Accession No.	3. Recipient's Catalog No.
4. Title and Subtitle Shear Wave Velocity Measurements		5. Report Date June 2025 Published: June 2025
		6. Performing Organization Code
7. Author(s) Evgeniy "Eugene" Torgashov, Ph.D., https://orcid.org/0000-0002-1908-1125 Neil Anderson, Ph. D., https://orcid.org/0000-0002-4830-8683 Thomas J. Casey, P.E., https://orcid.org/0009-0006-0524-943X		8. Performing Organization Report No.
9. Performing Organization Name and Address SCI Engineering, Inc. 130 Point West Boulevard St. Charles, Missouri 63301		10. Work Unit No. (TRAIS)
		11. Contract or Grant No. MoDOT project # TR202403
12. Sponsoring Agency Name and Address Missouri Department of Transportation (SPR-B) Construction and Materials Division P.O. Box 270 Jefferson City, Missouri 65102		13. Type of Report and Period Covered Final Report (August 2023-June 2025)
		14. Sponsoring Agency Code

15. Supplementary Notes
Conducted in cooperation with the U.S. Department of Transportation, Federal Highway Administration. MoDOT research reports are available in the Innovation Library at https://www.modot.org/research-publications.

16. Abstract
The Missouri Department of Transportation (MoDOT) commissioned SCI Engineering, Inc. to investigate cost-effective, non-intrusive geophysical methods for determining time-averaged shear wave velocity (Vs) profiles to a depth of 100 feet, based on anticipated updates to AASHTO seismic site classification specifications. Following a comprehensive literature review, eight candidate methods were identified. Of these, four methods—Active Multichannel Analysis of Surface Waves (Active MASW), Passive Multichannel Analysis of Surface Waves (Passive MASW), Active Refraction Microtremor (Active ReMi), and Passive Refraction Microtremor (Passive ReMi)—were selected for field testing based on their practicality and effectiveness. Field evaluations were conducted at three sites: the SCI Office in O'Fallon, Illinois; the I-270 Chain of Rocks Bridge; and the MLK Connector in Illinois. The sites were selected based on access, availability of existing groundtruth subsurface soil information, as well as representing a variety of subsurface profiles. Various geophone spacings and array configurations were tested. Performance metrics included depth of investigation, ease of deployment, data quality, and interpretability. Results demonstrated that combining Active and Passive MASW methods offered the most reliable and practical solution, providing consistent results, minimal operational complexity, and shared equipment and software requirements.
SCI Engineering developed a comprehensive User Manual and conducted field demonstrations to train MoDOT personnel in the acquisition, processing, and interpretation of MASW data. Adoption of these methods will streamline MoDOT's seismic site classification processes, align practices with forthcoming AASHTO requirements, and enhance MoDOT's internal technical capacity.

17. Key Words Shear wave velocity; Multichannel analysis of surface waves; Active MASW; Passive MASW; ReMi; Refraction microtremor; Seismic refraction; Refraction tomography; Reflection seismic; HVSR	18. Distribution Statement No restrictions. This document is available through the National Technical Information Service, Springfield, VA 22161.

19. Security Classification (of this report) Unclassified	20. Security Classification (of this page) Unclassified	21. No. of Pages 166	22. Price

Form DOT F 1700.7 (8-72) Reproduction of completed page authorized

Copyright

Disclaimer

Acknowledgments

The research was conducted by SCI Engineering, Inc., with Evgeniy V. Torgashov, PhD serving as the principal investigator and coordinating the project. Thomas J. Casey, P.E. serving as the technical project lead, and Neil L. Anderson, PhD, who made significant contributions, were the co-principal investigators on the project.

The authors would like to express their gratitude to the individuals that made this research project possible. First, the authors extend a sincere thank you to the Missouri Department of Transportation (MoDOT) for their financial support and for their forward-thinking vision in integrating geophysical technology into the AASHTO guidelines. The successful completion of this project would not have been possible without the guidance and valuable feedback from MoDOT's project team: Jenni Hosey, Jennifer Harper, Zachary J. Troesser, Lydia B. Brownell, and Suresh Patel. Special acknowledgment is also due to Ricardo Todd and Matthew G. Kistler for their contributions to the hardware and software manual review.

The authors would also like to thank the Kansas Geological Survey for their essential software support and guidance, which were crucial to the success of the project.

Lastly, the authors express their appreciation for the administrative assistants, geophysical and geotechnical department staff at SCI – especially Tammy Wolfe, Sara Province and Paul Bess – whose assistance and support were vital to the successful completion of this project.

Table of Contents

List of Tables

List of Figures

List of Appendices

List of Equations

List of Abbreviations and Acronyms

1-D ..... One-dimensional

2-D ..... Two-dimensional

3-D ..... Three-dimensional

AADT ..... Average Annual Daily Traffic

AASHTO..... American Association of State Highway and Transportation Officials

COR ..... Chain of Rocks (Bridge)

DC ..... Dispersion curve

F_{0HV}..... shear wave resonance frequency

ft/s ..... feet per second

Hz ..... Frequency Hertz

HVSR ..... Horizontal to vertical spectral ratio

IDOT ..... Illinois Department of Transportation

MASW ..... Multichannel Analysis of Surface Waves

mm..... millimeters

MoDOT..... Missouri Department of Transportation

MLK..... Martin Luther King

msec..... millisecond

N/A..... Not applicable

OFN ..... O'Fallon

OT ..... Overtone

QC ..... Quality Control

ReMi..... Refraction Microtremor

s ..... seconds

SCI ..... SCI Engineering, Inc.

SESAME ..... Site EffectS assessment using AMbient Excitations

Vs ..... Shear wave velocity

Vs_{30}..... Average shear wave velocity for the upper 30-meter depth

Vs_{100} ..... Average shear wave velocity for the upper 100-foot depth

Executive Summary

The Missouri Department of Transportation (MoDOT), in preparation for anticipated updates to the AASHTO seismic site classification specifications, commissioned SCI Engineering, Inc. to conduct a comprehensive investigation into cost-effective and reliable non-intrusive methods for determining time-averaged shear wave velocity (Vs) profiles to a depth of 100 feet. The outcome is intended to guide procedural refinements and equipment recommendations for MoDOT's seismic site assessments.

The primary goal of this project was to identify and validate field-deployable geophysical methods capable of generating reliable Vs data while minimizing operational complexity, cost, and personnel requirements. SCI has conducted a thorough literature search and identified eight (8) potentially applicable methods for generating shear wave velocity profiles to a depth of 100 feet, including the following methods:

- Active multichannel analysis of surface waves (Active MASW),
- Passive multichannel analysis of surface waves (Passive MASW),
- Active refraction microtremor (Active ReMi),
- Passive refraction microtremor (Passive ReMi),
- Conventional shear wave seismic refraction,
- Seismic shear wave refraction tomography,
- Horizontal to vertical spectral ratio (HVSR),
- Seismic shear wave reflection.

Four (4) of these methods, namely Active MASW, Passive MASW, Active ReMi and Passive ReMi, were selected based on their practicality and potential effectiveness. These four methods were then field-tested at three sites:

- SCI office, O'Fallon, Illinois
- I-270 Chain of Rock Bridge (COR) over the Mississippi River, Missouri and Illinois
- Martin Luther King (MLK) Connector, Illinois

The sites were selected based on access, availability of existing groundtruth data, and represented a variety of differing subsurface conditions. Various array configurations and geophone spacings were used to assess performance under varying field conditions. Performance metrics included depth of investigation, ease of deployment, data quality, and interpretability. Comparative data analysis highlighted that a combination of Active MASW and Passive MASW offered the most reliable and practical solutions. These methods shared equipment and software, demonstrated consistent results across field conditions, and allowed flexibility in array configurations.

A combination of Active and Passive MASW methods was identified as the preferred seismic methods for determining time-averaged shear wave velocity (Vs) profiles to a depth of 100 feet and implementation into the MoDOT Engineering Policy Guide (EPG).

SCI has conducted field demonstrations to showcase how a 1- or 2-person crew could effectively deploy the MASW methods to obtain Vs profiles to 100 feet. MoDOT personnel were trained on acquisition, processing, and interpretation procedures. A User Manual was developed for MoDOT personnel's use.

The adoption of the recommended MASW methods will:

- Enable MoDOT to perform more efficient and accurate seismic site classifications.
- Streamline field operations through minimal equipment and personnel needs.
- Ensure compliance with evolving AASHTO guidelines.
- Enhance internal capacity through dedicated training and documentation.

Chapter 1 Introduction

The overarching objective of the "**Shear Wave Velocity Measurements**" project was to update and refine the Missouri Department of Transportation (MoDOT) seismic site investigation and analysis procedures in anticipation of upcoming changes to American Association of State Highway and Transportation Officials (AASHTO) specifications. To achieve this overarching objective:

1. SCI Engineering (herein referred to as SCI) conducted a comprehensive literature search to identify non-intrusive testing methods that can be used to obtain cost-effective and reliable time-average shear wave velocity (Vs) data to a depth of 100 feet for use in AASHTO guidelines. The focus was on identifying effective methods with limited equipment, source, and personnel requirements. It was also essential that data analysis and interpretation be relatively straightforward. Eight (8) potentially relevant non-intrusive testing methods were identified based on the literature search. Comprehensive summaries of these methods are presented in the section of this report entitled "**Literature Search**".
2. SCI assessed the potential applicability of the identified non-intrusive testing methods based on the literature search, personal experience and input from practitioners and identified the four (4) most applicable (selected) methods. The relative utility of these eight (8) methods and the criterion used to select the four (4) most applicable (selected) methods are described in the section of this report entitled "**Relative Utility of the Selected Test Methods**".
3. SCI field-tested the four (4) most applicable selected methods. Example field-test data are presented in the section entitled "**Field Testing of the Four (4) Most Applicable Methods"**
4. SCI assessed the relative utility of the four (4) field-tested methods. A summary of this assessment is presented in the section entitled "**Comparative Analyses of Test Field Data"**
5. SCI submitted and presented a technical brief with method and equipment recommendations. Based on the literature search, the field-test results, solicited input from users of the four (4) methods, and discussions with vendors, SCI recommended MoDOT utilize the following two (2) methods: Active MASW and Passive MASW. Although these methods employ different sources, they utilize the same field equipment, recording instrumentation, and processing software, and provide both complemental and supplemental outputs. The SCI recommendations are presented in the section entitled "**Method and Equipment (including Hardware and Software) Recommendations"**.
6. SCI gave a field demonstration of the Active MASW and Passive MASW methods and demonstrated how a small 1- or 2-person crew could cost-effectively acquire shear wave velocity data to a depth of 100 feet. Example data acquired during the demonstration are presented in the section entitled "**Field Demonstration of the Recommended Method at the Test Site"**

7. SCI developed a **User Manual (Acquisition, Processing, and Interpretation)** for incorporation into the MoDOT's Engineering Policy Guide. SCI also trained selected MoDOT personnel.

- SCI prepared and submitted a **synthesis final report (Project TR202403**; **Shear Wave Velocity Measurements)**. The results of this investigation will enable MoDOT to update and refine seismic site investigation and analysis procedures in anticipation of upcoming changes to AASHTO specifications.

A user manual consisting of two (2) sections, General Guideline for MASW Field Surveying and MASW Manual, is presented in Appendix A and Appendix B, respectively.

The General Guideline for MASW Field Surveying document (Appendix A) outlines the guidelines for conducting MASW field surveys in various conditions at six selected MoDOT bridge sites. The primary objective was to provide effective survey parameters to ensure high-quality geophysical data collection for geotechnical analysis. The key recommendations include the geophone array setup and the traverse placement, considering site conditions at these six selected locations. Refer to Appendix A for detailed description.

The MASW manual (Appendix B) provides comprehensive guidelines for field equipment setup, acquisition, processing and interpretation of MASW data, used for shear wave velocity profiling. However, it is important to note that the recommended workflow is based on the specific test data collected during this project and may require adjustments to accommodate varying site conditions or project-specific requirements. The use of incorrect acquisition or processing parameters can potentially lead to significant misinterpretation of subsurface conditions. For advanced MASW data processing refer to the relevant software documentation.

Chapter 2 Literature Search

The goal of the comprehensive literature search was to identify methods that could be used to obtain cost-effective and reliable time-average shear wave velocity (Vs) data to a depth of 100 feet for use in following AASHTO guidelines. The focus was on identifying effective methods with limited equipment, source, and personnel requirements. It was also essential that data analysis and interpretation be relatively straightforward.

During the literature search, eight (8) potentially applicable non-intrusive methods for determining the shear wave velocity of the subsurface to a depth of 100 feet were identified and preliminarily assessed. These 8 methods are:

- Active multichannel analysis of surface waves (Active MASW).
- Passive multichannel analysis of surface waves (Passive MASW).
- Active refraction microtremor (active ReMi).
- Passive refraction microtremor (Passive ReMi).
- Conventional shear wave seismic refraction.
- Seismic shear wave refraction tomography.
- Horizontal to vertical spectral ratio (HVSR).
- Seismic shear wave reflection.

The detailed overview of each method is presented in the subsequent sections.

2.1. Active Multichannel Analysis of Surface Waves (Active MASW)

2.1.1 Brief Overview of the Active MASW Method

Multichannel analysis of surface waves (MASW) software can be used to transform recorded fundamental mode Rayleigh waves (a type of surface wave) generated using an active acoustic source into a 10-layered one-dimensional (1-D) shear wave velocity profile of the subsurface.

Active Rayleigh wave energy is normally generated using a proximal source such as a sledgehammer, weight drop or small explosive that is discharged at the surface by the MASW survey crew. The active sources that are used to image the subsurface to depths on the order of 100 feet typically generate Rayleigh waves with frequencies ranging from 5 to 60 hertz (Hz). The higher frequency (shorter wavelength) Rayleigh waves extend to shallow depths; the lower frequency (longer wavelength) Rayleigh waves extend to greater depths. Ideally, the recorded Rayleigh waves with the lowest frequencies will involve particle motion to depths of at least 100 feet. If depths of investigation greater than 100 feet are desired, the MASW crew should consider acquiring Passive MASW data or a combination of Active/Passive MASW data.

Rayleigh wave energy is dispersive meaning that different frequencies travel with different velocities. More specifically, each frequency travels with a phase velocity that is mostly a

function of the average shear wave velocity of the subsurface from the ground surface to the base of particle motion associated with that frequency (wavelength).

Active Rayleigh wave data are normally recorded using a linear array of geophones. MASW software analyzes the recorded Rayleigh wave data and calculates the phase velocities of a representative range of frequencies (from highest to lowest frequency Rayleigh waves). These phase velocity data are used to estimate the effective base of particle motion associated with each frequency and to estimate the average shear wave velocity over that depth range of particle motion. The subsurface can then be subdivided into a finite number of layers (one layer for each frequency analyzed; from the ground surface to the base of particle motion associated with lowest frequency analyzed). Interval shear wave velocities can then be assigned to each layer.

The output of a single Active MASW data set is a 10-layered 1-D shear wave velocity profile of the subsurface. In certain situations, a suite of MASW data sets is collected at intervals along the length of a traverse and the output 1-D shear wave velocity profiles are used to generate a pseudo-two-dimensional (2-D) shear wave velocity profile of the subsurface. Three-dimensional (3-D) shear wave velocity images of the subsurface can also be generated.

The active refraction microtremor (ReMi; Section 2.3 of this report) method is very similar to the active multichannel analysis of surface wave (MASW) method. The most significant difference is the processing software.

Note: Active MASW data can be acquired underwater using hydrophones coupled to the water bottom. In this case, Scholte waves are recorded. Scholte wave data can be processed using MASW software. The output is a 1-D shear wave velocity profile of the subsurface.

Note: Active MASW data can be acquired using horizontally polarized shear wave geophones. In this case, Love waves are recorded. Love wave data can be processed using MASW software. The output is a 1-D shear wave velocity profile of the subsurface.

For detailed data acquisition and processing instructions refer to Appendix B “MASW Manual”.

2.1.2 Data Acquisition

2.1.2.1 Brief Overview of Field Procedure

A linear array of geophones (typically 24), an acoustic source, an engineering seismograph and a laptop are used to record active Rayleigh wave data that propagates along the axis of the geophone array (Figure 2.1). The geophones are generally spaced such that the length of the array is on the order of the desired maximum depth of investigation. For example, if the objective is to image the subsurface to a depth of 100 feet, the geophones are typically spaced at 5 feet and the geophone array is 115 feet in length.

Active MASW data is generated by a source controlled by the MASW field crew (such as a sledgehammer and strike plate). The source is discharged off one the end of the geophone array. If the intent is to image the subsurface to a depth of 100 feet, the source is typically discharged 25-30 feet from the closest geophone. When the active source is discharged, the seismograph is triggered, and data is recorded (typically for one second or less). To increase the signal to noise ratio, the source is typically discharged multiple times (stacked) at each location. Typically, the source is discharged 2-5 times at each location to increase statistical reliability and minimize the effects of random noise. Separate field records are generated for each discharge. The separate field records are analyzed collectively during data processing.

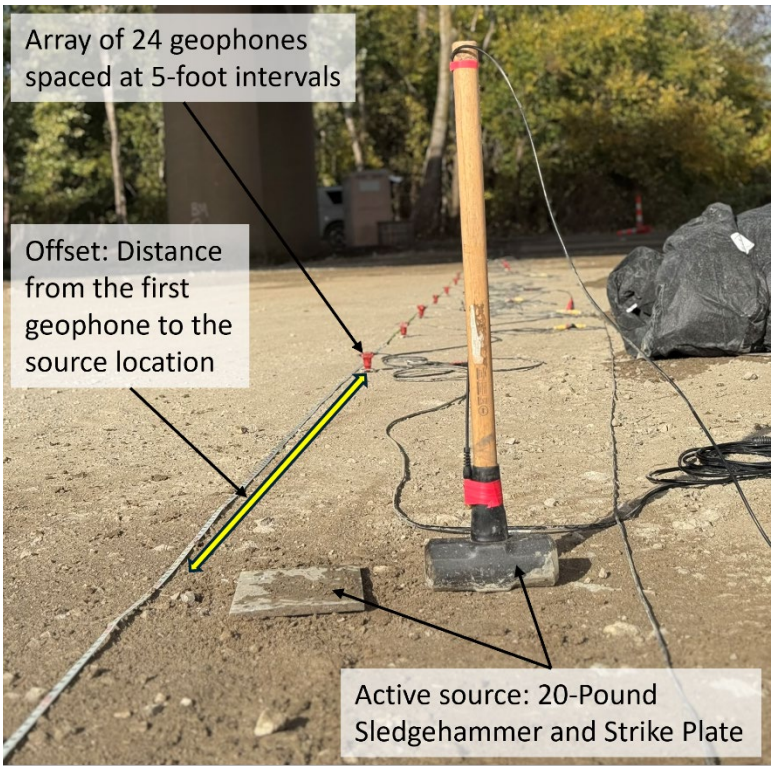

Figure 2.1 Photograph of a typical Active MASW field setup.

Field records can be visually assessed in the field for quality control (QC) purposes. Data can also be processed in a cursory manner in the field for QC purposes. If poor quality data have been recorded, the source can be discharged at the other end of the array of geophones.

If the recorded frequencies are relatively good quality but too high to image to a depth of 100 feet, a greater magnitude source can be employed.

2.1.2.2 Field Equipment

The portable equipment normally consists of an acoustic source, an engineering seismograph, a trigger switch, a laptop with installed acquisition and processing software, and, typically, an

array of 12-24 low-frequency vertically polarized geophones (either 4.5 Hz or 14 Hz geophones). Typically, a heavy sledgehammer source and a strike plate are employed.

2.1.2.3 Field Crew

Typically consists of 1-3 persons. A single person can acquire Active MASW data. However, if MASW data are to be acquired at multiple locations at a site, it is usually more efficient to field a crew consisting of 2-3 persons.

2.1.2.4 Considerations

Parameter entry. The correct acquisition parameters must be entered. An Active MASW field record is typically between 1.0 and 2.0 seconds in duration. The sampling interval is usually 0.5 milliseconds.

Size of test site. The test site must be large enough to allow for ease of placement of geophones and the offset active source. A typical Active MASW array (including the offset source) is typically about 145 feet in length.

Plotted location of the output 1-D shear wave velocity profile. A 10-layered 1-D shear wave velocity profile will be generated at each test location. The output shear wave velocity profile is more-or-less a function of the average shear wave velocity of the subsurface along the entire length of the geophone array. However, by convention, the shear wave velocity profile is plotted at the location of the center of the geophone array.

Vehicular access. All equipment can be hand-carried. Usually, the equipment and crew are transported in a single vehicle.

Surface topography. Active MASW data can be acquired across undulating ground surfaces or across steeply dipping terrain. However, elevation changes should be minimized where/if possible as data quality usually decreases as surface topographic relief increases. In these situations, 2 MASW data sets should be acquired. The active source should be discharged off both ends of the geophone array. To a certain extent, issues related to irregular surface topography can be dealt with or at least recognized during data processing. Often, the effects of irregular or dipping topography can be recognized on MASW field records. Rayleigh waves can be reflected (backscattered) from proximal surface topography such as stream beds, hillsides, and drainage ditches. Reflected Rayleigh wave can complicate data processing. Often, reflected Rayleigh wave energy can be recognized on the field records.

Subsurface topography. If there is a possibility that bedrock dips appreciably along the length of the geophone array, 2 MASW data sets should be acquired. The active source should be discharged off both ends of the geophone array. To a certain extent, issues related to irregular subsurface topography can be dealt with or at least recognized during data processing.

If features such as faults, solution-widened joints or voids are present beneath the geophone array or between the source and the array, it may not be possible to record useful Rayleigh

wave data. The discharged Rayleigh wave energy may not propagate uniformly along the length of the geophone array. Rather, it may be mostly reflected (backscattered) from the subsurface feature.

Often, reflected Rayleigh wave energy can be recognized on the field records.

Vegetation. Data can be acquired in heavily vegetated areas if the geophones and active source can be placed in the appropriate locations. However, dense vegetation does impede work and slows down field data acquisition. Usually, it is most efficient to clear the traverse ahead of time.

Background noise. Active MASW data can usually be acquired even in acoustically noisy environments. However, it may be necessary to increase the magnitude of the active source or to acquire multiple field records by discharging the source multiple times.

Anchoring requirements. The geophones are frequently coupled to the ground surface using short base spikes. However, base plates can be used in lieu of spikes and are usually used if data are acquired on pavement, rock or gravel. The geophones do need to be placed in stable, vertical positions on the ground surface.

Nature of ground surface. The geophones can be placed on soil, rock, fill, concrete, asphalt, etc. They should be stable, vertical, and effectively coupled. Data acquisition can be a problem if the ground surface is very soft or very loose. In such situations, it can be difficult to effectively couple the geophones and the source to the ground.

Different strike plates are often employed depending on the nature of the ground surface.

Placement of geophones and active source. Normally, a tape measure is laid out along the traverse and geophones are placed at their appropriate locations. If a few individual geophones are misplaced off by 5% or less, data quality should not be adversely affected, particularly if the geophones are shifted perpendicular to the traverse.

If the location of the source is in line with the geophone array but out by 10% or less, data quality should not be adversely affected.

Subsurface lithology or material. Active MASW data can be acquired across all types of soil and/or rock. MASW data can also be acquired across pavement, asphalt, fill, etc.

Depth of investigation. The maximum depth of investigation is a function mostly of the lowest frequency fundamental mode Rayleigh wave energy recorded and the length of the geophone array. If active data are being recorded, the lowest frequency recorded is a function of the energy generated by the source as greater magnitude sources generate lower frequency Rayleigh waves. Lower frequencies are more reliably analyzed when recorded using arrays with lengths on the order of the wavelength of those frequencies.

Proximity to buried structures and buried utilities. The Active MASW tool is non-invasive. Active data can be acquired in proximity to buried utilities and buried structures, unless there is concern that use of the acoustic source could damage built structures such as concrete or pavement. Issues with data quality can arise if the buried utilities or buried structures are beneath the geophone array or between the source and the array. Rayleigh waves that are reflected (backscattered) from subsurface features can complicate data processing.

Proximity to surface structures and surface utilities. The MASW tool is non-invasive. Active MASW data can be acquired in proximity to surface utilities and surface structures. Typically, the only clearance required is sufficient room to discharge the source. A sledgehammer source can damage concrete or pavement.

Sensitivity to background noise. The Active MASW technique is relatively insensitive to noise. However, in certain instances (such as in proximity to moving trains, operating heavy equipment, buildings with air conditioners, etc.) it can be very difficult to acquire useable data. If an MASW traverse located close to bridge foundations, vehicle induced noise transmitted by bridge piers could be potentially minimized by strategically discharging an active source (i.e., sledgehammer with a strike plate) in timeframes of lower traffic volume.

Permitting requirements. Generally, only permission from the surface rights holder is required.

Notification requirements. Generally, only permission from the surface rights holder is required.

Other considerations. It may not be possible to generate an output shear wave velocity profile that extends to the desired depth of investigation if the magnitude of the active source is too small or if the signal to noise ratio is too low. Site and/or ground conditions may make it effectively impossible to image the subsurface to the desired depth.

2.1.2.5 Brief Description of Field Data

The field data are recorded digitally and stored on the laptop connected to the seismograph or to built-in flash memory. Generally, multiple active records (typically 1 second in length) are generated for each active test location. These records are effectively “stacked” during processing to increase the signal to noise ratio.

2.1.2.6 Estimated Cost to Acquire MASW Field Data at One Test Site

Basic field costs include: a) 1 hour of crew time plus travel time; b) equipment rental and/or depreciation; and c) vehicle rental and/or depreciation plus fuel. It typically takes a 2-person crew 1 hour to acquire a single Active MASW data set (using a sledgehammer source and a 24-geophone array).

2.1.2.7 Potential for Errors

There is little likelihood that field errors will lead to misinterpretation.

Human. Human error, which leads to misinterpretation, is unlikely because the only critical non-automated processes are the placement of the geophones and the discharge of the active source. If the incorrect geophone separation is inadvertently entered as a processing parameter, significant errors can result. If the source is discharged too far from or too close to the geophone array, or if the source is too small, poor quality field data may be acquired.

Equipment. Equipment problems are unlikely to generate errors that will lead to misinterpretation. Care must be taken to ensure geophones are properly coupled to the ground surface.

2.1.2.8 Reproducibility of Field Tests

If good quality Active MASW field data can be recorded, field results can be reproduced with a relatively high degree of consistency.

2.1.2.9 Quality Control

Acquired data can be visually assessed in the field for QC purposes. Data can also be processed in a cursory manner in the field for QC purposes. If poor quality data sets have been recorded, the source can be discharged at the other end of the array of geophones or a greater magnitude source can be employed. Alternatively, the array can be reoriented or moved.

2.1.3 Data and/or Laboratory Processing

2.1.3.1 Brief Overview of Data Processing

In the initial phase of data processing (step 1), each uploaded MASW field record (example shown in Figure 4.5) is manually edited (selective muting) by the processor to remove coherent energy such as refractions, reflections, and higher mode Rayleigh waves. The processor also inputs the field acquisition parameters including geophone spacing, source offset and source location.

In step 2 of data processing, the edited MASW field record is analyzed, and an image panel (overtone record) is generated. The image panel is a phase velocity vs. frequency plot of energy accumulation pattern. It is constructed using a 2-D (time and space) wavefield transformation method that employs several pattern-recognition approaches and does not require any interactive input from the interpreter. This transformation eliminates all the ambient noise from human activities as well as source-generated noise such as scattered waves from buried objects (foundations, culverts, boulders, etc.). The image panel shows the relationship between phase velocity and frequency for those waves propagated horizontally directly from the impact point to the receiver line. These waves include fundamental and higher modes of surface waves as well as direct body (compressional) waves.

In step 3, the dispersion curve is extracted (usually subjectively “picked”) from the energy accumulation pattern in the image panel (example shown in Figure 4.8b). The extracted

dispersion curve is finally used as a reference to back-calculate the variation in Vs with depth below the surveyed area. This back-calculation is called inversion.

In step 4, the selected dispersion curve is inverted without any qualitative input from the interpreter. The output is a 10-layered 1-D shear wave velocity profile (example shown in Figure 4.8c).

If the output shear wave velocity profile is questionable, the Rayleigh wave data are normally reprocessed using different subjective parameters (i.e., muting, picking, etc.).

It should be noted that the propagation velocity of a Rayleigh wave is a uniform medium is described by

Equation 2.1 Relationship of Rayleigh, Shear and Compressional Wave Velocities:

$$V_R^6 - 8\beta^2 V_R^4 + (24 - 16\beta^2/\alpha^2)\beta^4 V_R^2 + 16(\beta^2/\alpha^2 - 1)\beta^6 = 0, \quad (2.1)$$

where:

V_R = Rayleigh wave velocity,

β = shear wave velocity, and

α = compressional wave velocity.

As noted, V_R is a function of both β and α. To transform Rayleigh wave velocities into shear wave velocities, the software package uses a predetermined value of Poisson's Ratio to remove the compressional wave velocity term (α) from the expression. This is a robust approach, but it does introduce some error into the output estimate of shear wave velocities.

2.1.3.2 Output of Data Processing

The output from a single test location is a 10-layered 1-D shear wave velocity profile. If data are collected at multiple test locations along the length of a traverse or an array, the output 1-D shear wave velocity profiles can be used to generate a 2-D or 3-D shear wave velocity profile. Creating a 2-D cross-section will allow the user to image the lateral variations in the shear wave velocity.

2.1.3.3 Estimated Cost to Process Field Data from One Test Site

Basic processing costs include about 1 hour of processor's time and hardware/software rental and/or depreciation.

2.1.3.4 Potential for Error

Human. Steps 2 and 4 (the transformation of the muted MASW field data into an overtone data and the inversion of the "picked" dispersion curve) do not require interpreter input. Step 1

(muting and parameter entry) and step 3 (the "picking" of the optimal dispersion curve) are subjective although usually straightforward.

In certain instances, it is difficult to "pick" an optimum dispersion curve. Problems can arise for one of a number of reasons: suitable fundamental mode Rayleigh wave energy may not have been recorded; the acoustic source may have been too small; the geophone array may have been too long or too short; lateral velocity variations along the length of the geophone array may have resulted in "smoothing" or "smearing" of phase velocity data on the overtone record; excessive topographic relief may have caused "smoothing" or "smearing"; geologic conditions (faulting for example) may have been such that surface wave energy of the desired frequency could not be recorded in the study area.

It is possible for a processor to misidentify higher mode Rayleigh wave energy as fundamental mode Rayleigh wave energy. In such situations, the output shear wave velocities will be anomalously high.

If the processor arbitrarily extends the dispersion curve (via extrapolation and with the objective of extending the shear wave velocity profile to greater depths) beyond the lowest confidently "pickable" frequency on the overtone record serious errors can arise.

Equipment. The Active MASW data acquisition equipment and processing software should not be defective. Data processing software may be glitchy, that could be typically resolved by simply closing and relaunching the software and reopening the data file.

2.1.3.5 Reproducibility of Field Tests

If the MASW field data are good quality, trained processors will generate consistent 1-D shear wave velocity profiles over the range of frequencies that were generated by the source in the field.

2.1.4 Interpretation

2.1.4.1 Brief Overview of Interpretation of Processed Data

The output of data processing is a 10-layered 1-D shear wave profile of the subsurface. If multiple Active MASW data sets are acquired, 2-D or 3-D shear wave velocity images of the subsurface can be generated.

Usually, the interpreter establishes relationships between lithology (if borehole control is available) and acoustic velocity and transforms the output 1-D shear velocity model into a geologic model of the subsurface. If geologic control is not available, the depth to bedrock (if imaged) can generally be estimated based on the visual assessment of the shear wave velocity profile.

If the MASW data are acquired for site classification purposes, the average shear wave velocity to a depth of 100 feet is normally calculated.

2.1.4.2 Deliverable(s)

1-D, 2-D, or 3-D geological and shear wave velocity models.

If the MASW data are acquired for site classification purposes, the average shear wave velocity to a depth of 100 feet is normally calculated.

A 10-layered 1-D shear wave velocity profile will be generated at each test location. The output shear wave velocity profile is more-or-less a function of the average shear wave velocity of the subsurface along the entire length of the geophone array. However, by convention, the shear wave velocity profile is plotted at the center of the respective geophone array.

2.1.4.3 Depth Range (Top/Bottom)

If a 20-pound sledgehammer source is employed, the output shear wave velocity profile will typically extend to a depth on the order of 100-120 feet. Greater depths of investigation can be achieved if a greater magnitude source is employed.

2.1.4.4 Lateral Resolution

Rayleigh wave data are acquired along the entire length of the geophone array. If the velocity of the subsurface varies laterally along the length of the array, lateral velocity smoothing will occur. However, some weighting is involved as the source/receiver separation is generally selected such that higher frequencies are excessively attenuated at the farthest geophones whereas the lowest frequencies are not recorded on the closest geophones.

The output 1-D shear wave velocity profile is more-or-less a function of the average shear wave velocity of the subsurface along the entire length of the geophone array. However, by convention, the output shear wave velocity profile is plotted at the center of the geophone array. Lateral resolution can be increased by decreasing the geophone spacing and sometimes the magnitude of the source. However, this approach usually decreases the overall depth of investigation as well.

Zones of anomalously low or high velocity on the output 10-layered 1-D shear wave velocity profile should not be misinterpreted as indicative of the presence of a boulder or clay-filled void/karstic feature, respectively, immediately beneath the center of the geophone array.

2.1.4.5 Vertical Resolution

The output of processing is a 10-layered shear wave velocity profile of the subsurface. The thickness of each layer is a pre-set software function of the total depth to the top of the 11^{th} layer. The thickness of the layers increases with depth. Layer boundaries are set by the processing software and do not usually correspond precisely to lithologic boundaries.

Additionally, Rayleigh wave data are acquired along the entire length of the geophone array. The shear wave velocity assigned to a specific layer is a function of the average velocity of that layer along the entire length of the geophone array.

The depth to significant features such as the top of rock can usually be estimated to within ±10%.

2.1.4.6 Time Required to Interpret Field Data (One Test Site)

If ground truth is available and if velocity/lithologic relationships can be established, the interpretation of the shear wave velocity data is normally relatively rapid and straightforward.

2.1.4.7 Potential for Error

Human. There is little potential for error if the interpreter understands that the output shear wave velocity profile generated at each test location represents the average shear wave along the length of the array. Layer velocities do not necessarily represent the precise shear wave velocity of the subsurface at the mid-point of the geophone array. The processor should be exercising caution when picking dispersion curve points.

Equipment. There is little potential for error.

2.1.4.8 Reproducibility of Deliverable

If ground truth is available, different experienced interpreters should come up with similar interpretations. If ground truth is not available, unreliable interpretations are a possibility.

2.1.5 Deliverables

2.1.5.1 Brief Overview of Deliverable(s)

1-D (or 2-D or 3-D) geologic and shear wave velocity models.

2.1.5.2 Utility of Deliverable(s)

Geologic and shear wave velocity models provide information about variations in lithology, porosity, engineering properties, rippability of rock, diggability of soil, depth to top of rock, etc.

The shear wave velocity profiles can also be used for earthquake site classification purposes.

2.1.5.3 Accuracy

The final interpretations are generally reliable if good quality Active MASW field data are recorded and if ground truth is available. Use of an experienced interpreter is essential.

2.1.6 Advantages

Advantages include:

- output is a shear wave velocity profile of the subsurface that typically extends to a depth of 100+ feet,
- depth to bedrock can usually be estimated to within ±10%,
- other lithologic units can often be identified and mapped on basis of shear wave velocity,
- relatively low cost,
- portability of equipment,
- relative insensitivity to background noise,
- typically employs a 1–3-person crew,
- field records can be visually assessed in the field for QC purposes,
- ability to rapidly process data in the field (for QC purposes),
- rapid processing of field data in lab,
- few restrictions with respect to surface conditions (soil, rock, pavement, etc.),
- non-invasive,
- limited potential for human error if operators and processors are trained,
- reproducibility of field data,
- reproducibility of processing results,
- reproducibility of interpretations, particularly if geologic control is available,
- multiple applications (determination of lithology, porosity, rippability, depth to bedrock, location of voids, shear strength),
- permitting is not required,
- tool can be used across and in proximity to utilities and built structures as the method is relatively insensitive to background acoustic noise,
- Active MASW data can be acquired underwater using hydrophones coupled to the water bottom (Scholte waves are recorded and processed),
- Active MASW data can be acquired using horizontally polarized shear wave geophones (Love waves are recorded and processed).

2.1.7 Disadvantages

Disadvantages include:

- desired maximum depths of investigation may not be realized if the source is too low magnitude given subsurface geologic conditions,
- site must be large enough to accommodate the geophone array and source,

- reliability of output shear wave velocity data decreases as lateral and vertical heterogeneity of soil/rock increases,
- significant surface topography can make it difficult to acquire useful data,
- significant subsurface topography can make it difficult to acquire useful data,
- features such as faults, solution-widened joints and voids may make it difficult to acquire useful data,
- underground utilities can make it difficult to acquire useful data,
- vegetation can pose problems during data acquisition,
- geophones and source must be effectively coupled to the ground surface; acquiring quality data on very soft or loose soil can be difficult,
- in certain limited situations, background noise may be overwhelming, layer boundaries on shear wave velocity profile do not correspond exactly to lithologic boundaries.

2.2. Passive Multichannel Analysis of Surface Waves (Passive MASW)

2.2.1 Brief Overview of the Passive MASW Method

Multichannel analysis of surface waves (MASW) software can be used to transform recorded fundamental Rayleigh waves (type of surface wave) generated using a passive acoustic source into a 10-layered 1-D shear wave velocity profile of the subsurface.

Passive Rayleigh wave energy (ambient noise) is not generated by the MASW field crew. Rather, passive Rayleigh wave energy is generated by external sources that can include microseismic activity, lightning strikes, vehicle traffic, etc. Passive sources typically generate Rayleigh waves with frequencies ranging from 1 to 30 Hz. The higher frequency (shorter wavelength) Rayleigh waves extend to shallow depths; the lower frequency (longer wavelength) Rayleigh waves extend to greater depths. Ideally, the lowest recorded frequency Rayleigh waves will involve particle motion to depths of several hundred feet.

As noted, Rayleigh wave data generated using a passive source are normally lower frequency than Rayleigh wave data generated using an active source (Section 2.1 of this report). Because the passive Rayleigh data are normally lower frequency, the output shear wave velocity profile generally provides for relatively poorer vertical resolution in the upper 100 feet. On the upside, Passive MASW data can be often used to image the subsurface to depths greater than several hundreds of feet. Combination Active/Passive MASW data sets can provide for both high vertical resolution at depths and greater depths of investigation.

Rayleigh wave energy is dispersive meaning that different frequencies travel with different velocities. More specifically, each frequency travels with a phase velocity that is mostly a function of the average shear wave velocity of the subsurface from the ground surface to the base of particle motion associated with that frequency (wavelength).

Passive MASW (Table 3.1) data are recorded using either a linear or a non-linear symmetric array of geophones. The use of a linear array is recommended if the source of the passive energy is known (for example, data being acquired along a roadway and vehicle traffic is being used as a source). The use of a non-linear symmetric array is recommended if the location of the passive source is unknown.

MASW software analyzes the recorded Rayleigh wave data and calculates the phase velocities of a representative range of frequencies (from highest to lowest frequency Rayleigh waves). These phase velocity data are used to estimate the effective base of particle motion associated with each frequency and to estimate the average shear wave velocity over that depth range of particle motion. The subsurface can then be subdivided into a finite number of layers (one layer for each frequency analyzed; from the ground surface to the base of particle motion associated with lowest frequency analyzed). Interval shear wave velocities can then be assigned to each layer.

The output of a single Passive MASW data set is a 10-layered 1-D shear wave velocity profile of the subsurface. In certain situations, a suite of MASW data sets is collected at intervals along the length of a traverse and the output 1-D shear wave velocity profiles are used to generate a pseudo-2-D shear wave velocity profile of the subsurface. 3-D shear wave velocity images of the subsurface can also be generated.

The passive refraction microtremor (ReMi; Section 2.4of this report) method is very similar to the passive multichannel analysis of surface wave (MASW) method. There are two significant differences: 1) MASW and ReMi processing software are different; and 2) ReMi software cannot be used to process data acquired using a non-linear array.

Note: Passive MASW data can be acquired underwater using hydrophones coupled to the water bottom. In this case, Scholte waves are recorded. Scholte wave data can be processed using MASW software. The output is a 1-D shear wave velocity profile of the subsurface.

Note: Passive MASW data can be acquired using horizontally polarized shear wave geophones. In this case, Love waves are recorded. Love wave data can be processed using MASW software. The output is a 1-D shear wave velocity profile of the subsurface.

For detailed data acquisition and processing instructions refer to Appendix A “MASW Manual”.

2.2.2 Data Acquisition

2.2.2.1 Brief Overview of Field Procedure

A linear or non-linear symmetric array of geophones (typically 12 to 24), an engineering seismograph and a laptop are used to record passive Rayleigh wave data. The geophones are generally spaced such that the length of the linear array or the width of the non-linear symmetric array is on the order of the desired maximum depth of investigation. For example, if the objective is to image the subsurface to a depth of 100 feet using a linear array, the geophones are typically spaced at 5 feet and the array is 115 feet in length (Figure 2.1).

Passive Rayleigh wave energy (ambient noise) is not generated by the MASW field crew. Rather, passive Rayleigh wave energy occurs naturally and can be generated by external sources that can include microseismic activity, lightning strikes, construction equipment, vehicle traffic, etc. Passive data are generated by triggering the seismograph manually and recording “random” data, typically for about 30 seconds or more. Passive data are never stacked, but multiple separate 30 plus second records are usually recorded at each test location to increase the probability that useful passive Rayleigh wave energy has propagated through the array. The separate field records are analyzed collectively during data processing.

If a linear array is used, Rayleigh wave energy must propagate through the array in a direction more-or-less parallel to the axis of the array. Rayleigh wave energy that propagates parallel to the axis of a linear array will exhibit lower apparent velocities (greater slowness) than energy that propagates through the same array at an angle.

Passive MASW field records cannot normally be visually assessed in the field for QC purposes and normally are not processed in the field for quality control purposes.

If combination Active/Passive data are required, an active source can be discharged while the 30 second passive data sets are being recorded. Alternatively, both active and Passive MASW data can be recorded separately and combined during processing.

2.2.2.2 Field Equipment

The Passive MASW method utilizes equipment typically employed in conventional seismic refraction surveys, except for the source. The acquisition equipment consists of an engineering seismograph, a laptop with installed acquisition and processing software, and an array of 24 low-frequency vertically polarized geophones (4.5 Hz recommended, however, 14 Hz geophones could be used in some cases). If passive data (only) are being recorded, an operational source is not required. If both active and passive data are being recorded, an acoustic source is employed.

2.2.2.3 Field Crew

Consists of 1-3 persons. A single person can acquire Passive MASW data. However, if MASW data are to be acquired at multiple locations at a site, it is usually more efficient to field a crew consisting of 2-3 persons.

2.2.2.4 Considerations

Parameter entry. The correct acquisition parameters must be entered. A Passive MASW field record is typically 30 seconds in duration, with 30 field records (files). The sampling interval is usually 2 milliseconds.

Size of test site. The test site must be large enough to allow for ease of placement of geophones. The diameter of a non-linear Passive MASW array is typically equal to the desired depth of investigation. The length of a linear Passive MASW array is typically equal to the desired depth of investigation.

Plotted location of the output 1-D shear wave velocity profile. A 10-layered 1-D shear wave velocity profile will be generated at each test location. The output shear wave velocity profile is assumed to be a function of the average shear wave velocity of the subsurface beneath the geophone array. However, by convention, the shear wave velocity profile is plotted at the center of the geophone array.

Vehicular access. All equipment can be transported by hand. Usually, the equipment and crew are transported in a single vehicle.

Surface topography. Passive MASW data can be acquired across undulating ground surfaces or across steeply dipping terrain. However, elevation changes should be minimized where/if possible as data quality usually decreases as surface topographic relief increases.

Subsurface topography. If features such as faults, solution-widened joints or voids are present beneath the geophone array, it may not be possible to record useful passive Rayleigh wave data.

Vegetation. Data can be acquired in heavily vegetated areas. However, dense vegetation does impede work and slows down field data acquisition. Usually, it is most efficient to clear the study site ahead of time.

Background noise. Passive MASW data can usually be acquired even in acoustically noisy environments. Coherent background noise such as highway traffic can constitute a useful source of passive Rayleigh wave energy.

Anchoring requirements. The geophones are frequently coupled to the ground surface using short base spikes. However, base plates can be used in lieu of spikes and are usually used if data are acquired on pavement, rock or gravel. The geophones do need to be placed in stable, vertical positions on the ground surface.

Nature of ground surface. The geophones can be placed on soil, rock, fill, concrete, asphalt, etc. They should be stable and vertical. Data acquisition can be a problem if the surficial soils are very loose. In such situations, it can be difficult to effectively couple the geophones to the ground.

Subsurface lithology or material. Passive MASW data can be acquired across all types of soil and/or rock. MASW data can also be acquired across pavement, asphalt, fill, etc.

Placement of geophones and active source. Normally, a tape measure is laid out and geophones are placed at their appropriate locations. If a few individual geophones are misplaced by 6 inches or less, data quality should not be adversely affected.

Depth of investigation. The maximum depth of investigation is a function mostly of the lowest frequency fundamental mode Rayleigh wave energy recorded and the length or diameter of the geophone array. The lowest frequency recorded is a function of the magnitude of recorded passive Rayleigh acoustic energy. Lower frequencies are more reliably analyzed when recorded using arrays with lengths on the order of the wavelength of those frequencies.

Proximity to buried structures and buried utilities. The MASW tool is non-invasive. Active data can be acquired in proximity to buried utilities and buried structures, unless there is concern that the acoustic source could damage built structures such as concrete or pavement. Ambient seismic ‘noise’ or microtremors, which occur constantly as cultural and natural background noise, can be as source of passive Rayleigh waves.

Proximity to surface structures and surface utilities. The Passive MASW tool is non-invasive. Passive data can be acquired in proximity to surface utilities and structures. Ambient seismic ‘noise’ (microtremors), which occur constantly as cultural and natural background noise, can be as source of passive Rayleigh waves.

Sensitivity to background noise. Background (ambient noise) can be a useful source of passive energy.

Permitting requirements. Generally, only permission from the surface rights holder is required.

Notification requirements. Generally, only permission from the surface rights holder is required.

Other considerations. Good quality Passive MASW data cannot be recorded unless suitable passive energy passes through the array while the seismograph is activated.

2.2.2.5 Brief Description of Field Data

The field data are recorded digitally and stored on the laptop connected to the seismograph or to built-in flash memory. Generally, multiple non-stacked passive records (each typically 30 seconds in length) are generated for each passive test location. These records are effectively "stacked" during processing to increase the signal to noise ratio.

2.2.2.6 Estimated Cost to Acquire MASW Field Data at One Test Site

Basic field costs include: a) 1-3 hours of crew time plus travel time; b) equipment rental and/or depreciation; and c) vehicle rental and/or depreciation plus fuel. Depending on the complexity of the array employed, it typically takes 2-person crew 1-3 hours to acquire a single MASW data set (24-geophone array).

2.2.2.7 Potential for Errors

There is little likelihood that field errors will lead to misinterpretation.

Human. Human error, leading to misinterpretation, is unlikely because the only critical non-automated process is the placement of the geophones. If the incorrect geophone separation is inadvertently entered as a processing parameter, significant errors can result. If suitable passive Rayleigh wave energy does not pass through the array while data are being recorded, the output 1-D shear wave velocity profile will not be reliable.

Equipment. Equipment problems are unlikely to generate errors that will lead to misinterpretation.

2.2.2.8 Reproducibility of Field Tests

If good quality Active MASW field data can be recorded, field results can be reproduced with a relatively high degree of consistency.

2.2.2.9 Quality Control

Field records cannot normally be visually assessed in the field for QC purposes.

However, data can also be processed in a cursory manner in the field for quality control purposes. If poor quality data have been recorded, the additional data can be collected. Alternatively, the array can be reoriented or moved.

2.2.3 Data and/or Laboratory Processing

2.2.3.1 Brief Overview of Data Processing

In step 1, the processor also inputs the field acquisition parameters including geophone spacing, source offset and source location (Appendix B).

In step 2 of data processing, the edited MASW field record is analyzed, and an image panel (overtone record) is generated. The image panel is a phase velocity vs. frequency plot of energy accumulation pattern. It is constructed using a 2-D (time and space) wavefield transformation method that employs several pattern-recognition approaches and does not require any interactive input from the interpreter (Appendix B). This transformation eliminates all the ambient noise from human activities as well as source-generated noise such as scattered waves from buried objects (foundations, culverts, boulders, etc.). The image panel shows the relationship between phase velocity and frequency for those waves propagated horizontally directly from the impact point to the receiver line. These waves include fundamental and higher modes of surface waves as well as direct body (compressional) waves.

In step 3, the dispersion curve is extracted (usually subjectively "picked") from the energy accumulation pattern in the image panel (Appendix B). The extracted dispersion curve is finally used as a reference to back-calculate the variation in Vs with depth below the surveyed area. This back-calculation is called inversion.

In step 4, the selected dispersion curve is inverted without any qualitative input from the interpreter. The output is a 10-layered 1-D shear wave velocity profile.

If the output shear wave velocity profile is questionable, the Rayleigh wave data are normally reprocessed using different subjective parameters (i.e., picking of dispersion curve, etc.).

It should be noted that the propagation velocity of a Rayleigh wave is a uniform medium is described by Equation 2.1 "Relationship of Rayleigh, Shear and Compressional Wave Velocities", where V_R is a function of both β and α. To transform Rayleigh wave velocities into shear wave velocities, the software package uses a predetermined value of Poisson's Ratio to remove the compressional wave velocity term (α) from the expression. This is a robust approach, but it does introduce some error into the output estimate of shear wave velocities.

2.2.3.2 Output of Data Processing

The output from a single test location is a 10-layered 1-D shear wave velocity profile. If data are collected at multiple test locations along the length of a traverse, the output 1-D shear wave velocity profiles can be used to generate a 2-D shear wave velocity profile. Creating a 2-D

cross-section will allow the user to image the lateral variations in the shear wave velocity. These profiles constitute the final deliverable.

2.2.3.3 Estimated Cost to Process Field Data from One Test Site

Basic processing costs include about 2 hours of processor's time and hardware/software rental and/or depreciation.

2.2.3.4 Potential for Error

Human. Steps 2 and 4 (the transformation of the muted MASW field data into an overtone data and the inversion of the "picked" dispersion curve) do not require interpreter input. Step 1 (parameter entry) is straightforward. Step 3 (the "picking" of the optimal dispersion curve) is subjective although usually straightforward.

In certain instances, it is difficult to "pick" an optimum dispersion curve. Problems can arise for one of a number of reasons: suitable fundamental mode Rayleigh wave energy may not have been recorded; the geophone array may have been too short; lateral velocity variations beneath the geophone array may have resulted in "smoothing" or "smearing" of phase velocity data on the overtone record; excessive topographic relief may have caused "smoothing" or "smearing"; geologic conditions (faulting for example) may have been such that surface wave energy of the desired frequency could not be recorded in the study area.

It is possible for a processor to misidentify higher mode Rayleigh wave energy as fundamental mode Rayleigh wave energy. In such situations, the output shear wave velocities will be anomalously high.

If the processor arbitrarily extends the dispersion curve (via extrapolation and with the objective of extending the shear wave velocity profile to greater depths) beyond the lowest confidently "pickable" frequency on the overtone record, serious errors can arise.

Equipment. The Passive MASW data acquisition equipment and processing software should not be defective. Data processing software may be glitchy, that could be typically resolved by simply closing and relaunching the software and reopening the data file.

2.2.3.5 Reproducibility of Field Tests

If the MASW field data are good quality, trained processors will generate consistent 1-D shear wave velocity profiles over the range of frequencies that were generated by the passive source.

2.2.4 Interpretation

2.2.4.1 Brief Overview of Interpretation of Processed Data

The output of data processing is a 10-layered 1-D shear wave profile of the subsurface. If multiple Active MASW data sets are acquired, 2-D or 3-D shear wave velocity images of the subsurface can be generated.

Usually, the interpreter establishes relationships between lithology (if control is available) and acoustic velocity and transforms the output 1-D shear velocity model into a geologic model of the subsurface. If geologic control is not available, the depth to bedrock (if imaged) can generally be estimated based on the visual assessment of the shear wave velocity profile.

If the MASW data are acquired for site classification purposes, the average shear wave velocity to a depth of 100 feet is normally calculated.

2.2.4.2 Deliverable(s)

1-D, 2-D, or 3-D geologic and shear wave velocity models.

If the MASW data are acquired for site classification purposes, the average shear wave velocity to a depth of 100 feet is normally calculated.

A 10-layered 1-D shear wave velocity profile will be generated at each test location. The output shear wave velocity profile is more-or-less a function of the average shear wave velocity of the subsurface along the entire length of the geophone array. However, by convention, the shear wave velocity profile is plotted at the center of the respective geophone array.

2.2.4.3 Depth Range (Top/Bottom)

Surface to depths on the order of multiple hundreds of feet. Greater depths of investigation can be achieved if very low frequency passive Rayleigh wave data are recorded.

2.2.4.4 Lateral Resolution

Rayleigh wave data are acquired along the entire breadth of the geophone array. If the velocity of the subsurface varies laterally beneath the array, lateral velocity smoothing will occur.

The output 1-D shear wave velocity profile is more-or-less a function of the average shear wave velocity of the subsurface across the entire breadth of the geophone array. However, by convention, the output shear wave velocity profile is plotted at the center of the geophone array. Lateral resolution can be increased by decreasing the geophone spacing. However, this approach usually decreases the overall depth of investigation as well.

Zones of anomalously low or high velocity on the output 10-layered 1-D shear wave velocity profile should not be misinterpreted as indicative of the presence of a boulder or clay-filled void/karstic feature, respectively, immediately beneath the center of the geophone array.

2.2.4.5 Vertical Resolution

The output of processing is a 10-layered shear wave velocity profile of the subsurface. The thickness of each layer is a pre-set software function of the total depth to the top of the 11th layer. The thickness of the layers increases with depth. Layer boundaries are set by the processing software and do not usually correspond precisely to lithologic boundaries.

Additionally, Rayleigh wave data are acquired across the entire breadth of the geophone array. The velocity assigned to a specific layer is a function of the average velocity of that layer across the entire breadth of the geophone array.

Significant features such as the top of rock can usually be estimated to within $\pm$10%.

2.2.4.6 Time Required to Interpret Field Data (One Test Site)

If ground truth is available and if velocity/lithologic relationships can be established, the interpretation of the shear wave velocity data is normally relatively rapid and straightforward.

2.2.4.7 Potential for Error

Human. There is little potential for error, if the interpreter understands that the output shear wave velocity profile generated at each test location represents the average shear wave along the length of the array. It does not represent the precise shear wave velocity of the subsurface at the mid-point of the geophone array.

Equipment. There is little potential for error.

2.2.4.8 Reproducibility of Deliverable

If ground truth is available, different experienced interpreters should come up with similar interpretations. If ground truth is not available, unreasonable interpretations are a very real possibility.

2.2.5 Deliverables

2.2.5.1 Brief Overview of Deliverable(s)

1-D (or 2-D or 3-D) geologic and shear wave velocity models.

2.2.5.2 Utility of deliverable(s)

Geologic and shear wave velocity models provide information about variations in lithology, porosity, engineering properties, rippability of rock, diggability of soil, depth to top of rock, etc.

The shear wave velocity profiles can also be used for earthquake site classification purposes.

2.2.5.3 Accuracy

The final interpretations are generally reliable if good quality Passive MASW field data are recorded and if ground truth is available. Use of an experienced interpreter is essential.

2.2.6 Advantages

Advantages include:

- output is a shear wave velocity profile of the subsurface that typically extends to a depth of multiple hundreds of feet,
- depth to bedrock can usually be estimated to within ±10%,
- other lithologic units can often be identified and mapped on basis of shear wave velocity,
- relatively low cost,
- portability of equipment,
- relatively insensitive to background noise,
- typically employ a 1–3-person crew,
- relatively rapid processing of field data in lab,
- few restrictions with respect to surface conditions (soil, rock, pavement, etc.),
- non-invasive,
- limited potential for human error if operators and processors are trained,
- reproducibility of field data,
- reproducibility of processing results,
- reproducibility of interpretations, particularly if geologic control is available,
- multiple applications (determination of lithology, porosity, rippability, depth to bedrock, location of voids, shear strength).
- permitting is not required,
- tool can be used across and in proximity to utilities and built structures as the method is relatively insensitive to background acoustic noise,
- Passive MASW data can be acquired underwater using hydrophones coupled to the water bottom (Scholte waves are recorded and processed),
- Passive MASW data can be acquired using horizontally polarized shear wave geophones (Love waves are recorded and processed).

2.2.7 Disadvantages

Disadvantages include:

- desired maximum depths of investigation may not be realized if low frequency passive Rayleigh wave data are not recorded,
- site must be large enough to accommodate the geophone array and source,
- difficult to QC data in the field,
- data are not usually processed in the field for QC purposes,
- reliability of output shear wave velocity data decreases as lateral and vertical heterogeneity of soil/rock increases,
- significant surface topography can make it difficult to acquire useful data,
- significant subsurface topography can make it difficult to acquire useful data,
- features such as faults, solution-widened joints and voids may make it difficult to acquire useful data,
- underground utilities can make it difficult to acquire useful data,
- vegetation can pose problems during data acquisition,
- geophones must be effectively coupled to the ground surface; acquiring quality data on very soft or loose soil can be difficult,
- in certain limited situations, proximal background noise may be overwhelming, layer boundaries on the shear wave velocity profile do not correspond exactly to lithologic boundaries.

2.3. Active Refraction Microtremor (Active ReMi) Method

2.3.1 Brief Overview of the Active ReMi Method

Refraction microtremor (ReMi) software can be used to transform recorded fundamental mode Rayleigh waves (type of surface wave) generated using an active acoustic source into a multi-layer (typically limited to 4) 1-D shear wave velocity profile of the subsurface.

Active Rayleigh wave energy is normally generated using a proximal source such as a sledgehammer, weight drop or small explosive that is discharged by the ReMi survey crew. The active sources that are used to image the subsurface to depths on the order of 100 feet typically generate Rayleigh waves with frequencies ranging from 5 to 60 Hz. The higher frequency (shorter wavelength) Rayleigh waves extend to shallow depths; the lower frequency (longer wavelength) Rayleigh waves extend to greater depths. Ideally, the recorded Rayleigh waves with the lowest frequencies will involve particle motion to depths of at least 100 feet. If depths of investigation greater than 100 feet are desired, the ReMi crew should consider acquiring Passive ReMi data or combination Active/Passive ReMi data.

Rayleigh wave energy is dispersive meaning that different frequencies travel with different velocities. More specifically, each frequency travels with a phase velocity that is mostly a function of the average shear wave velocity of the subsurface from the ground surface to the base of particle motion associated with that frequency (wavelength).

Active Rayleigh wave data are normally recorded using a linear array of geophones. ReMi software analyzes the recorded Rayleigh wave data and calculates the phase velocities of a representative range of frequencies (from highest to lowest frequency Rayleigh waves). These phase velocity data are used to estimate the effective base of particle motion associated with each frequency and to estimate the average shear wave velocity over that depth range of particle motion. The subsurface can then be subdivided into a finite number of layer (one layer for each frequency analyzed; from the ground surface to the base of particle motion associated with lowest frequency analyzed). Interval shear wave velocities can then be assigned to each layer.

The output of a single Active ReMi data set is a multi-layer (typically limited to 4) 1-D shear wave velocity profile of the subsurface. In certain situations, a suite of ReMi data sets is collected at intervals along the length of a traverse and the output 1-D shear wave velocity profiles are used to generate a pseudo-2-D shear wave velocity profile of the subsurface. 3-D shear wave velocity images of the subsurface can also be generated.

The active multichannel analysis of surface wave (MASW; Section 2.1of this report) method is very similar to the active refraction microtremor (ReMi) method. The most significant difference is the processing software.

2.3.2 Data Acquisition

2.3.3.1 Brief Overview of Field Procedure

A linear array of geophones (typically 12 to 24), an acoustic source, an engineering seismograph and a laptop are used to record active Rayleigh wave data that propagates along the axis of the geophone array (Figure 2.1). The geophones are generally spaced such that the length of the array is on the order of the desired maximum depth of investigation. For example, if the objective is to image the subsurface to a depth of 100 feet, the geophones are typically spaced at 5 feet and the array is 115 feet in length.

Active ReMi data are generated using a man-made source (such as a sledgehammer and strike plate). The source is discharged off one the end of the geophone array. If the intent is to image the subsurface to a depth of 100 feet, the source is typically discharged 25-30 feet from the closest geophone. When the active source is discharged, the seismograph is triggered, and data is recorded (typically for one second or less). To increase the signal to noise ratio, the source is typically discharged multiple times (stacked) at each location. Typically, the source is discharged 2-5 times at each location to increase statistical reliability and minimize the effects of random noise. Separate field records are generated for each discharge. The separate field records are analyzed collectively during data processing.

Field records can be visually assessed in the field for quality control purposes. Data can also be processed in a cursory manner in the field for quality control purposes. If poor quality data have been recorded, the source can be discharged at the other end of the array of geophones or a greater magnitude source can be employed. Alternatively, the array can be reoriented or moved.

If the recorded frequencies are relatively good quality but too high to image to a depth of 100 feet, a greater magnitude source can be employed.

2.3.2.2 Field Equipment

The portable equipment consists of an active source, an engineering seismograph, a trigger switch, a laptop with installed acquisition and processing software, and, typically, an array of 12-24 low-frequency vertically polarized geophones (either 4.5 Hz or 14 Hz geophones). Typically, a heavy sledgehammer source and a strike plate are employed.

2.3.2.3 Field Crew

Typically consists of 1-3 persons. A single person can acquire Active ReMi data. However, if ReMi data are to be acquired at multiple locations at a site, it is usually more efficient to field a field crew consisting of 2-3 persons.

2.3.2.4 Considerations

Parameter entry. The correct acquisition parameters must be entered. An Active ReMi field record is typically between 0.5 and 1.0 seconds in duration. The sampling interval is usually 0.5 milliseconds.

Size of test site. The test site must be large enough to allow for ease of placement of geophones and the offset active source. A typical Active ReMi array (including the offset source) is typically about 145 feet in length.

Plotted location of the output 1-D shear wave velocity profile. A multi-layered 1-D shear wave velocity profile will be generated at each test location. The output shear wave velocity profile is more-or-less a function of the average shear wave velocity of the subsurface along the entire length of the geophone array. However, by convention, the shear wave velocity profile is plotted at the center of the geophone array.

Vehicular access. All equipment can be transported by hand. Usually, the equipment and crew are transported in a single vehicle.

Surface topography. Active ReMi data can be acquired across undulating ground surfaces or across steeply dipping terrain. However, elevation changes should be minimized where/if possible as data quality usually decreases as surface topographic relief increases. In these situations, 2 ReMi data sets should be acquired. The active source should be discharged off both ends of the geophone array. To a certain extent, issues related to irregular surface topography can be dealt with or at least recognized during data processing. Often, the effects of irregular or dipping topography can be recognized on ReMi field records.

Rayleigh waves can be reflected from proximal surface topography such as stream beds, hillsides, and drainage ditches. Reflected Rayleigh wave can complicate data processing. Often, reflected Rayleigh wave energy can be recognized on the field records.

Subsurface topography. If there is a possibility that bedrock dips appreciably along the length of the geophone array, 2 ReMi data sets should be acquired. The active source should be discharged off both ends of the geophone array. To a certain extent, issues related to irregular subsurface topography can be dealt with or at least recognized during data processing.

If features such as faults, solution-widened joints or voids are present beneath the geophone array or between the source and the array, it may not be possible to record useful Rayleigh wave data. The discharged Rayleigh wave energy may not propagate uniformly along the length of the geophone array. Rather, it may be mostly backscattered (reflected) from these subsurface features, causing signal loss or distortion.

Often, backscattered Rayleigh wave energy can be recognized on the field records.

Vegetation. Data can be acquired in heavily vegetated areas if the geophones and active source can be placed in the appropriate locations. However, dense vegetation does impede work and

slows down field data acquisition. Usually, it is most efficient to clear the traverse ahead of time.

Background noise. Active ReMi data can usually be acquired even in acoustically noisy environments. However, it may be necessary to increase the magnitude of the active source or to stacking multiple field records.

Anchoring requirements. The geophones are frequently coupled to the ground surface using short base spikes. However, base plates can be used in lieu of spikes and are usually used if data are acquired on pavement, rock or gravel. The geophones do need to be placed in stable, vertical positions on the ground surface.

Nature of ground surface. The geophones are frequently coupled to the ground surface using short base spikes. However, base plates can be used in lieu of spikes and are usually used if data are acquired on pavement, rock or gravel. The geophones do need to be placed in stable, vertical positions on the ground surface.

Placement of geophones and active source. Normally, a tape measure is laid out along the traverse and geophones are placed at their appropriate locations. If a few individual geophones are misplaced off by 5% or less, data quality should not be adversely affected, particularly if the geophones are shifted perpendicular to the traverse.

If the location of the source is in line with the geophone array but out by 10% or less, data quality should not be adversely affected.

Subsurface lithology or material. Active ReMi data can be acquired across all types of soil and/or rock. ReMi data can also be acquired across pavement, asphalt, fill, etc.

Depth of investigation. The maximum depth of investigation is a function mostly of the lowest frequency fundamental mode Rayleigh wave energy recorded and the length of the geophone array. If active data are being recorded, the lowest frequency recorded is a function of the energy generated by the source as greater magnitude sources generate lower frequency Rayleigh waves. Lower frequencies are more reliably analyzed when recorded using arrays with lengths on the order of the wavelength of those frequencies.

Proximity to buried structures and buried utilities. The Active ReMi tool is non-invasive. Active data can be acquired in proximity to buried utilities and buried structures, unless there is concern that the acoustic source could damage built structures such as concrete or pavement. Issues with data quality can arise if the buried utilities or buried structures are beneath the geophone array or between the source and the array. Rayleigh waves that are reflected from subsurface features can complicate data processing.

Proximity to surface structures and surface utilities. The ReMi tool is non-invasive. Active data can be acquired in proximity to surface utilities and surface structures. ReMi data can be acquired in proximity to surface utilities and built structures. Typically, the only clearance

required is sufficient room to discharge the source. The sledgehammer can damage concrete or pavement.

Sensitivity to background noise. The Active ReMi technique is relatively insensitive to noise. However, in certain instances (such as in proximity to moving trains, operating heavy equipment, buildings with air conditioners, etc.) it can be very difficult to acquire data.

Permitting requirements. Generally, only permission from the surface rights holder is required.

Notification requirements. Generally, only permission from the surface rights holder is required.

Other considerations. It may not be possible to generate an output shear wave velocity profile that extends to the desired depth of investigation if the magnitude of the active source is too small or if the signal to noise ratio is too low. Site and/or ground conditions may make it effectively impossible to image the subsurface to the desired depth.

2.3.2.5 Brief Description of Field Data

The field data are recorded digitally and stored on the laptop connected to the seismograph or to built-in flash memory. Generally, multiple active records (typically 1 second in length) are generated for each active test location. These records are effectively "stacked" during processing to increase the signal to noise ratio.

2.3.2.6 Estimated Cost to Acquire REMI Field Data at One Test Site

Basic field costs include: a) 1 hour of crew time plus travel time; b) equipment rental and/or depreciation; and c) vehicle rental and/or depreciation plus fuel. It typically takes a 2-person crew 1 hour to acquire a single Active MASW data set (using a sledgehammer source and a 24-geophone array).

2.3.2.7 Potential for Errors

There is little likelihood that field errors will lead to misinterpretation.

Human. Human error, which leads to misinterpretation, is unlikely because the only critical non-automated processes are the placement of the geophones and the discharge of the active source. If the incorrect geophone separation is inadvertently entered as a processing parameter, significant errors can result. If the source is discharged too far from or too close to the geophone array, or if the source is too low magnitude, poor quality field data may be acquired.

Equipment. Equipment problems are unlikely to generate errors that will lead to misinterpretation, but care must be taken.

2.3.2.8 Reproducibility of Field Tests

If good quality Active ReMi field data can be recorded, field results can be reproduced with a relatively high degree of consistency.

2.3.2.9 Quality Control

Acquired data can be visually assessed in the field for quality control purposes. Data can also be processed in a cursory manner in the field for quality control purposes. If poor quality data have been recorded, the source can be discharged at the other end of the array of geophones or a greater magnitude source can be employed. Alternatively, the array can be reoriented or moved.

2.3.3 Data and/or Laboratory Processing

2.3.3.1 Brief Overview of Data Processing

In the initial phase of data processing (step 1), each uploaded ReMi field record is manually edited (selective muting) by the processor to remove coherent energy such as refractions and higher mode Rayleigh waves. The processor also inputs the field acquisition parameters including geophone spacing, source offset and source location.

In step 2 of data processing, the edited ReMi field record is analyzed, and an image panel is generated. The image panel is a slowness vs. frequency plot of energy accumulation pattern. It is constructed using a 2-D (time and space) wavefield transformation method that employs several pattern-recognition approaches and does not require any interactive input from the interpreter. This transformation eliminates all the ambient noise from human activities as well as source-generated noise such as scattered waves from buried objects (foundations, culverts, boulders, etc.).

The image panel shows the relationship between slowness and frequency for those waves propagated horizontally directly from the impact point to the receiver line. These waves include fundamental and higher modes of surface waves as well as direct body (compressional) waves.

In step 3, the dispersion curve is extracted (usually subjectively “picked”) from the energy accumulation pattern in the image panel. The extracted dispersion curve is finally used as a reference to back-calculate the variation in Vs with depth below the surveyed area. This back-calculation is called inversion.

In step 4, the selected dispersion curve is inverted without any qualitative input from the interpreter. The output is a 10-layered 1-D shear wave velocity profile.

If the output shear wave velocity profile is questionable, the Rayleigh wave data are normally reprocessed using different subjective parameters (i.e., muting, picking, etc.).

It should be noted that the propagation velocity of a Rayleigh wave is a uniform medium is described by the Equation 2.1 "Relationship of Rayleigh, Shear and Compressional Wave Velocities", where V_R is a function of both β and α. To transform Rayleigh wave velocities into shear wave velocities, the software package uses a predetermined value of Poisson's Ratio to remove the compressional wave velocity term (α) from the expression. This is a robust approach, but it does introduce some error into the output estimate of shear wave velocities.

2.3.3.2 Output of Data Processing

The output from a single test location is a 10-layered 1-D shear wave velocity profile. If data are collected at multiple test locations along the length of a traverse, the output 1-D shear wave velocity profiles can be used to generate a 2-D or 3-D shear wave velocity profile. Creating a 2-D cross-section will allow the user to image the lateral variations in the shear wave velocity.

2.3.3.3 Estimated Cost to Process Field Data from One Test Site

Basic processing costs include about 1 hour of processor's time and hardware/software rental and/or depreciation.

2.3.3.4 Potential for Error

Human. Steps 2 and 4 (the transformation of the muted ReMi field data into an overtone data and the inversion of the "picked" dispersion curve) do not require interpreter input. Step 1 (muting and parameter entry) and step 3 (the "picking" of the optimal dispersion curve) are subjective although usually straightforward.

In certain instances, it is difficult to "pick" an optimum dispersion curve. Problems can arise for one of a number of reasons: suitable fundamental mode Rayleigh wave energy may not have been recorded; the acoustic source may have been too small; the geophone array may have been too long or too short; lateral velocity variations along the length of the geophone array may have resulted in "smoothing" or "smearing" of phase velocity data on the overtone record; excessive topographic relief may have caused "smoothing" or "smearing"; geologic conditions (faulting for example) may have been such that surface wave energy of the desired frequency could not be recorded in the study area.

It is possible for a processor to misidentify higher mode Rayleigh wave energy as fundamental mode Rayleigh wave energy. In such situations, the output shear wave velocities will be anomalously high.

If the processor arbitrarily extends the dispersion curve (via extrapolation and with the objective of extending the shear wave velocity profile to greater depths) beyond the lowest confidently "pickable" frequency on the overtone record serious errors can arise.

Equipment. The Active ReMi processing software should not be defective.

2.3.3.5 Reproducibility of Field Tests

If the ReMi field data are good quality, trained processors will generate consistent 1-D shear wave velocity profiles over the range of frequencies that were generated by the source in the field.

2.3.4 Interpretation

2.3.4.1 Brief Overview of Interpretation of Processed Data

The output of data processing is a 10-layered 1-D shear wave profile of the subsurface. If multiple Active ReMi data sets are acquired, 2-D or 3-D shear wave velocity images of the subsurface can be generated.

Usually, the interpreter establishes relationships between lithology (if control is available) and acoustic velocity and transforms the output 1-D shear velocity model into a geologic model of the subsurface. If geologic control is not available, the depth to bedrock (if imaged) can generally be estimated based on the visual assessment of the shear wave velocity profile.

If the ReMi data are acquired for site classification purposes, the average shear wave velocity to a depth of 100 feet is normally calculated.

2.3.4.2 Deliverable(s)

1-D, 2-D, or 3-D geologic and shear wave velocity models.

If the ReMi data are acquired for site classification purposes, the average shear wave velocity to a depth of 100 feet is normally calculated.

A multi-layered 1-D shear wave velocity profile will be generated at each test location. The output shear wave velocity profile is more-or-less a function of the average shear wave velocity of the subsurface along the entire length of the geophone array. However, by convention, the shear wave velocity profile is plotted at the center of the respective geophone array.

2.3.4.3 Depth Range (Top/Bottom)

If a 20-pound sledgehammer source is employed, the output shear wave velocity profile will typically extend to a depth on the order of 100-120 feet. Greater depths of investigation can be achieved if a larger magnitude source is employed.

2.3.4.4 Lateral Resolution

Rayleigh wave data are acquired along the entire length of the geophone array. If the velocity of the subsurface varies laterally along the length of the array, lateral velocity smoothing will occur. However, some weighting is involved as the source/receiver separation is generally

selected such that higher frequencies are excessively attenuated at the farthest geophones whereas the lowest frequencies are not recorded on the closest geophones.

The output 1-D shear wave velocity profile is more-or-less a function of the average shear wave velocity of the subsurface along the entire length of the geophone array. However, by convention, the output shear wave velocity profile is plotted at the center of the geophone array. Lateral resolution can be increased by decreasing the geophone spacing and sometimes the magnitude of the source. However, this approach usually decreases the overall depth of investigation as well.

Zones of anomalously low or high velocity on the output multi-layer (typically limited to 4) 1-D shear wave velocity profile should not be misinterpreted as indicative of the presence of a boulder or clay-filled void/karstic feature, respectively, immediately beneath the center of the geophone array.

2.3.4.5 Vertical Resolution

The output of processing is a multi-layer (typically limited to 4) shear wave velocity profile of the subsurface. The thickness of each layer is a pre-set software function of the total depth to the top of the basal layer. The thickness of the layers increases with depth. Layer boundaries are set by the processing software and do not usually correspond precisely to lithologic boundaries.

Additionally, Rayleigh wave data are acquired along the entire length of the geophone array. The velocity assigned to a specific layer is a function of the average velocity of that layer along the entire length of the geophone array.

Significant features such as the top of rock can usually be estimated to within $\pm$10%.

2.3.4.6 Time Required to Interpret Field Data (One Test Site)

If ground truth is available and if velocity/lithologic relationships can be established, the interpretation of the shear wave velocity data is normally relatively rapid and straightforward.

2.3.4.7 Potential for Error

Human. There is little potential for error if the interpreter understands that the output shear wave velocity profile generated at each test location represents the average shear wave along the length of the array. Layer velocities do not necessarily represent the precise shear wave velocity of the subsurface at the mid-point of the geophone array.

Equipment. There is little potential for error.

2.3.4.8 Reproducibility of Deliverable

If ground truth is available, different experienced interpreters should come up with similar interpretations. If ground truth is not available, unreasonable interpretations are a very real possibility.

2.3.5 Deliverables

2.3.5.1 Brief Overview of Deliverable(s)

1-D (or 2-D or 3-D) geologic and shear wave velocity models.

2.3.5.2 Utility of Deliverable(s)

Geologic and shear wave velocity models provide information about variations in lithology, porosity, engineering properties, rippability of rock, diggability of soil, depth to top of rock, etc.

The shear wave velocity profiles can also be used for earthquake site classification purposes.

2.3.5.3 Accuracy

The final interpretations are generally reliable if good quality Active ReMi field data are recorded and if ground truth is available. Use of an experienced interpreter is essential.

2.3.6 Advantages

Advantages include:

- output is a shear wave velocity profile of the subsurface that typically extends to a depth of 100+ feet,
- depth to bedrock can usually be estimated to within ±10%,
- other lithologic units can often be identified and mapped on basis of shear wave velocity,
- relatively low cost,
- portability of equipment, relative insensitivity to background noise,
- typically employ a 1–3-person crew,
- field records can be visually assessed in the field for QC purposes,
- ability to rapidly process data in the field (for QC purposes),
- rapid processing of field data in lab, however, may be more complicated compared to MASW,
- few restrictions with respect to surface conditions (soil, rock, pavement, etc.),
- non-invasive,
- limited potential for human error if operators and processors are trained,

- reproducibility of field data,
- reproducibility of processing results,
- reproducibility of interpretations, particularly if geologic control is available,
- multiple applications (determination of lithology, porosity, rippability, depth to bedrock, location of voids, shear strength).
- permitting is not required,
- tool can be used across and in proximity to utilities and built structures as the method is relatively insensitive to background acoustic noise.

2.3.7 Disadvantages

Disadvantages include:

- desired maximum depths of investigation may not be realized if the source is too small given subsurface geologic conditions,
- site must be large enough to accommodate the geophone array and source,
- reliability of output shear wave velocity data decreases as lateral and vertical heterogeneity of soil/rock increases,
- significant surface topography can make it difficult to acquire useful data,
- significant subsurface topography can make it difficult to acquire useful data,
- features such as faults, solution-widened joints and voids may make it difficult to acquire useful data,
- underground utilities can make it difficult to acquire useful data,
- vegetation can pose problems during data acquisition,
- geophones and source must be effectively coupled to the ground surface; acquiring quality data on very soft or loose soil can be difficult,
- in certain limited situations, background noise may be overwhelming, layer boundaries on shear wave velocity profile do not correspond exactly to lithologic boundaries.

2.4. Passive Refraction Microtremor (Passive ReMi) Method

2.4.1 Brief Description of the Passive ReMi Method

Refraction microtremor (ReMi) software can be used to transform recorded fundamental Rayleigh waves (type of surface wave) generated using a passive acoustic source into a multi-layered (typically 4) 1-D shear wave velocity profile of the subsurface.

Passive Rayleigh wave energy (ambient noise) is not generated by the ReMi field crew. Rather, passive Rayleigh wave energy is generated by external ambient sources that can include microseismic activity, lightning strikes, vehicle traffic, etc. Passive sources typically generate Rayleigh waves with frequencies ranging from 1 to 30 Hz. The higher frequency (shorter wavelength) Rayleigh waves extend to shallow depths; the lower frequency (longer wavelength) Rayleigh waves extend to greater depths. Ideally, the lowest recorded frequency Rayleigh waves will involve particle motion to depths of several hundred feet.

As noted, Rayleigh wave data generated using a passive source are normally lower frequency than Rayleigh wave data generated using an active source. Because the passive Rayleigh data are normally lower frequency, the output shear wave velocity profile generally provides for relatively poorer vertical resolution in the upper 100 feet. On the upside, Passive ReMi data can be often used to image the subsurface to depths greater than several hundreds of feet. Combination Active/Passive ReMi data sets can provide for both high vertical resolution at shallow depths and greater depths of investigation.

Rayleigh wave energy is dispersive meaning that different frequencies travel with different velocities. More specifically, each frequency travels with a phase velocity that is mostly a function of the average shear wave velocity of the subsurface from the ground surface to the base of particle motion associated with that frequency (wavelength).

Passive ReMi data are recorded using a linear symmetric array of geophones. The linear array should be directed towards the location of the primary source of ambient noise if known.

ReMi software analyzes the recorded Rayleigh wave data and calculates the phase velocities of a representative range of frequencies (from highest to lowest frequency Rayleigh waves). These phase velocity data are used to estimate the effective base of particle motion associated with each frequency and to estimate the average shear wave velocity over that depth range of particle motion. The subsurface can then be subdivided into a finite number of layer (one layer for each frequency analyzed; from the ground surface to the base of particle motion associated with lowest frequency analyzed). Interval shear wave velocities can then be assigned to each layer.

The output of a single Passive ReMi data set is a multi-layered 1-D shear wave velocity profile of the subsurface. In certain situations, a suite of ReMi data sets is collected at intervals along the length of a traverse and the output 1-D shear wave velocity profiles are used to generate a

pseudo-2-D shear wave velocity profile of the subsurface. 3-D shear wave velocity images of the subsurface can also be generated.

The Passive MASW method (Section 2.2 of this report) method is very similar to the Passive ReMi method. There are two significant differences: 1) MASW and ReMi processing software are different; and 2) MASW software can be used to process data acquired using a non-linear array; ReMi software cannot.

2.4.2 Acquisition of Active ReMi Data

2.4.2.1 Brief Overview of Field Procedure

A linear array of geophones (typically 24), an engineering seismograph and a laptop are used to record passive Rayleigh wave data. The geophones are generally spaced such that the length of the linear array is on the order of the desired maximum depth of investigation. For example, if the objective is to image the subsurface to a depth of 100 feet using a linear array, the geophones are typically spaced at 5 feet and the array is 115 feet in length (Figure 2.1).

Passive Rayleigh wave energy (ambient noise) is not generated by the ReMi field crew. Rather, passive Rayleigh wave energy occurs naturally and can be generated by external sources that can include microseismic activity, lightning strikes, construction equipment, vehicle traffic, etc. Passive data are generated by triggering the seismograph manually and recording "random" data, typically for about 30 seconds or more. Passive data are never stacked, but multiple separate 30 plus second records are usually recorded at each test location to increase the probability that useful passive Rayleigh wave energy has propagated through the array. The separate field records are analyzed collectively during data processing.

A reliable shear wave velocity profile will be output only if measurable Rayleigh wave energy propagates through the array and in a direction parallel to the axis of the array. Rayleigh wave energy that propagates parallel to the axis of a linear array will exhibit lower apparent velocities (greater slowness) than energy that propagates through the same array at an angle.

Field records cannot normally be visually assessed in the field for QC purposes.

Data are normally not processed in the field for quality control purposes.

If combination Active/Passive data are required, an active source can be discharged while the 30 second passive data sets are being recorded. Alternatively, both active and passive wave data can be recorded separately and combined during processing.

2.4.2.2 Field Equipment

The method utilizes equipment typically employed in conventional seismic refraction surveys. This equipment consists of an active source, an engineering seismograph, a laptop with installed acquisition and processing software, and an array of 24 low-frequency vertically polarized geophones (either 4.5 Hz or 14 Hz geophones). If passive data (only) are being

recorded, an operational source is not required. If both active and passive data are being recorded, an acoustic source is employed.

2.4.2.3 Field Crew

Consists of 1-3 persons. A single person can acquire Passive ReMi data. However, if ReMi data are to be acquired at multiple locations at a site, it is usually more efficient to field a field crew consisting of 2-3 persons.

2.4.2.4 Considerations

Parameter entry. The correct acquisition parameters must be entered. A Passive ReMi field record is typically between 30 seconds in duration. The sampling interval is usually 0.5 milliseconds.

Size of test site. The test site must be large enough to allow for ease of placement of geophones. The diameter of a non-linear passive ReMi array is typically approximately equal to the desired depth of investigation. The diameter of a linear Passive ReMi array is typically approximately equal to the desired depth of investigation.

Plotted location of the output 1-D shear wave velocity profile. A multi-layered 1-D shear wave velocity profile will be generated at each test location. The output shear wave velocity profile is assumed to be a function of the average shear wave velocity of the subsurface beneath the geophone array. However, by convention, the shear wave velocity profile is plotted at the center of the geophone array.

Vehicular access. All equipment can be transported by hand. Usually, the equipment and crew are transported in a single vehicle.

Surface topography. Passive ReMi data can be acquired across undulating ground surfaces or across steeply dipping terrain. However, elevation changes should be minimized where/if possible as data quality usually decreases as surface topographic relief increases.

Rayleigh waves can be reflected from proximal surface topography such as stream beds, hillsides, and drainage ditches. Reflected Rayleigh wave can complicate data processing. Often, reflected Rayleigh wave energy can be recognized on the field records.

Subsurface topography. If features such as faults, solution-widened joints or voids are present beneath the geophone array, it may not be possible to record useful passive Rayleigh wave data.

Vegetation. Data can be acquired in heavily vegetated areas. However, dense vegetation does impede work and slows down field data acquisition. Usually, it is most efficient to clear the study site ahead of time.

Background noise. Passive ReMi data can usually be acquired even in acoustically noisy environments. Coherent background noise such as highway traffic can constitute a useful source of passive Rayleigh wave energy.

Anchoring requirements. The geophones are frequently coupled to the ground surface using short base spikes. However, base plates can be used in lieu of spikes and are usually used if data are acquired on pavement, rock or gravel. The geophones do need to be placed in stable, vertical positions on the ground surface.

Nature of ground surface. The geophones can be placed on soil, rock, fill, concrete, asphalt, etc. They should be stable and vertical. Data acquisition can be a problem if the surficial soils are very loose. In such situations, it can be difficult to effectively couple the geophones to the ground.

Placement of geophones and active source. Normally, a tape measure is laid out and geophones are placed at their appropriate locations. If a few individual geophones are misplaced by 5% or less, data quality should not be adversely affected.

Subsurface lithology or material. Passive ReMi data can be acquired across all types of soil and/or rock. ReMi data can also be acquired across pavement, asphalt, fill, etc.

Depth of investigation. The maximum depth of investigation is a function mostly of the lowest frequency fundamental mode Rayleigh wave energy recorded and the length or diameter of the geophone array. The lowest frequency recorded is a function of the magnitude of recorded passive Rayleigh acoustic energy. Lower frequencies are more reliably analyzed when recorded using arrays with lengths on the order of the wavelength of those frequencies.

Proximity to buried structures and buried utilities. The Passive ReMi tool is non-invasive. Data can be acquired in proximity to buried utilities and buried structures, unless there is concern that the acoustic source could damage built structures such as concrete or pavement. Ambient seismic ‘noise’ or microtremors, which occur constantly as cultural and natural background noise, can be as source of useful passive Rayleigh waves.

Proximity to surface structures and surface utilities. The Passive ReMi tool is non-invasive. Passive data can be acquired in proximity to surface utilities and structures. Ambient seismic ‘noise’ (microtremors), which occur constantly as cultural and natural background noise, can be as source of useful passive Rayleigh waves.

Sensitivity to background noise. Excessive background noise generated by moving trains, heavy equipment, buildings with air conditioners, etc., can make it difficult to acquire quality field data unless the geophone array is aligned with the source of the noise.

Permitting requirements. Generally, only permission from the surface rights holder is required.

Notification requirements. Generally, only permission from the surface rights holder is required.

Other considerations. Good quality Passive ReMi data cannot be recorded unless suitable passive energy passes through the array and in a direction parallel to the array while the seismograph is activated.

2.4.2.5 Brief Description of Field Data

The field data are recorded digitally and stored on the laptop connected to the seismograph or to built-in flash memory. Generally, multiple non-stacked passive records (each typically 30 seconds in length) are generated for each passive test location. These records are effectively "stacked" during processing to increase the signal to noise ratio.

2.4.2.6 Estimated Cost to Acquire Field Data at One Test Site

Basic field costs include a) 1-2 hours of crew time plus travel time, b) equipment rental and/or depreciation, and c) vehicle rental and/or depreciation plus fuel. Depending on the complexity of the array employed, it typically takes 2-person crew 1-2 hours to acquire a single ReMi data set (24-geophone array).

2.4.2.7 Potential for Errors

There is little likelihood that field errors will lead to misinterpretation.

Human. Human error, leading to misinterpretation, is unlikely because the only critical non-automated process is the placement of the geophones. If the incorrect geophone separation is inadvertently entered as a processing parameter, significant errors can result. If suitable passive Rayleigh wave energy does not pass through the array while data are being recorded, the output 1-D shear wave velocity profile will not be reliable.

Equipment. Equipment problems are unlikely to generate errors that will lead to misinterpretation.

2.4.2.8 Reproducibility of Field Tests

If good quality Passive ReMi data can be recorded, field results can be reproduced with a high degree of consistency.

2.4.2.9 Quality Control

Field records cannot normally be visually assessed in the field for QC purposes. However, data can also be processed in a cursory manner in the field for quality control purposes. If poor quality data have been recorded, the additional data can be collected. Alternatively, the array can be reoriented or moved.

2.4.3 Data and/or Laboratory Processing

2.4.3.1 Brief Overview of Data Processing

In the initial phase of data processing (step 1), each uploaded ReMi field record is manually edited (selective muting) by the processor to remove coherent energy such as refractions and higher mode Rayleigh waves. The processor also inputs the field acquisition parameters including geophone spacing, source offset and source location.

In step 2 of data processing, the edited ReMi field record is analyzed, and an image panel is generated. The image panel is a slowness vs. frequency plot of energy accumulation pattern. It is constructed using a 2-D (time and space) wavefield transformation method that employs several pattern-recognition approaches and does not require any interactive input from the interpreter. This transformation eliminates all the ambient noise from human activities as well as source-generated noise such as scattered waves from buried objects (foundations, culverts, boulders, etc.).

The image panel shows the relationship between slowness and frequency for those waves propagating through the receiver array in any direction. These waves include fundamental and higher modes of surface waves as well as direct body (compressional) waves.

In step 3, the dispersion curve is extracted (usually subjectively "picked") from the energy accumulation pattern in the image panel. The extracted dispersion curve is finally used as a reference to back-calculate the variation in Vs with depth below the surveyed area. This back-calculation is called inversion.

In step 4, the selected dispersion curve is inverted without any qualitative input from the interpreter. The output is a multi-layered (typically 4) 1-D shear wave velocity profile.

If the output shear wave velocity profile is questionable, the Rayleigh wave data are normally reprocessed using different subjective parameters (i.e., picking, etc.).

It should be noted that the propagation velocity of a Rayleigh wave is a uniform medium is described by Equation 2.1 "Relationship of Rayleigh, Shear and Compressional Wave Velocities", where V_R is a function of both β and α. To transform Rayleigh wave velocities into shear wave velocities, the software package uses a predetermined value of Poisson's Ratio to remove the compressional wave velocity term (α) from the expression. This is a robust approach, but it does introduce some error into the output estimate of shear wave velocities.

In step 2, each uploaded Passive ReMi field record is transformed into an overtone record (plot of Rayleigh-wave versus frequency format) using standard, established mathematical processes that do not require any interactive input from the interpreter.

In step 3, the overtone record is analyzed qualitatively by the processor input and an optimum phase velocity versus frequency curve (dispersion curve) for the fundamental mode Rayleigh wave data is generated (subjectively "picked").

In step 4, the selected dispersion curve is inverted without any qualitative input from the interpreter. The output is a multi-layered 1-D shear wave velocity profile.

2.4.3.2 Output of Data Processing

The output from a single test location is a multi-layered (typically 4) 1-D shear wave velocity profile. If data are collected at multiple test locations along the length of a traverse or aerially, the output 1-D shear wave velocity profiles can be used to generate a 2-D or 3-D shear wave velocity profile. Creating a 2-D cross-section will allow the user to image the lateral variations in the shear wave velocity. These profiles constitute the final deliverable.

2.4.3.3 Estimated Cost to Process Field Data from One Test Site

Basic processing costs include about 2 hours of processor's time and hardware/software rental and/or depreciation.

2.4.3.4 Potential for Error

Human. Steps 2 and 4 (the transformation of the muted ReMi field data into an overtone data and the inversion of the "picked" dispersion curve) do not require interpreter input. Step 1 (parameter entry) is straightforward. Step 3 (the "picking" of the optimal dispersion curve) is subjective although usually straightforward.

In certain instances, it is difficult to "pick" an optimum dispersion curve. Problems can arise for one of a number of reasons: suitable fundamental mode Rayleigh wave energy may not have been recorded; the geophone array may have been too short; lateral velocity variations beneath the geophone array may have resulted in "smoothing" or "smearing" of phase velocity data on the overtone record; excessive topographic relief may have caused "smoothing" or "smearing"; geologic conditions (faulting for example) may have been such that surface wave energy of the desired frequency could not be recorded in the study area.

If the processor arbitrarily extends the dispersion curve (via extrapolation and with the objective of extending the shear wave velocity profile to greater depths) beyond the lowest confidently "pickable" frequency on the overtone record, serious errors can arise.

Equipment. The Passive ReMi processing software should not be defective.

2.4.3.5 Reproducibility of Field Tests

If the ReMi field data are good quality, trained processors will generate consistent 1-D shear wave velocity profiles over the range of frequencies that were generated by the passive source.

2.4.4 Interpretation

2.4.4.1 Brief Overview of Interpretation of Processed Data

The output of data processing is a multi-layered 1-D shear wave profile of the subsurface. If multiple Active ReMi data sets are acquired, 2-D or 3-D shear wave velocity images of the subsurface can be generated.

Usually, the interpreter establishes relationships between lithology (if control is available) and acoustic velocity and transforms the output 1-D shear velocity model into a geologic model of the subsurface. If geologic control is not available, the depth to bedrock (if imaged) can generally be estimated based on the visual assessment of the shear wave velocity profile.

If the ReMi data are acquired for site classification purposes, the average shear wave velocity to a depth of 100 feet is normally calculated.

2.4.4.2 Deliverable(s)

1-D, 2-D, or 3-D geologic and shear wave velocity models.

If the ReMi data are acquired for site classification purposes, the average shear wave velocity to a depth of 100 feet is normally calculated.

A multi-layered (typically 4) 1-D shear wave velocity profile will be generated at each test location. The output shear wave velocity profile is more-or-less a function of the average shear wave velocity of the subsurface along the entire length of the geophone array. However, by convention, the shear wave velocity profile is plotted at the center of the respective geophone array.

2.4.4.3 Depth Range (Top/Bottom)

Surface to depths on the order of multiple hundreds of feet. Greater depths of investigation can be achieved if very low frequency passive Rayleigh wave data are recorded.

2.4.4.4 Lateral Resolution

Rayleigh wave data are acquired along the entire breadth of the geophone array. If the velocity of the subsurface varies laterally beneath the array, lateral velocity smoothing will occur.

The output 1-D shear wave velocity profile is more-or-less a function of the average shear wave velocity of the subsurface beneath the geophone array. However, by convention, the output shear wave velocity profile is plotted at the center of the geophone array. Lateral resolution can often times be increased by decreasing the geophone spacing. However, this approach usually decreases the overall depth of investigation as well.

Zones of anomalously low or high velocity on the output multi-layered 1-D shear wave velocity profile should not be misinterpreted as indicative of the presence of a boulder or clay-filled void/karstic feature, respectively, immediately beneath the center of the geophone array.

2.4.4.5 Vertical Resolution

The output of processing is a multi-layered (typically 4) shear wave velocity profile of the subsurface. The thickness of each layer is a pre-set software function of the total depth to the top of the basal layer. The thickness of the layers increases with depth. Layer boundaries are set by the processing software and do not usually correspond precisely to lithologic boundaries.

Additionally, Rayleigh wave data are acquired along the entire length of the geophone array. The velocity assigned to a specific layer is a function of the average velocity of that layer along the entire length of the geophone array.

Significant features such as the top of rock can usually be estimated to within $\pm$10%.

2.4.4.6 Time Required to Interpret Field Data (One Test Site)

If ground truth is available and if velocity/lithologic relationships can be established, the interpretation of the shear wave velocity data is normally relatively rapid and straightforward.

2.4.4.7 Potential for Error

Human. There is little potential for error, if the interpreter understands that the output shear wave velocity profile generated at each test location represents the average shear wave along the length of the array. It does not represent the precise shear wave velocity of the subsurface at the mid-point of the geophone array.

Equipment. There is little potential for error.

2.4.4.8 Reproducibility of Deliverable

If ground truth is available, different experienced interpreters should come up with similar interpretations. If ground truth is not available, unreasonable interpretations are a very real possibility.

2.4.5 Deliverables

2.4.5.1 Brief Overview of Deliverable(s)

1-D (or 2-D or 3-D) geologic and shear wave velocity models.

2.4.5.2 Utility of Deliverable(s)

Geologic and velocity models provide information about variations in lithology, porosity, engineering properties, rippability of rock, diggability of soil, depth to top of rock, etc.

The shear wave velocity profiles can be used for earthquake site classification purposes.

2.4.5.3 Accuracy

The final interpretations are generally reliable if good quality Passive ReMi field data are recorded and if ground truth is available. Use of an experienced interpreter is essential.

2.4.6 Advantages

Advantages include:

- output is a shear wave velocity profile of the subsurface that typically extends to a depth of multiple hundreds of feet,
- depth to bedrock can usually be estimated to within ±10%,
- other lithologic units can often be identified and mapped on basis of shear wave velocity,
- relatively low cost,
- portability of equipment,
- relatively insensitive to background noise,
- typically employ a 1–3-person crew,
- relatively rapid processing of field data in lab (slightly more time consuming than Active MASW),
- few restrictions with respect to surface conditions (soil, rock, pavement, etc.),
- non-invasive,
- limited potential for human error if operators and processors are trained,
- reproducibility of field data,
- reproducibility of processing results,
- reproducibility of interpretations, particularly if geologic control is available,
- multiple applications (determination of lithology, porosity, rippability, depth to bedrock, location of voids, shear strength).
- permitting is not required,
- tool can be used across and in proximity to utilities and built structures as the method is relatively insensitive to background acoustic noise.

2.4.7 Disadvantages

Disadvantages include:

- desired maximum depths of investigation may not be realized if low frequency passive Rayleigh wave data are not recorded,
- site must be large enough to accommodate the geophone array and source,
- difficult to QC data in field,
- data are not usually processed in the field for QC purposes,
- reliability of output shear wave velocity data decreases as lateral and vertical heterogeneity of soil/rock increases,
- significant surface topography can make it difficult to acquire useful data,
- significant subsurface topography can make it difficult to acquire useful data,
- features such as faults, solution-widened joints and voids may make it difficult to acquire useful data,
- underground utilities can make it difficult to acquire useful data,
- vegetation can pose problems during data acquisition,
- geophones must be effectively coupled to the ground surface; acquiring quality data on very soft or loose soil can be difficult,
- in certain limited situations, proximal background noise may be overwhelming,
- layer boundaries on shear wave velocity profile do not correspond exactly to lithologic boundaries.

2.5 Conventional Shear Wave Refraction Seismic Method

2.5.1 Brief Overview of the Conventional Shear Wave Refraction Seismic Method

Conventional shear wave refraction seismic data are acquired using an array of geophones (acoustic receivers) placed at uniform intervals along the length of a traverse. Acoustic sources (typically a sledgehammer) are discharged at predetermined locations within and off the ends of the geophone array.

The travel time of the first shear wave energy (direct arrival or refracted arrival) to arrive at each geophone for each discharged source is recorded. This multiplicity of travel (arrival) time data is analyzed statistically and a layered 2-D shear wave velocity model of the subsurface with elevation control is output. The layers represent lithologic units with varying depths and thicknesses, and contrasting densities and/or shear wave velocities.

The output layered shear wave velocity model is usually transformed into a layered geologic model based on known or presumed velocity/lithology relationships. If the shallow subsurface cannot be accurately represented by a layered shear wave velocity model, the conventional refraction seismic method may produce unsatisfactory deliverables. In this case, the acquisition of shear wave refraction tomographic (Section 2.6 of this report) data may be the preferred option.

The shear wave refraction seismic technique is often a useful tool for mapping the top of rock and determining the average velocities of the shallow subsurface. Typically, if a sledgehammer source is employed, the subsurface is imaged to a maximum depth of about 30 feet.

Both conventional compressional wave and shear wave seismic refraction data can be acquired. Herein, we restrict our discussion to the acquisition of conventional shear wave refraction seismic data acquired along a single traverse with the primary objective of determining the shear wave velocity of the subsurface to a depth of 100 feet.

2.5.2 Data Acquisition

2.5.2.1 Brief Overview of Field Procedure

An array of geophones (usually 12, 24 or 48; connected to engineering seismograph) is placed at uniform intervals (typically 10 feet) along the length of a traverse. Acoustic (seismic) sources (typically a sledgehammer) are discharged at predetermined locations (generally nine or fewer, depending upon the number of geophones employed) within and off the ends of the geophone array (Figure 2.1).

The geophones record the arrival time and magnitude of the first shear wave energy to reach each geophone (either the direct arrival or a refracted arrival) and a limited time-window of earlier and later arriving acoustic energy. The arrival time of the first shear wave energy to reach each geophone after a source is discharged and the corresponding source-to-receiver

separation is the only information utilized by the processor of refraction seismic tomography data.

A typical shear wave seismic source consists of a 20-pound sledgehammer struck horizontally on a block that has been adequately coupled to the surface. The geophones are relatively low frequency (typically 14 Hz) and horizontally polarized. The geophones should be placed with an accuracy of at least 5%.

2.5.2.2 Field Equipment

Portable, and normally consisting of an impulsive shear wave energy source and strike block, a trigger switch cable, 12 to 48 horizontally polarized geophones, geophone cable, a 12 to 48-channel engineering seismograph, a 12-volt battery, and laptop computer.

2.5.2.3 Field Crew

Typically consists of 2-4 persons depending, in part, on the size of the array.

2.5.2.4 Considerations

Parameter entry. The correct acquisition parameters must be entered. A conventional shear wave refraction record is typically 1-2 seconds in duration. The sampling interval is usually 0.5 milliseconds. Geophone spacing employed is one estimate of maximum lateral resolution. Elevation control is required.

Size of test site. The size of test site must be large enough to allow for ease of placement of geophones and the safe use of the acoustic source. The length of the array of geophones must normally be about six times the maximum intended depth of investigation. Sources are discharged within and off both ends of the array at multiple predetermined locations.

Plotted location of the output 1-D shear wave velocity profile. The depth to each layer as determined for each geophone location from the statistical analyses of the entirety of the data set is plotted beneath that geophone. Each layer is assigned a shear wave velocity based on the statistical analyses of the entire seismic data set.

Vehicular access. All equipment can be transported by hand. Usually, the equipment and crew are transported in a single vehicle.

Surface topography. Data can be acquired across steeply dipping terrain. However, elevation changes should be minimized where/if possible. Elevation control must be acquired.

Subsurface topography. The output of processing is a layered velocity model of the subsurface with elevation control. Conventional refraction data are normally acquired with the objective of mapping subsurface structure.

Vegetation. Data can be acquired in heavily vegetated areas. However, dense vegetation does impede work and slows down field data acquisition. Usually, it is most efficient to clear the traverses ahead of time.

Background noise. Good quality shear wave refraction data are difficult to acquire in an acoustically noisy environment (e.g., adjacent to busy roadway). Data quality (signal-to-noise ratio) can be often improved by using a more powerful source or stacking (discharging a source multiple times at each location and summing recorded records).

It can be very difficult to acquire good quality data on windy and/or rainy days.

Anchoring requirements. The geophones need to be stable, correctly placed, and correctly oriented. Whenever possible, the geophones are connected to spikes that are inserted into the soil for maximum connectivity.

Nature of ground surface. The geophones can be placed on soil, rock, fill, concrete, asphalt, etc. However, they must be coupled, stable and vertical. Whenever possible, the geophones are connected to spikes that are inserted into the soil for maximum connectivity.

Placement of geophones and active source. Normally, a tape measure is laid out along the traverse and geophones are placed at their appropriate locations. If a few individual geophones are misplaced off by 5% or less, data quality should not be adversely affected, particularly if the geophones are shifted only perpendicular to the traverse.

If the location of the discharged source is out by 6 inches or less (assuming a 10-foot geophone spacing), data quality should not be adversely affected.

Subsurface lithology or material. Conventional shear wave refraction data can be acquired across all types of soil and/or rock. Data can also be acquired across pavement, asphalt, fill, etc.

Depth of investigation. The maximum depth of investigation is ideally about one sixth of the length of the geophone array. However, if a 20-pound sledgehammer source is employed, it is usually difficult to image refractive interfaces at depths greater than 30 feet. Higher magnitude acoustic sources will provide for greater depths of investigation. Longer arrays and longer source-to-receiver offsets should be used to image the subsurface at greater depths.

Proximity to buried structures and buried utilities. The seismic refraction method is non-invasive. Data can be acquired in proximity to buried utilities and buried structures, unless there is concern that the source could damage built structures such as concrete or pavement.

Proximity to surface structures and surface utilities. Seismic refraction data can be acquired in proximity to surface utilities and built structures. The only clearance required is sufficient room to discharge the source.

Sensitivity to background noise. Relative to the MASW and ReMi methods, the seismic refraction method is much more sensitive to background noise. Vehicle traffic, for example, can effectively mask the desired signal especially at longer source to geophone offsets.

Permitting requirements. Generally, only permission from the surface rights holder is required.

Notification requirements. Generally, only permission from the surface rights holder is required.

Other considerations. Horizontally polarized geophones are generally more expensive compared to vertically polarized geophones.

2.5.2.5 Brief Description of Field Data

The raw field data, consisting of common-shot records (typically less than 2 seconds in length), are recorded digitally and stored on the laptop connected to the seismograph or to built-in flash memory. Surface wave energy, reflected energy, refracted shear wave energy, compressional shear wave energy, and noise is present on the field records. However, the only information that is of interest to the processor is the arrival time of the first shear wave energy (either direct arrival or refraction) to reach each geophone each time the source is discharged. It can be difficult to identify the first shear wave arrivals, particularly at greater source to receiver separations.

2.5.2.6 Estimated Cost to Acquire Field Data at One Test Site

Basic field costs include: a) crew time plus travel time; b) equipment rental and/or depreciation; and c) vehicle rental and/or depreciation plus fuel. It typically takes a 3-person crew about 2-3 hours to acquire a single conventional refraction data set (24-geophone array). Elevation data are required.

2.5.2.7 Potential for Errors

There is little likelihood that field errors will lead to misinterpretation.

Human. If appropriate acquisition parameters (array length, array orientation, geophone spacing, source, source locations, recording parameters, etc.) are selected, human error, leading to misinterpretation, is unlikely because the only critical non-automated processes are the placement of the geophones and the discharge of the source. If the magnitude of the source is too small, if the geophones are not properly coupled to the ground, or if the site is too noisy, poor quality field data may be acquired.

Equipment. Equipment problems are unlikely to generate errors that will lead to misinterpretation.

2.5.2.8 Reproducibility of Field Tests

If good quality data can be recorded, field results can be reproduced with a high degree of consistency.

2.5.2.9 Quality Control

Shot gathers can be visually assessed in the field for quality control purposes. If the data are noisy, stacking or the use of a greater magnitude source can be options.

2.5.3 Data and/or Laboratory Processing

2.5.3.1 Brief Overview of Data Processing

The arrival time of the first shear wave energy as recorded by each geophone every time the acoustic source is discharged is determined based on the manual or automated analyses of the common-shot field records. This is referred to as "picking the first shear wave arrivals". Because the first shear wave arrivals are preceded by direct and refracted compressional waves, it can be very difficult to determine the arrival time of the first shear wave energy, particularly at greater source to receiver offsets. A skilled processor is required. The travel time data and the corresponding source/receiver separations are analyzed statistically in an automated manner by the processing software and a layered 2-D shear wave velocity model of the subsurface is generated.

2.5.3.2 Output of Data Processing

The output is a layered 2-D shear wave velocity model of the subsurface. A typical output 2-D velocity model generally consists of no more than 5 layers (a typical 2 layered model would consist of soil and bedrock). Each layer, except for the shallowest layer, is assigned a single velocity. Low-velocity layers and thin high-velocity are not imaged. This velocity model constitutes the output of data processing.

2.5.3.3 Estimated Cost to Process Field Data from One test Site

Basic processing costs include: a) processor's time; and b) hardware/software rental and/or depreciation. It typically takes an experienced interpreter about 4 hours to process a single conventional shear wave refraction seismic data set (24-geophone array).

2.5.3.4 Potential for Error

Human. The determination of accurate first shear wave arrival times requires interpreter input and can be a source of error. Errors are generally introduced when the field data are poor quality (low signal-to-noise ratio), and first shear wave arrival times cannot be determined with a high degree of precision.

Equipment. The processing software should not be defective. However, conventional seismic refraction software is not capable of imaging low-velocity layers and thin high-velocity layers. This can lead to significant misinterpretations. Also, the software analyzes the travel time data (statistically) and outputs a 2-D best-fit layered velocity model of the subsurface. If the subsurface cannot be reliably represented by a 2-D layered velocity model, the output velocity model may be unreasonable.

2.5.3.5 Reproducibility of Field Tests

If the field data are good quality, experienced processors will generate consistent 2-D layered velocity models. Output velocity models will vary slightly if different processing software is used.

2.5.4 Interpretation

2.5.4.1 Brief Overview of Interpretation of Processed Data

The output of data processing is a layered 2-D shear wave velocity model of the subsurface. Normally, the interpreter establishes relationships between lithology and acoustic velocity and transforms the output velocity model into a layered lithologic (geologic) model. This geologic model usually constitutes the final deliverable.

2.5.4.2 Deliverable(s)

2-D lithologic (geologic) model, normally with 5 or fewer layers, that typically extends to a depth of no more than 30 feet if a sledgehammer source is employed. A typical 2-layered geologic model might consist of a soil layer overlying bedrock.

2.5.4.3 Depth Range (Top/Bottom)

The maximum depth of investigation is ideally about one-sixth of the length of the geophone array or the depth to the deepest prominent (mappable) refractor, whichever is shallower.

2.5.4.4 Lateral Resolution

Effectively the same as the geophone spacing.

2.5.4.5 Vertical Resolution

Vertical resolution depends on the subsurface lithology. Generally, the only lithologic interfaces which can be imaged are those that separate units with significantly different acoustic properties (e.g., soil/bedrock, shale/limestone, etc.). Low-velocity layers and thin high-velocity layers cannot be imaged.

2.5.4.6 Time Required to Interpret Field Data (One Test Site)

If ground truth is available and if velocity/lithology relationships can be established, the interpretation of conventional shear wave seismic refraction data is normally relatively straightforward.

2.5.4.7 Potential for Error

Human. The interpreter must establish relationships between shear wave velocity and the geology. Ground truth significantly increases the reliability of the final interpretations.

Equipment. The software analyzes the input travel time data (statistically) and outputs a best-fit layered velocity model of the subsurface. If the subsurface cannot be reliably represented by a layered velocity model, the output velocity model may be unreasonable. In this case, the geologic model generated by the interpreter will also be unreasonable.

2.5.4.8 Reproducibility of Deliverable

If ground truth is available and if the earth can be reasonably well represented by a layered velocity model, different experienced interpreters should come up with similar geologic interpretations. If ground truth is not available, unreasonable geologic interpretations are a very real possibility.

2.5.5 Deliverables

2.5.5.1 Brief Overview of Deliverable(s)

2-D lithologic (geologic) model and velocity/depth models, normally with 5 or fewer layers, that typically extends to a depth of no more than 30 feet if a sledgehammer source is employed. A typical 2-layered geologic model might consist of a soil layer overlying bedrock.

2.5.5.2 Utility of Deliverable(s)

Geologic and velocity/depth models provide information about variations in lithology, porosity, the engineering properties of soil and rock, rippability of rock, diggability of soil, depth to top of rock, etc.

2.5.5.3 Accuracy

The final interpretations (geologic models) are generally reliable if good quality field data are recorded, if ground truth is available and if the shallow subsurface can be reasonably well-represented by a layered velocity model. Use of an experienced interpreter is essential.

2.5.6 Advantages

Advantages include:

- output is a layered shear wave velocity profile of the subsurface,
- 2-D geologic model can be generated if ground truth is available,
- variations in the depth to the different layers is depicted,
- depth to bedrock can usually be estimated to within ±10%,
- other imaged lithologic units can often be identified and mapped on basis of shear wave velocity,
- relatively low cost compared to seismic refraction tomography (Table 3.2) or seismic reflection methods (Table 3.2),
- portability of equipment,
- typically employ a 2 to 3-person crew,
- field records can be visually assessed in the field for QC purposes,
- few restrictions with respect to surface conditions (soil, rock, pavement, etc.),
- non-invasive,
- data can be assessed in the field for quality control purposes,
- limited potential for human error if operators and processors are trained,
- reproducibility of field data if good quality,
- reproducibility of processing results if data are good quality,
- reproducibility of interpretations, if data are good quality and geologic control is available,
- multiple applications (determination of lithology, porosity, rippability, depth to bedrock, location of voids, shear strength),
- permitting is not required.

2.5.7 Disadvantages

Disadvantages include:

- each layer (except for the first layer) is assigned a single velocity,
- relatively sensitive to noise,
- elevation control is required,
- maximum depths of investigation are on the order of 30 feet if a sledgehammer source is employed,
- site must be large enough to accommodate the geophone array and source,
- data cannot be processed in the field for quality control purposes,
- reliability of output shear wave velocity data decreases as lateral and vertical heterogeneity of soil/rock increases,
- relatively high cost compared to MASW and ReMi methods,
- vegetation can pose problems during data acquisition,

- geophones and source must be effectively coupled to the ground surface; acquiring quality data on very soft or loose soil can be difficult.

2.6. Shear Wave Refraction Seismic Tomography

2.6.1 Brief Overview of the Shear Wave Refraction Seismic Tomography Method

Shear wave refraction tomography seismic data are acquired using an array of geophones placed at uniform intervals along the length of a traverse. Shear wave acoustic sources are discharged between each pair of geophones and at multiple predetermined locations off the ends of the geophone array.

The travel time of the first shear wave energy (direct arrival or refracted arrival) to arrive at each geophone for each discharged source is recorded. During processing, the subsurface beneath the geophone array is divided into pixels. The lateral separation between each pixel is equal to geophone spacing. The multiplicity of travel (arrival) time data is then statistically analyzed, and each pixel is assigned a shear wave velocity. The output is a 2-D tomographic velocity model of the subsurface with elevation control.

There are 2 main differences between a conventional refraction (Section 2.5 of this report) model and a refraction tomography model. First, in a tomography model, the acoustic velocity within the model varies both laterally and vertically. Second, in a tomographic model, low velocity zones and thin high-velocity zones can be imaged.

The output shear velocity model is generally transformed into a geologic model based on known or presumed velocity/lithology relationships.

This technique is usually a useful tool for mapping the top of rock. Lateral and vertical lithologic changes within soil and rock can also be mapped if characterized by interpretable velocity variations.

Both compressional wave and shear wave seismic refraction tomography data can be acquired. Herein, we restrict our discussion to the acquisition of shear wave refraction tomography seismic data acquired along a single traverse with the primary objective of determining the shear wave velocity of the subsurface to a depth of 100 feet.

2.6.2 Data Acquisition

2.6.2.1 Brief Overview of Field Procedure

An array of geophones (usually 12, 24 or 48; connected to engineering seismograph) is placed at predetermined uniform intervals along the length of a traverse. Acoustic (seismic) sources are discharged between each pair of geophones and at multiple predetermined locations off the ends of the geophone array. The geophones record the arrival time and magnitude of the first shear wave energy to reach each geophone (either the direct arrival or a refracted arrival) and a limited time-window of earlier and later arriving acoustic energy. The arrival time of the first shear wave energy to reach each geophone after a source is discharged and the

corresponding source-to-receiver separation is the only information utilized by the processor of shear wave refraction seismic tomography data.

A typical shear wave seismic source consists of a 20-pound sledgehammer struck horizontally on a block that has been adequately coupled to the surface. The geophones are relatively low frequency (typically 14 Hz) and horizontally polarized. The geophones should be placed with an accuracy of at least 5%.

2.6.2.2 Field Equipment

Portable, and normally consisting of an impulsive shear wave acoustic source and strike block, a trigger switch cable, 12 to 48 horizontally polarized geophones, geophone cable, a 12 to 48-channel engineering seismograph, a 12-V battery, and laptop computer.

2.6.2.3 Field Crew

Typically consists of 3-4 persons depending, in part, on the size of the array.

2.6.2.4 Considerations

Parameter entry. The correct acquisition parameters must be entered. A conventional shear wave refraction record is typically 1-2 seconds in duration. The sampling interval is usually 0.5 milliseconds. Geophone spacing employed is one estimate of maximum lateral resolution. Elevation control is required.

Size of test site. The size of test site must be large enough to allow for ease of placement of geophones and the safe use of the acoustic source. The array of geophones must normally be about 3 times the maximum desired depth of investigation. Sources are discharged within and off the ends of the array at multiple predetermined locations.

Plotted location of the output 1-D shear wave velocity profile. Each pixel in the output model is assigned a shear wave velocity. The shear wave velocities plotted as a function of depth immediately beneath each geophone are assumed to represent the velocity of the subsurface immediately beneath that geophone.

Vehicular access. All equipment can be transported by hand. Usually, the equipment and crew are transported in a single vehicle.

Surface topography. Data can be acquired across steeply dipping terrain. However, elevation changes should be minimized where/if possible.

Subsurface topography. The output of processing is a shear wave velocity model of the subsurface with elevation control. Refraction tomography data are normally acquired with the objective of mapping subsurface structure.

Vegetation. Data can be acquired in heavily vegetated areas. However, dense vegetation does impede work and slows down field data acquisition. Usually, it is most efficient to clear the traverses ahead of time.

Background noise. Good quality shear wave refraction tomography data are difficult to acquire in an acoustically noisy environment (e.g., adjacent to busy roadway). Data quality (signal-to-noise ratio) can be often improved by using a more powerful source or stacking (discharging a source multiple times at each location and summing recorded records).

It can be very difficult to acquire good quality data on windy and/or rainy days.

Anchoring requirements. The geophones need to be stable, correctly placed, and correctly oriented. Whenever possible, the geophones are connected to spikes that are inserted into the soil for maximum connectivity.

Nature of ground surface. The geophones can be placed on soil, rock, fill, concrete, asphalt, etc. However, they must be coupled, stable and vertical. Whenever possible, the geophones are connected to spikes that are inserted into the soil for maximum connectivity.

Placement of geophones and active source. Normally, a tape measure is laid out along the traverse and geophones are placed at their appropriate locations. If a few individual geophones are misplaced off by 5% or less, data quality should not be adversely affected, particularly if the geophones are shifted perpendicular to the traverse.

If the location of the discharged source is out by 6 inches or less (assuming a 10-foot geophone spacing), data quality should not be adversely affected.

Subsurface lithology or material. Refraction seismic tomography data can be acquired across all types of soil and/or rock as well as across pavement, asphalt, fill, etc.

Depth of investigation. The maximum depth of the investigation is highly variable and depends on subsurface conditions. Often, the depth of investigation is comparable to one-half the length of the geophone array. A 20-pound sledgehammer source is often sufficient for mapping subsurface velocities at depths on the order of 60 feet. Higher magnitude acoustic sources will provide for greater depths of investigation. Longer arrays and longer source-to-receiver offsets should be used to image the subsurface to greater depths.

Proximity to buried structures and buried utilities. The refraction seismic tomography method is non-invasive. Data can be acquired in proximity to buried utilities and buried structures, unless there is concern that the source could damage built structures such as concrete or pavement.

Proximity to surface structures and surface utilities. Seismic refraction data can be acquired in proximity to surface utilities and built structures. The only clearance required is sufficient room to discharge the source.

Sensitivity to background noise. Relative to the MASW and ReMi methods, the seismic refraction tomography method is much more sensitive to background noise. Vehicle traffic, for example, can effectively mask the desired signal especially at longer source to geophone offsets.

Permitting requirements. Generally, only permission from the surface rights holder is required.

Notification requirements. Generally, only permission from the surface rights holder is required.

Other considerations. Wind conditions can degrade seismic data quality by introducing ambient surface noise, leading to a lower signal-to-noise ratio. Horizontally polarized geophones are generally more expensive compared to vertically polarized geophones.

2.6.2.5 Brief Description of Field Data

The field data, consisting of common-shot records (typically less than 1 second in length), are recorded digitally, and stored on the laptop connected to the seismograph or to built-in flash memory. Surface wave energy, reflected energy, refracted shear wave energy, compressional shear wave energy, and noise is present on the field records. However, the only information that is of interest to the processor is the arrival time of the first shear wave energy (either direct arrival or refraction) to reach each geophone each time the source is discharged. It can be difficult to identify the first shear wave arrivals, particularly at greater source to receiver separations.

2.6.2.6 Estimated Cost to Acquire Field Data at One Test Site

Basic field costs include: a) crew time plus travel time; b) equipment rental and/or depreciation; and c) vehicle rental and/or depreciation plus fuel. It typically takes a 3-person crew 4-5 hours to acquire a single conventional refraction data set (24-geophone array). Elevation data are required.

2.6.2.7 Potential for Errors

There is little likelihood that field errors will lead to misinterpretation.

Human. If appropriate acquisition parameters (array length, array orientation, geophone spacing, source, source locations, recording parameters, etc.) are selected, human error, leading to misinterpretation, is unlikely because the only critical non-automated processes are the placement of the geophones and the discharge of the source. If the incorrect geophone separation is inadvertently entered as a processing parameter, significant errors can result. If the magnitude of the source is too small, if the geophones are not properly coupled to the ground, or if the site is too noisy, poor quality field data may be acquired.

Equipment. Equipment problems are unlikely to generate errors that will lead to misinterpretation.

2.6.2.8 Reproducibility of Field Tests

If good quality data can be recorded, field results can be reproduced with a high degree of consistency.

2.6.2.9 Quality Control

Shot gathers can be visually assessed in the field for quality control purposes. If the data are noisy, stacking or the use of a higher magnitude source could be considered.

2.6.3 Data and/or Laboratory Processing

2.6.3.1 Brief Overview of Data Processing

The arrival time of the first shear wave energy as recorded by each geophone every time the acoustic source is discharged is determined based on the manual or automated analyses of the common-shot field records. This is referred to as "picking the first shear wave arrivals". Because the first shear wave arrivals are preceded by direct and refracted compressional waves, it can be very difficult to determine the arrival time of the first shear wave energy, particularly at greater source to receiver offsets. A knowledgeable processor is required.

During processing, the subsurface beneath the geophone array is divided into pixels that extend into the subsurface to the maximum depth imaged by the acquired data. The lateral and vertical separation between each pixel is equal to geophone spacing. The multiplicity of travel (arrival) time data is then statistically analyzed, and each pixel is assigned a shear wave velocity. The output is a 2-D tomographic velocity model of the subsurface with elevation control.

2.6.3.2 Output of Data Processing

The output is a 2-D seismic cross-section of velocity distribution within the subsurface. Unlike the conventional refraction seismic method, a tomographic velocity profile incorporates both lateral velocity and vertical variations over distances on the order of the geophone spacing. Velocity inversions and thin high velocity layers can also be mapped. This shear wave velocity model constitutes the output of data processing.

2.6.3.3 Estimated Cost to Process Field Data from One Test Site

Basic processing costs include: a) processor's time; and b) hardware/software rental and/or depreciation. It typically takes an experienced interpreter about 6-8 hours to process a single shear wave refraction tomography seismic set (24-geophone array).

2.6.3.4 Potential for Error

Human. The determination of accurate first shear wave arrival times requires interpreter input and can be a source of error. Errors are generally introduced when the field data are poor

quality (low signal-to-noise ratio), and first shear wave arrival times cannot be determined with a high degree of precision.

Equipment. The processing software should not be defective. The software analyzes the travel time data (statistically) and outputs a 2-D best-fit shear wave velocity model of the subsurface. If the subsurface cannot be reliably represented by a 2-D velocity model, the output velocity model may be unreasonable.

2.6.3.5 Reproducibility of Field Tests

If the field data are good quality, experienced processors will generate consistent 2-D tomographic shear wave velocity models. Output tomographic velocity models will vary slightly if different processing software is used.

2.6.4 Interpretation

2.6.4.1 Brief Overview of Interpretation of Processed Data

The output of data processing is a high-resolution (compared to the output of the conventional refraction seismic method) tomographic shear wave velocity model of the subsurface. Normally, the interpreter establishes relationships between lithology and acoustic velocity and transforms the output velocity model into a lithologic (geologic) model. Lateral and vertical lithologic changes within soil and bedrock can be mapped if characterized by interpretable velocity variations. This geologic model usually constitutes the final deliverable.

2.6.4.2 Deliverable(s)

High-resolution 2-D lithologic (geologic) model. A typical geologic model might consist of soil overlying bedrock. Lateral and vertical lithologic changes and changes in acoustic properties within soil and rock can be mapped if characterized by interpretable velocity variations.

2.6.4.3 Depth Range (Top/Bottom)

The maximum depth of investigation is highly variable and depends on subsurface conditions. Often, the depth of investigation is comparable to the one-half the length of the geophone array. A 20-pound sledgehammer source is often sufficient for mapping subsurface velocities at depths on the order of 60 feet. Higher magnitude acoustic sources will provide for greater depths of investigation. Longer arrays and longer source-to-receiver offsets should be used to image the subsurface to greater depths.

2.6.4.4 Lateral Resolution

Unlike, the conventional refraction seismic method, the tomographic velocity profile can incorporate velocity inversions and both lateral velocity and vertical variations over distances on the order of the geophone spacing.

2.6.4.5 Vertical Resolution

Unlike the conventional refraction seismic method, the tomographic velocity profile can incorporate both lateral velocity and vertical variations over distances on the order of the geophone spacing and velocity inversions. Resolution diminishes with depth.

2.6.4.6 Time Required to Interpret Field Data (One Test Site)

If ground truth is available and if velocity/lithology relationships can be established, the interpretation of shear wave refraction tomography data is normally relatively rapid and straightforward.

2.6.4.7 Potential for Error

Human. The interpreter must establish relationships between shear wave velocity and the geology. Ground truth significantly increases the reliability of the final interpretations.

Equipment. The software analyzes the input travel time data (statistically) and outputs a best-fit velocity model of the subsurface. If the input travel time data is unreliable, the geologic model generated by the interpreter will also be unreasonable.

2.6.4.8 Reproducibility of Deliverable

If ground truth is available, different experienced interpreters may come up with slightly different interpretations. If ground truth is not available, unreasonable interpretations are a very real possibility.

2.6.5 Deliverables

2.6.5.1 Brief Overview of Deliverable(s)

High-resolution (relative to the conventional seismic refraction method) 2-D velocity and geologic models.

2.6.5.2 Utility of Deliverable(s)

Geologic and velocity models provide information about lateral and vertical variations in lithology and porosity, the engineering properties of soil and rock, rippability of rock, diggability of soil, depth to top of rock, etc.

2.6.5.3 Accuracy

The final interpretations are generally reliable if good quality field data are recorded, if ground truth is available. Use of an experienced processor and interpreter is essential.

2.6.6 Advantages

Advantages include:

- output is a 2-D shear wave velocity model of the subsurface,
- Lateral and vertical variations in shear wave velocity are depicted,
- 2-D geologic model can be generated if ground truth is available,
- depth to bedrock can usually be estimated to within ±10%,
- relatively low cost compared to seismic reflection method,
- portability of equipment,
- typically employ a 2–3-person crew,
- field records can be visually assessed in the field for QC purposes,
- few restrictions with respect to surface conditions (soil, rock, pavement, etc.),
- non-invasive,
- data can be assessed in the field for quality control purposes,
- limited potential for human error if operators and processors are trained,
- reproducibility of field data if data are good quality,
- reproducibility of processing results if data are good quality,
- reproducibility of interpretations, if data are good quality and geologic control is available,
- multiple applications (determination of lithology, porosity, rippability, depth to bedrock, location of voids, shear strength),
- permitting is not required.

2.6.7 Disadvantages

Disadvantages include:

- relatively sensitive to noise,
- elevation control is required,
- maximum depths of investigation are typically on the order of 60 feet if a sledgehammer source is employed,
- relatively high cost compared to MASW, ReMi and conventional seismic refraction methods,
- site must be large enough to accommodate the geophone array and source,
- data cannot be processed in the field for quality control purposes,
- reliability of output shear wave velocity data decreases as lateral and vertical heterogeneity of soil/rock increases,
- vegetation can pose problems during data acquisition,

- geophones and source must be effectively coupled to the ground surface; acquiring quality data on very soft or loose soil can be difficult.

2.7. Microseismic Horizontal to Vertical Spectral Ratio (HVSR) Method

2.7.1 Brief Overview of the HVSR Method

The single-station microtremor horizontal-to-vertical spectral ratio (HVSR) method involves recording seismic ambient noise with a single very low frequency three-component seismometer and calculating the ratio of the horizontal-to-vertical Fourier amplitude spectra (HVSR).

Empirical evidence from sites with measured V_S profiles down to bedrock has shown that the lowest frequency HVSR peak occurs at the fundamental mode horizontal shear wave resonance frequency of the soil layer if there is a sufficiently strong impedance contrast at the soil/bedrock interface.

Note: An interpretable fundamental mode horizontal shear wave resonance frequency (f_{0HV}) will be output only if there is a significant contrast between the acoustic properties of the soil and underlying rock. The HVSR tool is not capable of imaging the subsurface beneath the top of intact rock.

If the fundamental mode horizontal shear wave resonance frequency (f_{0HV}) of the soil layer can be reliably measured, the depth to bedrock can be calculated only if the average shear wave velocity of the soil layer is known. The determination of f_{0HV} at a particular location, or the mapping of its spatial variability around a site or area (regional microzonation), and its conversion to sediment thickness have always been and still are the predominant uses of the HVSR method.

Conversely, if the fundamental mode horizontal shear wave resonance frequency (f_0) of the soil layer can be reliably measured, the average shear wave velocity of the soil layer can be calculated only if the depth to bedrock is known.

It is important to note that the interpretation of the HVSR curve is complicated by a lack of understanding regarding the precise composition of the microtremor wavefield. Whether the wavefield composition is primarily body waves, surface waves, and/or highly scattered (diffuse) combinations thereof (total wavefield) is still largely debated. Studies of microtremors have shown that the analytical expression exists for all real-world conditions contribution of different wave types varies with frequency, from site to site, and that Love waves are often a dominant part of the surface wave component of the microtremor wavefield. Therefore, no single theoretical model comprehensively explains all observed HVSR behaviors across varying environments. This variability underscores the importance of site-specific calibration, supplementary geotechnical or geophysical data (e.g., borehole logs or other shear wave surveys), and careful consideration during both processing and interpretation stages to avoid misrepresenting subsurface characteristics.

2.7.2 Acquisition of Active HVSR Data

2.7.2.1 Brief Overview of Field Procedure

HVSR data are recorded by a single operator using a single tri-axial seismometer. Microtremor (ambient noise) data are normally recorded for tens of minutes to hours.

Poor choices (mostly site conditions) made by the practitioner during data acquisition have the potential to impact the HVSR by introducing artificial resonance frequencies (HVSR peaks) and altering the HVSR amplitude. The natural site-related resonance frequencies are relatively robust and likely to be obtained even if the data acquisition is not ideal. This latter point combined with the minimal required equipment is the appeal of the HVSR method. The greatest difficulty is at the interpretation stage; the practitioner should therefore seek to minimize errors during the data acquisition and analysis stages.

2.7.2.2 Field Equipment

The most suitable recording instrument is a three-component seismometer (velocimeter) with a noise floor lower than the seismic noise level over the frequency band of interest (i.e., 0.1–25 Hz).

2.7.2.3 Field Crew

Typically consists of 1 person.

2.7.2.4 Considerations

Parameter entry. An HVSR field record is typically tens of minutes to hours in duration. Window length is inversely proportional to minimum frequency. Longer time windows should be used for sites with expected low fundamental frequencies (i.e., long fundamental periods; $T_0 = 1/f_0$).

Size of test site. The test site must be large enough to allow for ease of placement of the triaxial geophone.

Plotted location of the output resonance frequency. The output resonance frequency is assumed to be indicative of the fundamental mode horizontal shear wave resonance frequency (f_{0HV}) of the subsurface immediately beneath the triaxial geophone. This is the case only if there is a sufficiently strong impedance contrast at the soil/bedrock interface.

Vehicular access. All equipment can be hand-carried. The equipment and crew can be transported in a single vehicle.

Surface topography. Human-constructed surfaces or pavements should be removed prior to sensor-ground coupling. However, in urbanized settings, this is almost never possible, and most recordings will be collected on human constructed pavements, e.g., asphalt, concrete, and stone.

Subsurface topography. An interpretable resonance frequency will be output only if there is a significant contrast between the acoustic properties of the soil and underlying rock.

Recording over subsurface cavities will alter the HVSR curve. Cavities that are shallow and wide violate the free-field requirement.

Avoid recording on stiffer substrate than the underlying ground. Can cause velocity inversion.

Vegetation. Avoid recording near trees. Vegetation should be removed. The sensor base should be inserted firmly into the ground surface.

Background noise. The sensor base should be inserted firmly into the ground surface with protection from other natural phenomena including temperature fluctuation and wind or rain vibrations. Measurements should be avoided during wind and heavy rain. A cover can help shade and keep the seismometer cool but can also lead to transmitting wind or rain droplet vibration into the ground due to its surface area. Waiting for a less windy day or use of an umbrella with fewer contact points is often better solutions towards mitigating recording wind and rain vibration. Avoid recording near operating equipment.

Anchoring requirements. The sensor base should be inserted firmly into the ground surface with protection from other natural phenomena including temperature fluctuation and wind or rain vibrations.

Nature of ground surface. The sensor base should be inserted firmly into the ground surface with protection from other natural phenomena including temperature fluctuation and wind or rain vibrations.

Human-constructed surfaces or pavements should be removed prior to sensor-ground coupling. However, in urbanized settings, this is almost never possible, and most recordings will be collected on human constructed pavements, e.g., asphalt, concrete, and stone.

Placement of geophone. The sensor base should be inserted firmly into the ground surface with protection from other natural phenomena including temperature fluctuation and wind or rain vibrations.

Subsurface lithology or material. An interpretable fundamental mode horizontal shear wave resonance frequency (f_{0HV}) will be output only if there is a significant contrast between the acoustic properties of the soil and underlying rock.

Depth of investigation. The HVSR tool is not capable of imaging the subsurface beneath the top of intact rock.

If the fundamental mode horizontal shear wave resonance frequency (f_{0HV}) of the soil layer can be reliably measured, the depth to bedrock can be calculated only if the average shear wave velocity of the soil layer is known.

Conversely, if the fundamental mode horizontal shear wave resonance frequency (*f0*) of the soil layer can be reliably measured, the average shear wave velocity of the soil layer can be calculated only if the depth to bedrock is known.

Proximity to buried structures and buried utilities. The active HVSR tool is non-invasive. Active data can be acquired in proximity to buried utilities and buried structures, unless there is concern that the acoustic source could damage built structures such as concrete or pavement. Issues with data quality can arise if the buried utilities or buried structures are beneath the geophone array or between the source and the array. Rayleigh waves that are reflected from subsurface features can complicate data processing.

Recording over buried human-constructed materials (e.g., electrical power lines or vents) will alter the HVSR curve. Data should not be acquired across such features if possible.

Proximity to surface structures and surface utilities. When acquiring data in proximity to urban infrastructure, a general criterion is to offset the recording location by a distance equivalent to the height of the structure. If this criterion must be violated, caution should be exercised when interpreting the results, as the resonance frequency of the structure may show up in the HVSR recording, notably when recording on the foundation of any built structure and near tall structures or long bridges.

Sensitivity to background noise. Measurements should be avoided during wind and heavy rain. A cover can help shade and keep the seismometer cool but can also lead to transmitting wind or rain droplet vibration into the ground due to its surface area. Waiting for a less windy day or use of an umbrella with fewer contact points is often better solutions towards mitigating recording wind and rain vibrations.

Permitting requirements. Generally, only permission from the surface rights holder is required.

Notification requirements. Generally, only permission from the surface rights holder is required.

Other considerations. An interpretable fundamental mode horizontal shear wave resonance frequency (f_{0HV}) will be output only if there is a significant contrast between the acoustic properties of the soil and underlying rock. The HVSR tool is not capable of imaging the subsurface beneath the top of intact rock.

2.7.2.5 Brief Description of Field Data

The field data are recorded digitally and stored on the laptop connected to the seismograph or to built-in flash memory. An HVSR field record is typically tens of minutes to hours in duration.

2.7.2.6 Estimated Cost to Acquire Field Data at One Test Site

Basic field costs include a) up to 3 hours of crew time plus travel time, b) equipment rental and/or depreciation, and c) vehicle rental and/or depreciation plus fuel. It typically takes a 1-person crew up to 3 hours to acquire HVSR data set at a single site.

2.7.2.7 Potential for Errors

Poor choices (mostly site conditions) made by the practitioner during data acquisition have the potential to impact the HVSR by introducing artificial resonance frequencies (HVSR peaks) and altering the HVSR amplitude. The natural site-related resonance frequencies are relatively robust and likely to be obtained even if the data acquisition is not ideal. This latter point combined with the minimal required equipment is the appeal of the HVSR method.

Human. Poor choices (mostly site conditions) made by the practitioner during data acquisition have the potential to impact the HVSR by introducing artificial resonance frequencies (HVSR peaks) and altering the HVSR amplitude.

Equipment. Equipment problems are unlikely to generate errors that will lead to misinterpretation.

2.7.2.8 Reproducibility of Field Tests

If good quality HVSR field data can be recorded, field results can be reproduced with a relatively high degree of consistency.

2.7.2.9 Quality Control

Field records cannot be visually assessed in the field for quality control purposes.

2.7.3 Data and/or Laboratory Processing

2.7.3.1 Brief Overview of Data Processing

The stability and reliability of the calculated HVSR depend on the processing and interpretation steps as much as on the equipment (acquisition system) and the quality of the in-situ acquisition. The general processing steps involved in computing an HVSR are first outlined below. Then important parameters that are highlighted in the general processing using bold, italicized, and underlined text are discussed in further detail.

The entire microtremor three-component time series is split into several time windows of equal or varying length. Fourier spectra are computed for each individual tapered time window and smoothed. Each time window should be at least 10 times longer than the estimated fundamental site period, as advised by the SESAME (Site EffectS assessment using AMbient Excitations; 2004) HVSR guidelines.

After smoothing, the ratio between horizontal and vertical spectra is calculated. Similar individual HVSRs confirm underlying soil homogeneity, while variable HVSRs between individual components may indicate spatially complex, spatially variable subsurface conditions. The azimuth dependence of HVSRs should be checked to find indications of two-dimensional (2-D) and three-dimensional (3-D) site effects including sedimentary basins and surface topography.

With additional processing, HVSR measurements have the potential to provide information on lateral variation of the subsurface, as well as 3-D variations. The average horizontal spectrum is valid for use once no azimuthal dependence of the HVSR is confirmed, i.e., assumptions of 1-D site effects can be reasonably accepted.

The final average HVSR for a testing location was historically calculated as the average of all HVSRs from the spectra of the combined horizontal components of each time window but is increasingly determined from the averaged spectra from all time windows of each component. Averaging of HVSRs from all selected time windows reduces variability in the mean HVSR curve, whereas averaging of each component spectra with time is more appropriate given the diffuse wavefield assumption.

The chosen window length involves a trade-off between spectral resolution and statistically meaningful results. As mentioned, each time window should be at least 10 times longer than the estimated fundamental site period. A stable HVSR will result with 20-time windows or more with 15–20 windows required to achieve Gaussian statistics. Sites with lower fundamental frequencies (longer fundamental periods) may require a total recording length up to an hour or more to ensure enough time windows are available for reliable processing.

The HVSR is the spectral ratio of horizontal-to-vertical component ground motions. While the vertical component is unambiguously defined, a single “horizontal” component must be defined from the two measured orthogonal components of horizontal motion.

HVSR calculations performed across all azimuths is the most robust way to determine the site’s representative horizontal spectrum. We note that most of the available software may automatically skip confirming azimuthal variability in the HVSR, displaying only the horizontal average HVSR but have the option of computing azimuthal HVSR curves.

The average HVSR curve is calculated for the recording site by averaging with time and the two horizontal components (i.e., source azimuth). It was noted that averaging of HVSRs from all selected time windows reduces variability in the mean HVSR curve compared to averaging of each component’s spectra with time and that the latter is considered more appropriate for use if the assumption is a diffuse wavefield.

2.7.3.2 Output of Data Processing

The fundamental mode horizontal shear wave resonance frequency (f_{0HV}) of the soil layer can be reliably measured, the depth to bedrock can be calculated only if the average shear wave velocity of the soil layer is known. The determination of f_{0HV} at a particular location, or the

mapping of its spatial variability around a site or area (regional microzonation), and its conversion to sediment thickness have always been and still are the predominant uses of the HVSR method.

Conversely, if the fundamental mode horizontal shear wave resonance frequency (*f0*) of the soil layer can be reliably measured, the average shear wave velocity of the soil layer can be calculated only if the depth to bedrock is known.

2.7.3.3 Estimated Cost to Process Field Data from One Test Site

Basic processing costs include about 4 hours of processor's time and hardware/software rental and/or depreciation.

2.7.3.4 Potential for Error

Human. Steps 2 and 4 (the transformation of the muted HVSR field data into an overtone data and the inversion of the "picked" dispersion curve) do not require interpreter input. Step 1 (muting and parameter entry) and step 3 (the "picking" of the optimal dispersion curve) are subjective although usually straightforward.

In certain instances, it is difficult to "pick" an optimum dispersion curve. Problems can arise for one of a number of reasons: suitable fundamental mode Rayleigh wave energy may not have been recorded; the acoustic source may have been too small; the geophone array may have been too long or too short; lateral velocity variations along the length of the geophone array may have resulted in "smoothing" or "smearing" of phase velocity data on the overtone record; excessive topographic relief may have caused "smoothing" or "smearing"; geologic conditions (faulting for example) may have been such that surface wave energy of the desired frequency could not be recorded in the study area.

It is possible for a processor to misidentify higher mode Rayleigh wave energy as fundamental mode Rayleigh wave energy. In such situations, the output shear wave velocities will be anomalously high.

If the processor arbitrarily extends the dispersion curve (via extrapolation and with the objective of extending the shear wave velocity profile to greater depths) beyond the lowest confidently "pickable" frequency on the overtone record serious errors can arise.

Equipment. The HVSR processing software should not be defective.

2.7.3.5 Reproducibility of Field Tests

If the HVSR field data are good quality, trained processors will generate consistent If the fundamental mode horizontal shear wave resonance frequency (f_{0HV}) of the soil layer.

2.7.4 Interpretation

2.7.4.1 Brief Overview of Interpretation of Processed Data

If the fundamental mode horizontal shear wave resonance frequency (f_{0HV}) of the soil layer can be reliably measured, the depth to bedrock can be calculated only if the average shear wave velocity of the soil layer is known. The determination of f_{0HV} at a particular location, or the mapping of its spatial variability around a site or area (regional microzonation), and its conversion to sediment thickness have always been and still are the predominant uses of the HVSR method.

Conversely, if the fundamental mode horizontal shear wave resonance frequency (*f0*) of the soil layer can be reliably measured, the average shear wave velocity of the soil layer can be calculated only if the depth to bedrock is known.

2.7.4.2 Deliverable(s)

If the fundamental mode horizontal shear wave resonance frequency (f_{0HV}) of the soil layer can be reliably measured, the depth to bedrock can be calculated only if the average shear wave velocity of the soil layer is known. The determination of f_{0HV} at a particular location, or the mapping of its spatial variability around a site or area (regional microzonation), and its conversion to sediment thickness have always been and still are the predominant uses of the HVSR method.

Conversely, if the fundamental mode horizontal shear wave resonance frequency (*f0*) of the soil layer can be reliably measured, the average shear wave velocity of the soil layer can be calculated only if the depth to bedrock is known.

2.7.4.3 Depth Range (Top/Bottom)

An interpretable fundamental mode horizontal shear wave resonance frequency (f_{0HV}) will be output only if there is a significant contrast between the acoustic properties of the soil and underlying rock. The HVSR tool is not capable of imaging the subsurface beneath the top of intact rock.

2.7.4.4 Lateral Resolution

If the fundamental mode horizontal shear wave resonance frequency (f_{0HV}) of the soil layer at a specific location can be reliably measured, the depth to bedrock at that location can be calculated if the average shear wave velocity of the soil layer is known. The determination of f_{0HV} at a particular location, or the mapping of its spatial variability around a site or area (regional microzonation), and its conversion to sediment thickness have always been and still are the predominant uses of the HVSR method.

Conversely, if the fundamental mode horizontal shear wave resonance frequency (*f0*) of the soil layer at a specific location can be reliably measured, the average shear wave velocity of the soil layer can be calculated if the depth to bedrock at that location is known.

2.7.4.5 Vertical Resolution

If the fundamental mode horizontal shear wave resonance frequency (f0HV) of the soil layer at a specific location can be reliably measured, the depth to bedrock at that location can be calculated if the average shear wave velocity of the soil layer is known. The determination of f0HV at a particular location, or the mapping of its spatial variability around a site or area (regional microzonation), and its conversion to sediment thickness have always been and still are the predominant uses of the HVSR method.

Conversely, if the fundamental mode horizontal shear wave resonance frequency (f0) of the soil layer at a specific location can be reliably measured, the average shear wave velocity of the soil layer can be calculated if the depth to bedrock at that location is known.

The HVSR tool is not capable of imaging the subsurface beneath the top of intact rock.

2.7.4.6 Time Required to Interpret Field Data (One Test Site)

If the fundamental mode horizontal shear wave resonance frequency (f_{0HV}) of the soil layer at a specific location can be reliably measured, the depth to bedrock at that location can be calculated if the average shear wave velocity of the soil layer is known. The determination of f_{0HV} at a particular location, or the mapping of its spatial variability around a site or area (regional microzonation), and its conversion to sediment thickness have always been and still are the predominant uses of the HVSR method.

Conversely, if the fundamental mode horizontal shear wave resonance frequency (*f0*) of the soil layer at a specific location can be reliably measured, the average shear wave velocity of the soil layer can be calculated if the depth to bedrock at that location is known.

The HVSR tool is not capable of imaging the subsurface beneath the top of intact rock.

2.7.4.7 Potential for Error

Human. If the HVSR data have been properly acquired and processed, there is little potential for error if either the average shear wave velocity of the soil or the depth to top of intact rock are known.

Equipment. There is little potential for error.

2.7.4.8 Reproducibility of Deliverable

If ground truth (average shear wave velocity of soil or depth to top of rock) is available, different experienced interpreters should come up with similar interpretations. If ground truth is not available, unreasonable interpretations are a very real possibility.

2.7.5 Deliverables

2.7.5.1 Brief Overview of Deliverable(s)

If the fundamental mode horizontal shear wave resonance frequency (f_{0HV}) of the soil layer at a specific location can be reliably measured, the depth to bedrock at that location can be calculated if the average shear wave velocity of the soil layer is known. The determination of f_{0HV} at a particular location, or the mapping of its spatial variability around a site or area (regional microzonation), and its conversion to sediment thickness have always been and still are the predominant uses of the HVSR method.

Conversely, if the fundamental mode horizontal shear wave resonance frequency (*f0*) of the soil layer at a specific location can be reliably measured, the average shear wave velocity of the soil layer can be calculated if the depth to bedrock at that location is known.

The HVSR tool is not capable of imaging the subsurface beneath the top of intact rock.

2.7.5.2 Utility of Deliverable(s)

Used for site classification purposes and estimates of depth to top of intact rock.

2.7.5.3 Accuracy

The final interpretations are generally reliable if good quality HVSR field data are recorded, if data are correctly processed and if ground truth is available. Use of an experienced interpreter is essential.

2.7.6 Advantages

Advantages include:

- estimate of depth to bedrock or estimates of average shear wave velocity of the subsurface (if ground truth is available),
- relatively low cost,
- minimal field space requirements
- portability of equipment,
- typically employ a 1-person crew,
- non-invasive,

- limited potential for human error if operators and processors are trained,
- reproducibility of field data,
- reproducibility of processing results,
- reproducibility of interpretations if geologic control is available,
- permitting is not required.

2.7.7 Disadvantages

Disadvantages include:

- estimate of depth to bedrock or estimates of average shear wave velocity of the subsurface only if ground truth is available,
- cannot image beneath top of rock,
- field records cannot be visually assessed in the field for QC purposes,
- inability to rapidly process data in the field (for QC purposes),
- relatively slow processing of field data in lab,
- sensitive to noise,
- human-constructed surfaces or significant subsurface topography can make it difficult to acquire useful data,
- features such as faults, solution-widened joints and voids may make it difficult to acquire useful data,
- underground utilities can make it difficult to acquire useful data,
- vegetation can pose problems during data acquisition,
- geophones must be effectively coupled to the ground surface; acquiring quality data on very soft or loose soil can be difficult.

2.8. Shear Wave Reflection Seismic Method

2.8.1 Brief Overview of the Shallow Reflection Seismic Method (with Emphasis on the Generation of 1-D Shear Wave Velocity Profiles)

An array of geophones (acoustic receivers) is placed at uniform intervals along the length of a traverse (Figure 2.1). Shear wave acoustic sources are discharged at predetermined locations within (typically between each receiver) and off the ends of the geophone array. Each time a source is discharged, the arrival times and magnitudes of acoustic energy reflected (as echoes) from prominent subsurface lithologic interfaces are recorded as a field record.

During data processing, the entirety of the field records is transformed into a single 2-D reflection seismic profile (image) of the subsurface. The horizontal axis is distance (along geophone array); the vertical axis is two-way travel time. On migrated data, the magnitude of reflected energy from prominent lithologic interfaces is plotted on the image at its point of origin in time and space.

During processing, a velocity-depth model of the subsurface is generated. Shear wave velocities are assigned only to those layers that generate relatively high magnitude identifiable reflections.

The shear wave reflection seismic technique can be a good tool for mapping the top of rock, and prominent lithologic interfaces within the soil and below the top of rock. However, the only interfaces that are imaged are those across which there is a significant change in acoustic impedance (product of shear wave velocity and density).

Both compressional wave and shear wave seismic reflection data can be acquired with the objective of imaging the subsurface to depths on the order of tens of thousands of feet. Herein, we restrict our discussion to the acquisition of shallow (imaging to depths of less than 300 feet) high-resolution shear wave reflection seismic data acquired along a single traverse with the primary objective of determining the shear wave velocity of the subsurface to a depth of 100 feet.

2.8.2 Data Acquisition

2.8.2.1 Brief Overview of Field Procedure

An array of geophones (usually 24 or 48; connected to engineering seismograph) is placed at uniform intervals (typically 10 to 20 feet) along the length of a traverse. Acoustic (shear wave) sources are discharged at predetermined locations within (typically between each receiver) and off the ends of the geophone array. Each time a source is discharged, the arrival times and magnitudes of acoustic energy reflected (as echoes) from prominent subsurface lithologic interfaces are digitally recorded and stored as a field record. The time-length of the window of recorded data is a function of the estimated two-way travel time of reflections from the lowest target horizon of interest.

If the traverse of interest is longer than of the geophone array, the entire array can be shifted along the traverse to ensure full subsurface coverage is acquired. Alternatively, a roll box and two or more interconnected arrays of geophones can be deployed.

Seismic reflection is the most complicated of all geophysical methods. The acquisition, processing and interpretation of reflection seismic data require significantly more expertise than any other commonly employed geophysical tool.

2.8.2.2 Field Equipment

Portable, and typically consisting of an impulsive shear wave energy source, trigger switch cable, 24-48 horizontally polarized high-frequency geophones, geophone cable, 24 or 48-channel seismograph, 12-V battery, and laptop.

2.8.2.3 Field Crew

Typically consists of 3-5 persons depending, in part, on the size of the array.

2.8.2.4 Considerations

Parameter entry. The correct acquisition parameters must be entered. A shallow high-resolution shear wave reflection record is typically 1.0 seconds in duration. The sampling interval is usually 0.5 milliseconds. Geophone spacing employed is one estimate of maximum lateral resolution. Elevation control is required.

Size of test site. The size of test site must be large enough to allow for ease of placement of geophones and the safe use of the acoustic source. The length of the array of geophones is normally equal to maximum depth of investigation. Sources are discharged within and off the ends of the array at predetermined locations.

Plotted location of the output 2-D shear wave velocity profile. The output of seismic processing is a 2-D reflection seismic profile (image) of the subsurface. The horizontal axis is distance (along geophone array); the vertical axis is 2-way travel time. On migrated data, the magnitude of reflected energy from prominent lithologic interfaces is plotted on the reflection seismic profile at its point of origin in time and space.

Vehicular access. All equipment can be hand-carried. The equipment and crew can be transported in a single vehicle.

Surface topography. Data can be acquired across steeply dipping terrain. However, elevation changes should be minimized where/if possible. Elevation control must be acquired.

Subsurface topography. The output of processing is a plot of reflection amplitude plotted as a function of distance and 2-way reflection arrival time. Shear wave reflection data are normally acquired with the objective of mapping subsurface structure.

Avoid recording on stiffer substrate than the underlying ground. Can cause velocity inversion.

Vegetation. Data can be acquired in heavily vegetated areas. However, dense vegetation impedes work and slows down field data acquisition. Usually, it is most efficient to clear the traverses ahead of time.

Background noise. It is usually difficult to acquire good quality reflection data in an acoustically noisy environment (e.g., adjacent to busy roadway). Data quality (signal-to-noise ratio) can be often improved by using a more powerful source or stacking. Data are stacked by discharging a source multiple times at each location and summing the recorded shot gathers (raw field records).

Geophones are often buried to minimize noise. It can be very difficult to acquire good quality data on windy and/or rainy days.

Anchoring requirements. The horizontally oriented geophones need to be coupled in stable, vertical positions to the ground surface and correctly oriented.

Nature of ground surface. The horizontally polarized shear wave geophones have spike bases that are normally inserted into relatively consolidated soil. It is very difficult to acquire quality data in areas (e.g., pavement, loose soil, exposed rock, etc.) where the geophones cannot be adequately coupled to the ground surface.

Placement of geophone. Normally, a tape measure is laid out along the traverse and geophones are placed at their appropriate locations. If a few individual geophones are misplaced off by 5% or less, data quality should not be adversely affected, particularly if the geophones are shifted only perpendicular to the traverse.

If the location of the discharged source is out by 6 inches or less (assuming a 10-foot geophone spacing), data quality should not be adversely affected.

Geophones are often buried to minimize noise.

Subsurface lithology or material. If the source and the geophones can be reliable coupled to the ground surface, shear wave reflection seismic data can be acquired across all types of soil and/or rock, pavement, asphalt, fill, etc.

Depth of investigation. A 20-pound sledgehammer source is usually sufficient for mapping reflective interfaces at depths on the order of a couple hundred feet. Higher magnitude acoustic sources will provide for greater depths of investigation. Longer arrays should be used to get the information about deeper horizons. Oil and gas exploration companies routinely use large (multiple pound) explosive sources to image the subsurface to depths on the order of tens of thousands of feet.

Proximity to buried structures and buried utilities. The reflection method is non-invasive. Data can be acquired in proximity to buried utilities and buried structures, unless there is concern that the source could damage built structures such as concrete or pavement.

The noise generated by subsurface structures and utilities can be relatively high magnitude and effectively can mask the relatively low magnitude reflections generated by subsurface lithologic interfaces of interest.

Proximity to surface structures and surface utilities. Reflection data can be acquired in proximity to surface utilities and built structures. The only clearance required is sufficient room to discharge the seismic source.

The noise generated by surface structures and utilities can be relatively high magnitude and effectively can mask the relatively low magnitude reflections generated by subsurface lithologic interfaces of interest.

Sensitivity to background noise. Measurements should be avoided during wind and heavy rain. A cover can help shade and keep the seismometer cool but can also lead to transmitting wind or rain droplet vibration into the ground due to its surface area. Waiting for a less windy day or use of an umbrella with fewer contact points is often better solutions towards mitigating recording wind and rain vibrations.

Permitting requirements. Generally, only permission from the surface rights holder is required.

Notification requirements. Generally, only permission from the surface rights holder is required.

Other considerations. Horizontally polarized geophones are generally more expensive compared to vertically polarized geophones.

2.8.2.5 Brief Description of Field Data

The raw field data, consisting of common-shot records (typically less than 1 second in length) are recorded digitally and stored on the laptop connected to the seismograph or to built-in flash memory. Surface wave energy, reflected compressional wave energy, reflected shear wave energy, refracted shear wave energy, compressional shear wave energy, and noise is present on the field records. However, the only information that is of interest to the processor is the arrival time and magnitude of the reflected shear waves.

2.8.2.6 Estimated Cost to Acquire Field Data at One Test Site

Basic field costs include a) crew time plus travel time, b) equipment rental and/or depreciation, and c) vehicle rental and/or depreciation plus fuel. It typically takes a 3-person crew about five hours to acquire a single shear wave reflection data set (24-geophone array). Elevation data are required.

2.8.2.7 Potential for Errors

There is little likelihood that field errors will lead to misinterpretation.

Human. If appropriate acquisition parameters (array length, array orientation, geophone spacing, source, source locations, recording parameters, etc.) are selected, human error, leading to misinterpretation, is unlikely because the only critical non-automated processes are the placement of the geophones and the placement/discharge of the source. If the source is too small, if the geophones are not properly coupled to the ground, or if the site is too noisy, poor quality field data (low signal-to-noise ratio) may be acquired.

Equipment. Equipment problems are unlikely to generate errors that will lead to misinterpretation.

2.8.2.8 Reproducibility of Field Tests

If good quality field data can be recorded, field results can be reproduced with a high degree of consistency.

2.8.2.9 Quality Control

Common shot gathers can be visually assessed in the field for quality control purposes. If the data are noisy, stacking or the use of a higher magnitude source can be options.

2.8.3 Data and/or Laboratory Processing

2.8.3.1 Brief Overview of Data Processing

The processing of reflection seismic data is very complex and sophisticated and requires interactive input from an experienced processor/interpreter.

Typical processing steps include 1) the downloading of field data from the seismograph, 2) the reformatting of the field data, 3) muting of field data to remove critically refracted waves and bad traces, 4) filtering (noise attenuation, and signal enhancement including deconvolution), 5) velocity analysis, 6) re-sorting of common shot gathers into common mid-point gathers, 7) application of normal moveout corrections, 8) stacking using previously defined velocities, and 9) migration. A 2-D seismic profile (vertical axis in time) is the primary output. The output 2-D profile can also be depth-migrated. In this case, the vertical axis of the output shear wave reflection seismic profile is transformed from 2-way travel time to in depth.

A secondary output is a shear wave velocity model of the subsurface. However, shear wave velocities are assigned only to those layers that generate relatively high magnitude identifiable reflections. Frequently, only the top of rock and prominent underlying lithologic units are imaged. In this case, the velocity model to a depth of 100 feet, might consist of 3 layers or fewer.

2.8.3.2 Output of Data Processing

The output is a 2-D reflection seismic profile of the subsurface (vertical axis in time). On migrated 2-D reflection seismic profile, the acoustic energy reflected from all those subsurface interfaces that could be imaged is assumed to be placed in its proper spatial location of origin (time and space). During data interpretation, the output seismic profiles are transformed into 2-D lithologic images.

2.8.3.3 Estimated Cost to Process Field Data from One Test Site

Basic processing costs include a) processor's time, and b) hardware/software rental and/or depreciation. It typically takes an experienced interpreter about five hours to process a single shallow reflection seismic data set (24-geophone array).

2.8.3.4 Potential for Error

Human. Each processing step requires input from an experienced data processor. The generation of the output 2-D seismic profile is subjective. The processing of reflection seismic data is very sophisticated and requires considerable expertise.

Equipment and Software. The processing software should not be defective. However, seismic reflection software is not capable of imaging lithologic units that are either too thin (< 10 feet) or too acoustically similar to overlying and/or underlying strata.

2.8.3.5 Reproducibility of Field Tests

If the field data are good quality, experienced processors will generate similar reflection seismic profiles for the same field data set.

2.8.4 Interpretation

2.8.4.1 Brief Overview of Interpretation of Processed Data

The primary output of processing is a migrated 2-D reflection seismic profile. Unless the data are depth-migrated, the vertical axis on the profile is in time; the horizontal axis represents distance along the traverse. If the data are depth-migrated, the vertical axis is in depth. During data interpretation, the output 2-D reflection seismic profile is transformed into 2-D lithologic (geologic) image of the subsurface. This is the primary deliverable.

2.8.4.2 Deliverable(s)

During data interpretation, the 2-D reflection seismic profiles are transformed into 2-D lithologic (geologic) images of the subsurface. This is the primary deliverable.

A secondary deliverable is the shear wave velocity model of the subsurface. However, shear wave velocities are assigned only to those layers that generate relatively high magnitude

identifiable reflections. Frequently, only the top of rock and prominent underlying lithologic units are imaged. In this case, the velocity model to a depth of 100 feet, might consist of 3 layers or fewer. Velocities can be out by 10%.

2.8.4.3 Depth Range (Top/Bottom)

Typically, the subsurface is imaged to depths on the order of 300 feet. Greater depths of investigation can be achieved if larger sources are employed.

2.8.4.4 Lateral Resolution

Effectively the same as one-half the geophone spacing.

2.8.4.5 Vertical Resolution

Depends on the subsurface lithology (thickness and acoustic velocity) and the dominant frequency of the processed reflection seismic data. Generally, the only lithologic interfaces which can be imaged are those that separate units with significantly different acoustic properties (e.g., clay/gravel, soil/bedrock, limestone/shale, etc.). Thinner layers can be imaged on higher frequency data.

2.8.4.6 Time Required to Interpret Field Data (One Test Site)

If ground truth is available and if velocity/lithologic relationships can be established, the interpretation of shallow reflection seismic data is often very reliable.

2.8.4.7 Potential for Error

Human. The interpreter must establish relationships between acoustic velocity and the lithology and identify the geologic interfaces that generate each prominent reflection. Ground truth significantly increases the reliability of the final interpretations. The use of an experienced interpreter is essential.

Equipment. There is little potential for error.

2.8.4.8 Reproducibility of Deliverable

If ground truth is available, different experienced interpreters should generate similar interpretations. If ground truth is not available, unreasonable interpretations are a very real possibility.

2.8.5 Deliverables

2.8.5.1 Brief Overview of Deliverable(s)

The primary deliverable of the shear wave reflection seismic method is a high-resolution 2D vertical cross-section of the subsurface along the length of the traverse, showing interpreted layers with different material shear wave impedance (shear wave velocity × density). In some applications, 3-D shear wave reflection data volumes may also be generated, depending on array geometry and acquisition extent.

2.8.5.2 Utility of Deliverable(s)

Geologic images provide information about lateral and vertical variations in lithology from the ground surface to the depth of the lowest horizon imaged.

A secondary deliverable is the shear wave velocity model of the subsurface. However, shear wave velocities are assigned only to those layers that generate relatively high magnitude identifiable reflections.

2.8.5.3 Accuracy

The final interpretations are generally reliable if good quality field data are recorded and if ground truth is available (to constrain and verify interpretations). Use of an experienced interpreter is essential.

2.8.6 Advantages

Advantages include portability of equipment, few restrictions with respect to surface conditions (soil, rock, pavement, etc.), non-invasive, depth penetration (in all types of soil and/or rock) on the order of 200 feet often times using only a sledgehammer source. The method has multiple applications (determination of lithology, depth to bedrock, mapping of lithologic interfaces beneath top of rock, location of voids, etc.). Additionally, permitting is not required, and the tool can be used across and in proximity to utilities and built structures.

Advantages include:

- the primary deliverable is an interpreted 2-D shear wave velocity profile of the subsurface to depth greater than 100 feet,
- if ground truth is available, the shear wave profile can be transformed into a geologic cross-section,
- depth to bedrock can usually be estimated to within $\pm$10%,
- other imaged lithologic units can often be identified and mapped on basis of shear wave velocity,

- a secondary deliverable is a shear wave velocity profile of the subsurface typically extending to depths greater than 100 feet,
- portability of equipment,
- field records can be visually assessed in the field for QC purposes,
- non-invasive,
- data can be assessed in the field for quality control purposes,
- limited potential for human error if operators and processors are trained,
- reproducibility of field data if good quality,
- reproducibility of processing results if data are good quality,
- reproducibility of interpretations, if data are good quality and geologic control is available,
- multiple applications (determination of lithology, porosity, depth to bedrock, location of voids),
- permitting is not required.

2.8.7 Disadvantages

Method is relatively expensive and time consuming. Significant experience is absolutely essential (acquisition, processing and interpretation). Ground truth is required to accurately constrain geologic correlations. Accuracy decreases with depth. Reliability of tool decreases as lateral and vertical heterogeneity of soil/rock increases.

Disadvantages include:

- only layers that are characterized by significant acoustical impedance contrasts are imaged,
- usually, relatively few layers are imaged at depths shallower than 100 feet,
- highly sensitive to noise,
- elevation control is required,
- site must be large enough to accommodate the geophone array and source,
- significant restrictions with respect to surface conditions (soil, rock, pavement, etc.) as geophones and source must be effectively coupled to the ground surface,
- data cannot be processed in the field for quality control purposes,
- reliability of output shear wave velocity data decreases as lateral and vertical heterogeneity of soil/rock increases,
- expert processors and interpreters are required,
- relatively high cost compared to surface wave and refraction seismic methods,
- vegetation can pose problems during data acquisition,
- typically employ a 3–5-person crew.

Chapter 3 Relative Utility of the Identified Testing Methods

Based on the literature search, eight (8) potential applicable methods for determining the shear wave velocity of the subsurface to a depth of 100 feet were assessed. The comparative utility of each of the eight methods is summarized in Tables 3.1 and 3.2 with the described attributes ranked from 1 to 4 (1 being the best and 4 being the worst), based on the following criteria:

1. Repeatability of results (data acquired at different times; data processed by different personnel).
2. Required field equipment and cost.
3. Source requirements (passive and/or active).
4. Field crew size.
5. Ease and straightforwardness of data acquisition.
6. Ease and effectiveness of quality control in field.
7. Time to acquire a single field data set.
8. Data acquisition limitations (e.g., surface topography, bedrock topography, surface vegetation, proximity to cultural features, soil thickness, presence of karst features, etc.).
9. Required processing software and cost.
10. Ease and straightforwardness of data processing.
11. Time to process a single data set.
12. Reliability of the output shear wave velocity data.
13. Ease and straightforwardness of interpretation (average Vs to depth of 100 feet, mapping of lithologic units including top-of-rock, etc.).
14. Maximum realizable depths of investigation (source dependent)
15. Resolution of Vs profile.

Only four (4) of the eight (8) methods evaluated during the literature review (Table 3.1) – active multichannel analysis of surface waves (MASW), passive multichannel analysis of surface waves (MASW), active refraction microtremor (ReMi), and Passive Refraction Microtremor (ReMi), were considered to be potentially suitable for determining the shear wave velocity of soil and rock to a depth of 100 feet. These four (4) selected methods were deemed to be most appropriate and were field tested for comparative assessment purposes.

One (1) of the eight (8) methods – Horizontal to vertical spectral ratio (HVSR; Table 3.2) was not considered to be a viable option for this study. This method was not recommended for several reasons, including:

- The deliverable is the resonant frequency of the soil layer only.
- The average shear wave velocity of the subsurface can only be calculated if depth to top of rock is known.
- The average shear wave velocity of the subsurface can only be calculated to top of rock.

- The acoustic properties of soil and rock must differ appreciably.

Three (3) of the eight (8) methods – conventional shear wave seismic refraction, seismic shear wave refraction tomography, and seismic shear wave reflection (Table 3.2), were not considered to be viable options for this study. These three (3) methods were not recommended for several reasons, including:

- They have no significant advantages over the four (4) selected methods (re: utility of deliverable).
- Data acquisition is more time-consuming and significantly more expensive compared to the four (4) selected methods.
- These three (3) methods are more sensitive to background noise.
- Highly skilled processors are required, more so than for the selected methods.
- Elevation control is required.
- Long geophone arrays are required compared to the four (4) selected methods.
- Specialized high-magnitude sources are required.

Table 3.1 Comparative assessment of the Active Multichannel Analysis of Surface Waves (MASW), Passive Multichannel Analysis of Surface Waves (MASW), Active Refraction Microtremor (ReMi), and Passive Refraction Microtremor (ReMi) methods. In each cell, the described attribute is ranked from 1-4 (best to worst). Where warranted, a specific attribute is ranked as tied.

	Active Multichannel Analysis of Surface Waves (MASW)	**Passive Multichannel Analysis of Surface Waves (MASW)**	**Active Refraction Microtremor (ReMi)**	**Passive Refraction Microtremor (ReMi)**
Field Equipment and Relative Cost	3: Acoustic source, 24-channel geophone array, engineering seismograph and dedicated laptop.	2: Passive source, 24-channel geophone array, engineering seismograph and dedicated laptop.	3: Acoustic Source, 24-channel geophone array, engineering seismograph and dedicated laptop.	2: Passive source, 24-channel geophone array, engineering seismograph and dedicated laptop.
Source	2: Active source. Sledgehammer or higher magnitude sources can be employed.	1: Passive source (ambient noise).	2: Active source. Sledgehammer or higher magnitude sources can be employed.	1: Passive source (ambient noise).
Ease of Data Acquisition (re: source and recording)	1: Source must be discharged multiple times. Relatively rapid once array and seismograph are set-up. Crew typically spends ~0.5 hours per location.	2: Passive data only are recorded. Relatively slow process as data is recorded for multiple minutes. Crew typically spends ~1.25 hours per location.	1: Source must be discharged multiple times. Relatively rapid once array and seismograph are set-up. Crew typically spends ~0.5 hours per location.	2: Passive data only are recorded. Relatively slow process as data is recorded for multiple minutes. Crew typically spends ~1.25 hours per location.
Crew Size	2: Typically, 1-3-person crew.	2: Typically, 1-3-person crew.	2: Typically, 1-3-person crew.	2: Typically, 1-3-person crew.
Quality Control in Field	1: Visual inspection for QC is the norm. Data can be quickly preprocessed in the field for QC purposes.	4: User cannot assess quality of data in field.	1: Visual inspection for QC is the norm. Data can be quickly preprocessed in the field for QC purposes.	4: User cannot assess quality of data in field.
Data Acquisition Cost (including set-up)	2: Multi-person crew. Crew typically spends ~0.5 hours per location.	3: Multi-person crew. Crew typically spends ~1.25 hours of acquisition time.	3: Multi-person crew. Crew typically spends ~0.5 hours per location.	2: Multi-person crew. Crew typically spends ~1.25 hours of acquisition time.
Field Space Requirements	2: Length of array and source is typically ~130 feet.	2: Length of array and source is typically ~130 feet.	2: Length of array and source is typically ~130 feet.	2: Length of array and source is typically ~130 feet.
Ease of Data Processing	1: Processing is relatively straightforward if good quality data are acquired. ~0.5 hours per data set.	1: Processing is relatively straightforward if good quality data are acquired. ~1 hour per data set.	1: Processing is relatively straightforward if good quality data are acquired. ~0.5 hour1 per data set.	1: Processing is relatively straightforward if good quality data are acquired. ~1 hour per data set.
Output of Processing	1: 10-layered 1-D shear wave velocity profile that typically extends to a depth of 100 feet.	1: 10-layered 1-D shear wave velocity profile that typically extends to a depth of 100 feet.	1: 10-layered 1-D shear wave velocity profile that typically extends to a depth of 100 feet.	1: 10-layered 1-D shear wave velocity profile that typically extends to a depth of 100 feet.

	Active Multichannel Analysis of Surface Waves (MASW)	Passive Multichannel Analysis of Surface Waves (MASW)	Active Refraction Microtremor (ReMi)	Passive Refraction Microtremor (ReMi)
Deliverable	1: 10-layered 1-D shear wave velocity profile that typically extends to a depth of 100 feet. The 1-D shear wave velocity profile represents the average shear wave velocity of the subsurface beneath the entire array. Higher frequencies are usually recorded. Hence, the resolution in upper 100 feet is relatively high.	2: 10-layered 1-D shear wave velocity profile that typically extends to a depth significantly greater than 100 feet. The 1-D shear wave velocity profile represents the average shear wave velocity of the subsurface beneath the entire array. Higher frequencies are usually not recorded. Hence, the resolution in upper 100 feet is relatively low.	2: 10-layered 1-D shear wave velocity profile that typically extends to a depth of 100 feet. The 1-D shear wave velocity profile represents the average shear wave velocity of the subsurface beneath the entire array. Higher frequencies are usually recorded. Hence, the resolution in upper 100 feet is relatively high.	1: 10-layered 1-D shear wave velocity profile that typically extends to a depth significantly greater than 100 feet. The 1-D shear wave velocity profile represents the average shear wave velocity of the subsurface beneath the entire array. Higher frequencies are usually not recorded. Hence, the resolution in upper 100 feet is relatively low.
Significant Disadvantages	• Space required to set up the array of geophones. • Surface topography can be a serious problem. • Subsurface topography can be a serious problem. • Subsurface structures and/or features can be a serious problem. • Lateral velocity variations beneath the geophone array can distort overtone image and cause interpretational issues.	• Space required to set up the array of geophones. • Surface topography can be a serious problem. • Subsurface topography can be a serious problem. • Subsurface structures and/or features can be a serious problem. • Lateral velocity variations beneath the geophone array can distort overtone image and cause interpretational issues. • There may not be a suitable source of passive noise. • Higher frequencies are usually not recorded. Hence, the resolution in upper 100 feet is relatively low.	• Space required to set up the array of geophones. • Surface topography can be a serious problem. • Subsurface topography can be a serious problem. • Subsurface structures and/or features can be a serious problem. • Lateral velocity variations beneath the geophone array can distort frequency vs slowness image and cause interpretational issues.	• Space required to set up the array of geophones. • Surface topography can be a serious problem. • Subsurface topography can be a serious problem. • Subsurface structures and/or features can be a serious problem. • Lateral velocity variations beneath the geophone array can distort frequency vs slowness image and cause interpretational issues. • There may not be a suitable source of passive noise, possibly because of the orientation of the linear array. • Higher frequencies are usually not recorded. Hence, the resolution in upper 100 feet is relatively low.
Significant Advantages	• Acquisition, processing, and interpretation is relatively straightforward. • Output is normally a 10-layered shear wave velocity model of the	• Acquisition, processing, and interpretation is relatively straightforward. • Output is normally a 10-layered shear wave velocity model of the	• Acquisition, processing, and interpretation is relatively straightforward. • Output is normally a 10-layered shear wave velocity model of the	• Acquisition, processing, and interpretation is relatively straightforward. • Output is normally a 10-layered shear wave velocity model of the

	Active Multichannel Analysis of Surface Waves (MASW)	Passive Multichannel Analysis of Surface Waves (MASW)	Active Refraction Microtremor (ReMi)	Passive Refraction Microtremor (ReMi)
	subsurface that extends to a depth of 100 feet. • Passive data can be simultaneously acquired, and depths of investigation can be extended to hundreds of feet. • Relatively insensitive to background noise. Passive MASW data can be simultaneously acquired. • Love wave MASW data can be acquired. • MASW data can be acquired on water bottom. • Higher mode Rayleigh wave data can be acquired and processed separately for comparative purposes.	subsurface that extends to a depth of 100 feet. • Active data can be simultaneously acquired, and resolution in the upper 100 feet can be significantly increased. • Relatively insensitive to background noise. Passive MASW data can be simultaneously acquired. • Love wave MASW data can be acquired. • MASW data can be acquired on water bottom. • Higher mode Rayleigh wave data can be acquired and processed separately for comparative purposes.	subsurface that extends to a depth of 100 feet. • Passive data can be simultaneously acquired, and depths of investigation can be extended to hundreds of feet. • Relatively insensitive to background noise.	subsurface that extends to a depth of 100 feet. • Active data can be simultaneously acquired, and resolution in the upper 100 feet can be significantly increased. • Relatively insensitive to background noise.
Other considerations	• MASW processing software, in our opinion, is more user friendly than ReMi processing software. • Non-linear array data can be processed using MASW software. This can be a significant advantage if passive data are recorded. • Higher mode Rayleigh wave data can be acquired and processed separately for comparative purposes. • MASW data can be acquired on water bottom. • Love wave MASW data can be acquired. Love wave data may be higher resolution than Rayleigh wave data.	• MASW processing software, in our opinion, is more user friendly than ReMi processing software. • Non-linear array data can be processed using MASW software. This can be a significant advantage if passive data are recorded. • Higher mode Rayleigh wave data can be acquired and processed separately for comparative purposes. • MASW data can be acquired on water bottom. • Love wave MASW data can be acquired. Love wave data may be higher resolution than Rayleigh wave data.	• ReMi processing software, in our opinion, is less sophisticated and less user friendly than MASW processing software. • Non-linear array data cannot be processed using ReMi software. • Non-linear array data cannot be processed using ReMi software. This can be a significant advantage if passive data are recorded. • Higher mode Rayleigh wave data cannot be acquired and processed separately for comparative purposes. • ReMi data cannot be acquired on water bottom. • Love wave MASW data cannot be processed.	• ReMi processing software, in our opinion, is less sophisticated and less user friendly than MASW processing software. • Non-linear array data cannot be processed using ReMi software. This can be a significant disadvantage if passive data are recorded. • Higher mode Rayleigh wave data cannot be acquired and processed separately for comparative purposes. • ReMi data cannot be acquired on water bottom. • Love wave ReMi data cannot be processed.

Table 3.2 Comparative assessment of the Conventional Shear Wave Refraction Seismic, Shear Wave Refraction Seismic Tomography, Horizontal to Vertical Spectral Ratio (HVSR), and Shear Wave Reflection Seismic methods. In each cell, the described attribute is ranked from 1-4 (best to worst). Where warranted, a specific attribute is ranked as tied.

	Conventional Shear Wave Refraction Seismic	**Shear Wave Refraction Seismic Tomography**	**Horizontal to Vertical Spectral Ratio (HVSR)**	**Shear Wave Reflection Seismic**
Field Equipment and Relative Cost	4: Specialized acoustic source, 24-channel geophone array, engineering seismograph and dedicated laptop.	4: Specialized acoustic source, 24-channel geophone array, engineering seismograph and dedicated laptop.	1: Single triaxial geophone, engineering seismograph and dedicated laptop.	4: Specialized acoustic source, 24-channel geophone array, engineering seismograph and dedicated laptop.
Source	3: Specialized active. A high magnitude shear wave must be employed.	3: Specialized active. A high magnitude shear wave source must be employed.	1: Passive source (ambient noise).	3: Specialized active. A high magnitude shear wave source must be employed.
Ease of Data Acquisition (re: source and recording)	3: Source must be discharged multiple times and at multiple (typically 5) locations assuming 12 geophone array is employed. Crew typically spends ~3 hours per location assuming single 12 geophone array.	3: Source must be discharged multiple times and at multiple (typically 30) locations assuming 12 geophone array is employed. Crew typically spends ~5 hours per location assuming single 12 geophone array.	2: Tens of minutes of passive data only are recorded. Relatively slow process. Crew typically spends ~2 hours per location.	3: Source must be discharged multiple times and at multiple (typically 30) locations assuming 12 geophone array is employed. Crew typically spends ~5 hours per location assuming single 12 geophone array.
Crew Size	3: Typically, 2-4-person crew.	4: Typically, 3-4-person crew.	1: Single person.	4: Typically, 3-4-person crew.
Quality Control in Field	2: Visual inspection for QC is the norm. Data cannot be preprocessed in the field for QC purposes.	3: Visual inspection for QC is the norm. Data cannot be preprocessed in the field for QC purposes.	4: Cannot assess quality of data in field.	3: Visual inspection only.
Data Acquisition Cost (including set-up)	4: multi-person crew; ~3 hours of acquisition time.	5: multi-person crew; ~5 hours of acquisition time.	1: 1-person crew; ~2 hours of acquisition time.	5: multi-person crew; ~5 hours of acquisition time.
Field Space Requirements	4: Length of array and source is typically ~700 feet.	3: Length of array and source is typically ~400 feet.	1: Single geophone is employed.	3: Length of array and source is typically ~300 feet.
Ease of Data Processing	3: Processing is somewhat challenging even if good quality data are acquired. Expert processor is required. More than 2 hours per data set.	4: Processing is somewhat challenging even if good quality data are acquired. Expert processor is required. More than 2 hours per data set.	2: Processing is challenging even if good quality data are acquired. Expert processor is required. More than 2 hours per data set.	5: Processing is challenging even if good quality data are acquired. Expert processor is required. More than 2 hours per data set.

	Conventional Shear Wave Refraction Seismic	Shear Wave Refraction Seismic Tomography	Horizontal to Vertical Spectral Ratio (HVSR)	Shear Wave Reflection Seismic
Output of Processing	3: Typically, a 3- to 5-layered 1-D shear wave velocity model that typically extends only to top of rock.	2: Typically, 1-D shear wave velocity model that can extend to a depth of 100 feet if a high magnitude source is employed.	4: Output of processing is the frequency of reverberations from top of rock.	2: Typically, a 3- to 5-layered 1-D shear wave velocity image that extends to a depth greater than 100 feet.
Deliverable	2: Typically, a 2- to 5-layered 2-D shear wave velocity model that typically extends only to top of rock. A sledgehammer source is usually not suitable.	1: Typically, a relatively high-resolution 2-D shear wave velocity model of the subsurface that can extend to a depth of 100 feet if a high magnitude source is employed. A sledgehammer source is usually not suitable.	3: If the average velocity of the soil layer is known, the depth to top of rock can be calculated. If the depth to top of rock is known, the average shear wave velocity of the soil layer can be calculated. Otherwise, only resonant frequency can be determined.	2: Typically, a 3- to 5-layered shear wave velocity model that extends to a depth greater than 100 feet. Expert interpreter is required.
Significant Disadvantages	• Space required to set up the array of geophones. • Typical output is a 2-layered velocity model. • Method usually images subsurface to top of rock only. • High magnitude source is required I bedrock is at a depth greater than about 30 feet. • Elevation control is required. • Long geophone arrays are required. • Sensitive to background noise.	• Space required to set up the array of geophones. • Cost. • Skilled processor is required. • High magnitude source is required. • Elevation control is required. • Long geophone arrays are required. • Sensitive to background noise.	• Deliverable is the resonant frequency of the soil layer. • Ground truth is required. For example, the depth to top of rock can be calculated only if the average shear wave velocity of the soil layer is known. Conversely, the average shear wave velocity of the soil layer can be calculated only if the depth to top of rock is known. • Method only images the subsurface to top of rock. • Acoustic properties of soil and rock must differ appreciably. • A skilled processor is required.	• Space required to set up the array of geophones. • Cost. • A highly skilled processor and a highly skilled interpreter are required. • High magnitude source may be required. • Elevation control is required. • Sensitive to background noise.
Significant Advantages	• No significant advantages over other methods.	• The output is a 2-D shear wave velocity image of the subsurface. • Lateral smoothing is not an issue.	• Minimal space required. Single geophone and recording equipment. geophones. • A single operator is required.	• No significant advantages over other methods.
Other considerations	• Most applicable in moderately consolidated soils or weathered rock. • Subsurface material, such as saturated clayey soils may	• Multiple source locations are required. • Field setup is more challenging due to the required high-magnitude shear wave source and	• The triaxial geophone must be placed on firm and flat ground for good coupling. Placing on a slope must be avoided.	• Multiple source locations are required. • Directly measures stiffness via shear wave velocities.

	Conventional Shear Wave Refraction Seismic	Shear Wave Refraction Seismic Tomography	Horizontal to Vertical Spectral Ratio (HVSR)	Shear Wave Reflection Seismic
	attenuate the signal and data interpretability.	horizontally polarized (shear wave) geophones. • May not be applicable at sites with low shear wave velocity contrast or complex stratigraphy.	• Does not provide shear wave velocity directly – only resonance frequency.	• Shear wave source and horizontally polarized (shear wave) geophones are required. • Less sensitive to pore fluid conditions

Chapter 4 Field Testing of Four Most Applicable Methods

SCI field tested the following four (4) methods with the goal of determining the method or methods that would be of most utility to MoDOT:

- Active MASW (Chapter 2.1; Table 3.1 in Chapter 3)
- Passive MASW (Chapter 2.2; Table 3.1 in Chapter 3)
- Active ReMi (Chapter 2.3; Table 3.1 in Chapter 3)
- Passive ReMi (Chapter 2.4; Table 3.1 in Chapter 3)

The intent was to identify the most effective method or methods based on the following criteria: 1) limited equipment, source, and personnel requirements for deployment; 2) straightforward data analysis; and 3) ease of interpretation of the results. The three (3) test sites are as follows:

1. SCI office in O'Fallon, Illinois (Coordinates 38.579899°, -89.925626°, Figures 4.1 and Figure 4.2);

2. I-270 Chain of Rocks (COR) Bridge over Mississippi River (Coordinates 38.766181°, -90.179479° and 38.762539°, -90.164550°, Figures 4.1 and Figure 4.3);

3. MLK connector, IDOT site (Coordinates 38.629338°, -90.163943°, Figures 4.1 and Figure 4.4).

For assessment and comparison purposes, field data were acquired for each method using at least two (2) array orientations, geophone spacings of 5 feet and 10 feet, and different source offsets where applicable. More specifically, the Active MASW and ReMi data were acquired using linear arrays of 24-4.5 Hz geophones spaced at both 5-foot and 10-foot intervals. The active source, consisting of a metal plate and a 20-pound sledgehammer, was discharged at offset distances of 10 feet, 20 feet, 25 feet, and 30 feet.

The Passive MASW and ReMi data were similarly acquired using linear arrays of 24-4.5 Hz geophones spaced at both 5-foot and 10-foot intervals. At the I-270 COR Bridge over the Mississippi River, Passive MASW data were also acquired using a non-linear (L-shaped) array of 24-4.5 Hz geophones. The Passive MASW and ReMi data were recorded using ambient surface wave energy as the source.

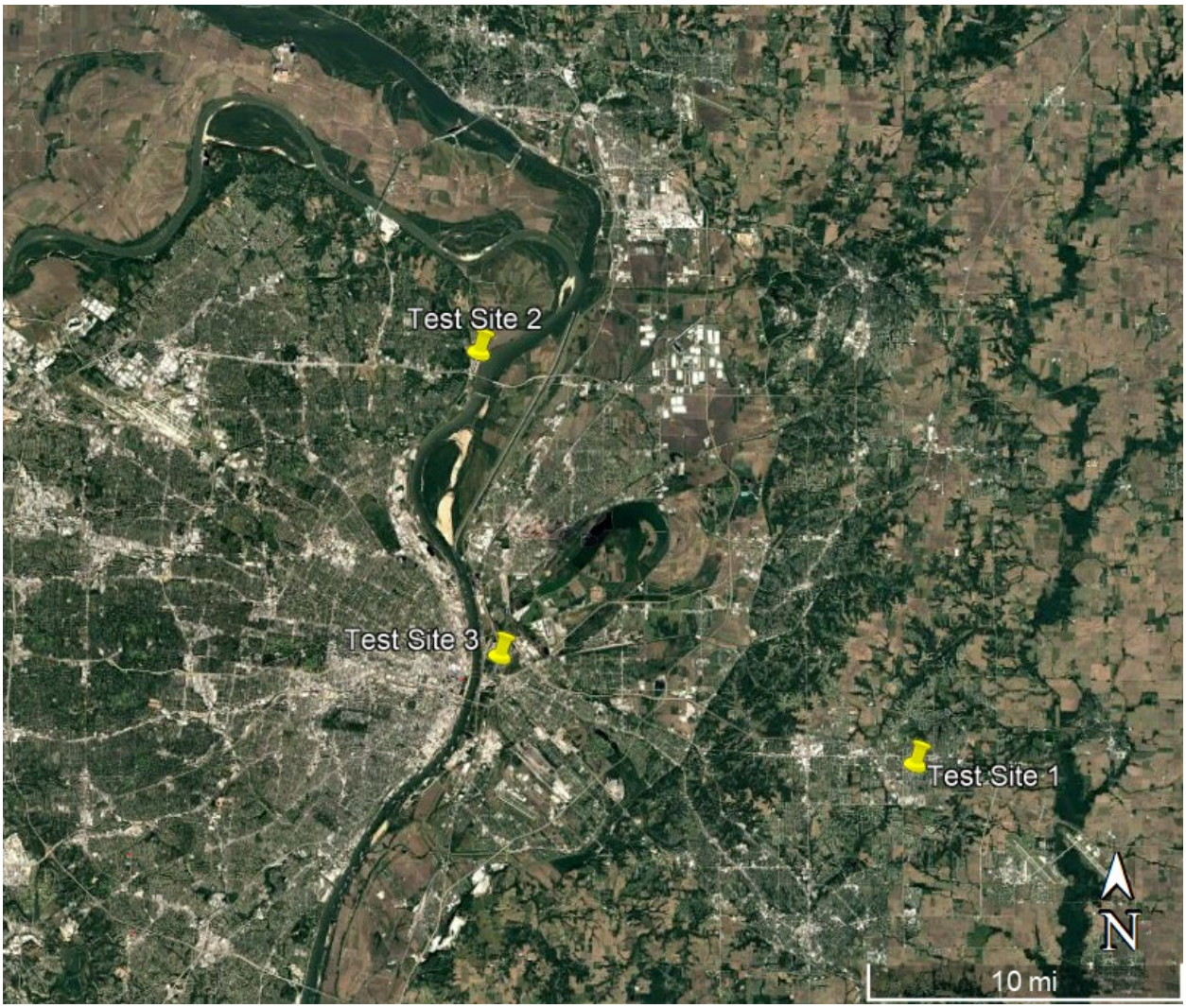

Figure 4.1 Locations of SCI Test Sites 1 (SCI office in O'Fallon, Illinois), 2 (I-270 COR Bridge over Mississippi River), and 3 (MLK connector, IDOT site).

4.1. Overview of the Data Acquired at the SCI Office in O'Fallon, Illinois Site (Test Site 1)

Active and Passive MASW and ReMi data were acquired along near-perpendicular traverses 1 and 2 at the SCI O'Fallon office site (Figure 4.2). Passive MASW data were also acquired along L-shaped traverse 3 shown in red in Figure 4.2. A tabularized summary of the field data acquired at SCI office in O'Fallon, Illinois (Test Site 1) is presented as Table 4.1.

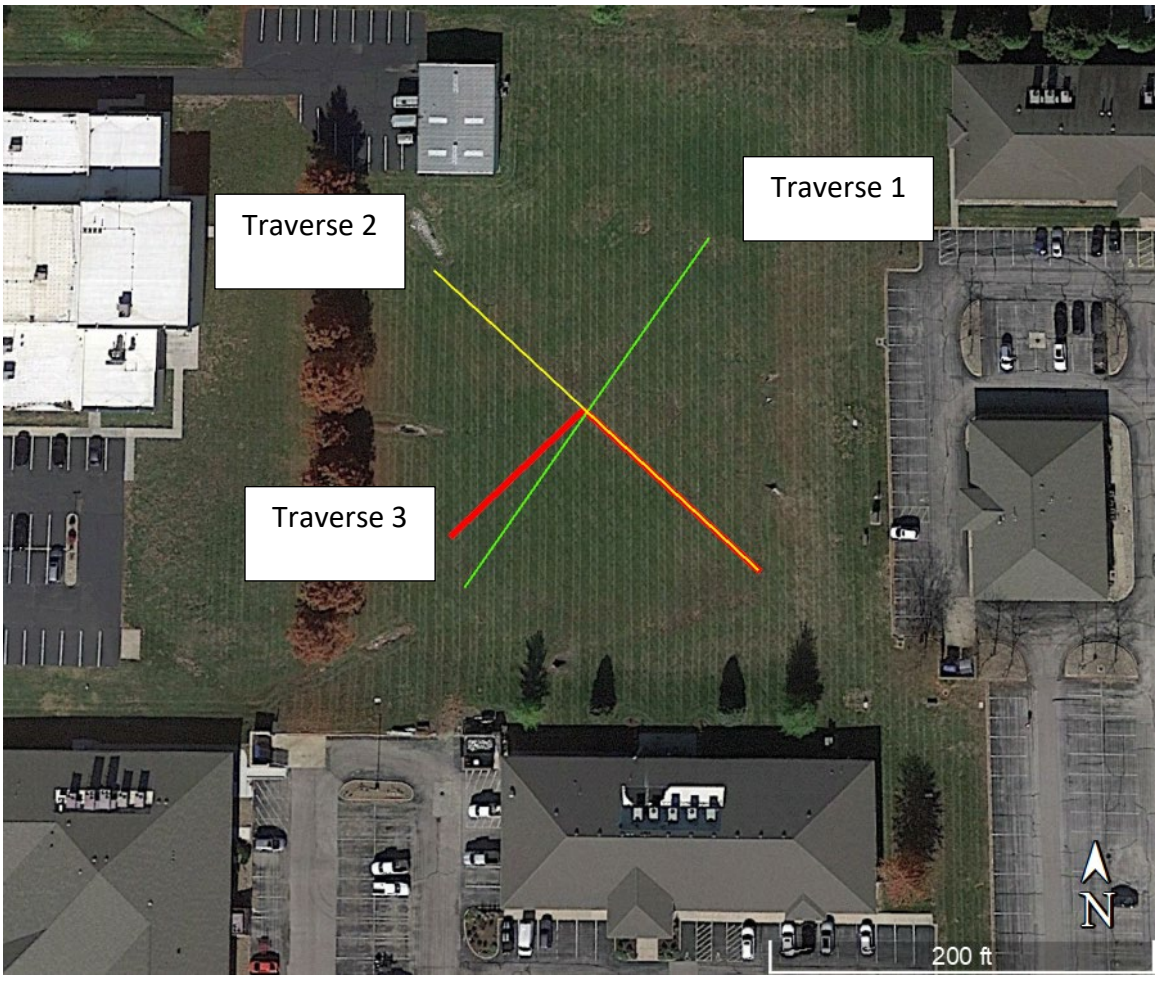

Figure 4.2 SCI office in O'Fallon, Illinois (Test Site 1; Figure 4.1) traverse locations.

Active and Passive MASW and ReMi data were acquired along the traverses 1 and 2 shown in green and yellow using both a 5-foot and a 10-foot geophone spacing. The active source, consisting of a metal plate and a 20-pound sledgehammer, was discharged at offset distances of 10 feet, 20 feet, 25 feet, and 30 feet. Passive MASW data were acquired along non-linear traverse 3 (L-shaped) shown in red.

Table 4.1 Tabularized summary of field data acquired at Test Site 1 (SCI office in O'Fallon, Illinois; Figures 4.1 and 4.2). Active and passive data were acquired along a linear traverse using a geophone spacing of 5 and 10 feet.

Data Set Number	Test Site and Traverse	Data Type	Geophone Spacing, feet	Offset, feet	Source Location	Record Length, seconds
1	OFN Traverse 1	Active	5	30	SW	1
2	OFN Traverse 1	Active	5	25	SW	1
3	OFN Traverse 1	Active	5	20	SW	1
4	OFN Traverse 1	Active	5	10	SW	1
5	OFN Traverse 1	Active	5	30	NE	1
6	OFN Traverse 1	Active	5	25	NE	1
7	OFN Traverse 1	Active	5	20	NE	1
8	OFN Traverse 1	Active	5	10	NE	1
9	OFN Traverse 1	Passive	5	N/A	N/A	30
10	OFN Traverse 1	Active	10	30	NE	1
11	OFN Traverse 1	Active	10	20	NE	1
12	OFN Traverse 1	Active	10	10	NE	1
13	OFN Traverse 1	Active	10	30	SW	1
14	OFN Traverse 1	Active	10	20	SW	1
15	OFN Traverse 1	Active	10	10	SW	N/A
16	OFN Traverse 1	Passive	10	N/A	N/A	N/A
1	OFN Traverse 2	Passive	5	N/A	N/A	30
2	OFN Traverse 2	Active	5	30	NW	1
3	OFN Traverse 2	Active	5	25	NW	1

Data Set Number	Test Site and Traverse	Data Type	Geophone Spacing, feet	Offset, feet	Source Location	Record Length, seconds
4	OFN Traverse 2	Active	5	20	NW	1
5	OFN Traverse 2	Active	5	10	NW	1
6	OFN Traverse 2	Active	5	30	SE	1
7	OFN Traverse 2	Active	5	25	SE	1
8	OFN Traverse 2	Active	5	20	SE	1
9	OFN Traverse 2	Active	5	10	SE	1
10	OFN Traverse 2	Active	10	30	SE	1
11	OFN Traverse 2	Active	10	20	SE	1
12	OFN Traverse 2	Active	10	10	SE	1
13	OFN Traverse 2	Active	10	30	NW	1
14	OFN Traverse 2	Active	10	20	NW	1
15	OFN Traverse 2	Active	10	10	NW	1
1	OFN Traverse 3	Passive	5	N/A	N/A	30

4.2. Overview of Data Acquired at the I-270 COR Bridge over Mississippi River Site (Test Sites 2a and 2b)

Active and Passive MASW and ReMi data were acquired along linear traverses at the I-270 COR bridge over Mississippi River Test Sites 2a and 2b (Figure 4.3). Passive MASW data were also acquired along an L-shaped traverse.

A tabularized summary of the field data acquired at the I-270 COR bridge over Mississippi River (Test Sites 2a and 2b) is presented as Table 4.2.

Figure 4.3 I-270 COR bridge over Mississippi River (Test Site 2a and 2b; Figure 4.1) traverse locations.

Active and Passive MASW and ReMi data were acquired along linear traverses using both a 5-foot and a 10-foot geophone spacing. The active source, consisting of a metal plate and a 20-pound sledgehammer, was discharged at offset distances of 10 feet, 20 feet, 25 feet, and 30 feet. Passive MASW data were acquired along a non-linear (L-shaped) traverse.

Table 4.2 Tabularized summary of field data acquired at Test Sites 2a and 2b (I-270 COR bridge over Mississippi River; Figures 4.1 and 4.3). Active and passive data were acquired along a linear traverse using a geophone spacing of 5 and 10 feet.

Data Set Number	Test Site and Line	Data Type	Geophone Spacing, feet	Offset, feet	Source Location	Record Length, seconds
0	I-270 Traverse 1 (MO)	Active	5	30	NW	1
1	I-270 Traverse 1 (MO)	Active	5	30	NW	1
2	I-270 Traverse 1 (MO)	Active	5	25	NW	1
3	I-270 Traverse 1 (MO)	Active	5	20	NW	1
4	I-270 Traverse 1 (MO)	Active	5	10	NW	1
5	I-270 Traverse 1 (MO)	Active	5	30	SE	1
6	I-270 Traverse 1 (MO)	Active	5	25	SE	1
7	I-270 Traverse 1 (MO)	Active	5	20	SE	1
8	I-270 Traverse 1 (MO)	Active	5	10	SE	1
9	I-270 Traverse 1 (MO)	Passive	5	N/A	N/A	30
10	I-270 Traverse 1 (MO)	Active	10	30	SE	1
11	I-270 Traverse 1 (MO)	Active	10	20	SE	1
12	I-270 Traverse 1 (MO)	Active	10	10	SE	1
13	I-270 Traverse 1 (MO)	Active	10	0	SE	1
14	I-270 Traverse 1 (MO)	Active	10	10	NW	1
15	I-270 Traverse 1 (MO)	Active	10	0	NW	1
16	I-270 Traverse 1 (MO)	Passive	10	N/A	N/A	30
1	I-270 Traverse 2 (IL)	Active	5	30	W	1
2	I-270 Traverse 2 (IL)	Active	5	25	W	1

Data Set Number	Test Site and Line	Data Type	Geophone Spacing, feet	Offset, feet	Source Location	Record Length, seconds
3	I-270 Traverse 2 (IL)	Active	5	20	W	1
4	I-270 Traverse 2 (IL)	Active	5	10	W	1
5	I-270 Traverse 2 (IL)	Active	5	30	E	1
6	I-270 Traverse 2 (IL)	Active	5	25	E	1
7	I-270 Traverse 2 (IL)	Active	5	20	E	1
8	I-270 Traverse 2 (IL)	Active	5	10	E	1
9	I-270 Traverse 2 (IL)	Active	5	10	E	1
10	I-270 Traverse 2 (IL)	Passive	5	N/A	N/A	30
301	I-270 Traverse 2 (IL)	Active	5	30	N	1
302	I-270 Traverse 2 (IL)	Active	5	25	N	1
303	I-270 Traverse 2 (IL)	Active	5	20	N	1
304	I-270 Traverse 2 (IL)	Active	5	10	N	1
305	I-270 Traverse 2 (IL)	Active	5	30	S	1
306	I-270 Traverse 2 (IL)	Active	5	25	S	1
307	I-270 Traverse 2 (IL)	Active	5	20	S	1
308	I-270 Traverse 2 (IL)	Active	5	10	S	1
309	I-270 Traverse 2 (IL)	Passive	5	N/A	N/A	30 sec

4.3. Overview of Data Acquired at the MLK Connector, IDOT Site (Test Site 3)

Active and Passive MASW and ReMi data were acquired along linear traverses at the MLK connector, IDOT site (Figure 4.4). Passive MASW data were also acquired along L-shaped traverses. A tabularized summary of the field data acquired at MLK connector, IDOT site (Test Site 3) is presented as Table 4.3.

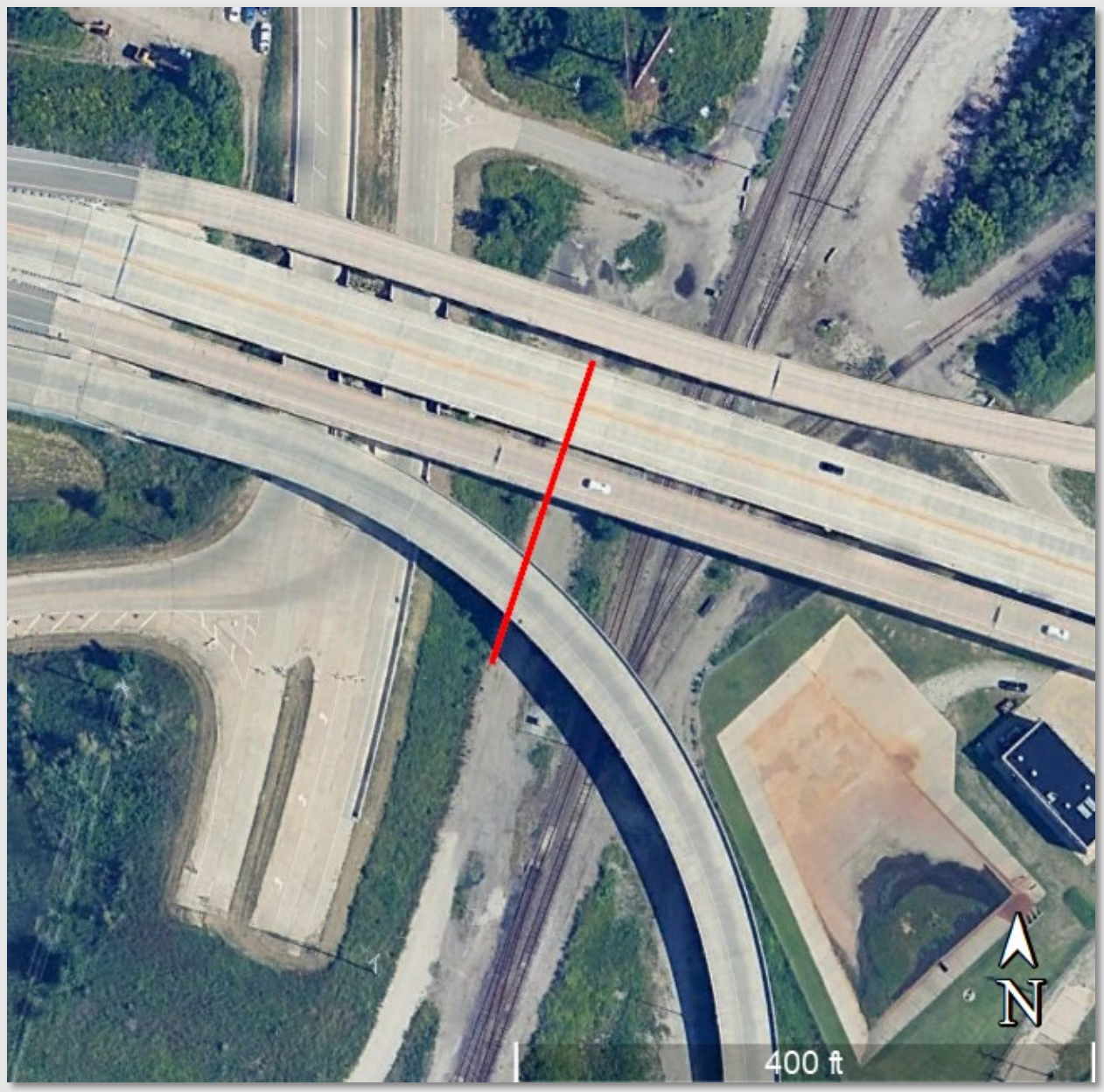

Figure 4.4 MLK connector, IDOT site (Test Site 3; Figure 4.1) traverse location. Active and Passive MASW and ReMi data were acquired along a linear array using both a 5-foot and a 10-foot geophone spacing. The active source, consisting of a metal plate and a 20-pound sledgehammer, was discharged at offset distances of 10 feet, 20 feet, 25 feet, and 30 feet.

Table 4.3 Tabularized summary of field data acquired at Test Site 3 (MLK connector, IDOT site; Figures 4.1 and 4.4). Active and passive data were acquired along a linear traverse using a geophone spacing of 5 and 10 feet.

Data Set Number	Test Site and Line	Data Type	Geophone Spacing, feet	Offset, feet	Source Location	Record Length, seconds
1	MLK Traverse 1	Passive	5	N/A	N/A	30
2	MLK Traverse 1	Active	5	30	NE	1
3	MLK Traverse 1	Active	5	25	NE	1
4	MLK Traverse 1	Active	5	20	NE	1
5	MLK Traverse 1	Active	5	10	NE	1
6	MLK Traverse 1	Active	5	30	SW	1
7	MLK Traverse 1	Active	5	25	SW	1
8	MLK Traverse 1	Active	5	20	SW	1
9	MLK Traverse 1	Active	5	10	SW	1
10	MLK Traverse 1	Active	10	10	NE	1
11	MLK Traverse 1	Active	10	0	NE	1
12	MLK Traverse 1	Active	10	0	SW	1
13	MLK Traverse 1	Active	10	30	SW	1
14	MLK Traverse 1	Active	10	20	SW	1
15	MLK Traverse 1	Active	10	10	SW	1
16	MLK Traverse 1	Passive	10	N/A	N/A	30

4.4. Comparative Analyses of the Acquired Test Field Data

SCI field-tested the four (4) non-invasive methods for determining the shear wave velocity of the subsurface to depths of 100 feet:

- Active MASW (Table 3.1);

- Passive MASW (Table 3.1);
- Active ReMi (Table 3.1);
- Passive ReMi (Table 3.1).

Test data were acquired at three (3) test sites:

1. SCI office in O'Fallon, Illinois (Figures 4.1 and 4.2);
2. I-270 COR bridge over Mississippi River (Figures 4.1 and 4.3);
3. MLK connector, IDOT site (Figures 4.1 and 4.4).

The intent was to identify the most effective method or methods based on the following criteria:

1. limited equipment, source, and personnel requirements for deployment;
2. straightforward data analysis; and
3. ease of interpretation of the results.

Based on the literature search, the field-test results, solicited input from users of the four (4) methods, and discussions with vendors, SCI recommended MoDOT utilize the following two (2) methods: Active MASW and Passive MASW. Although these methods employ different sources, they utilize the same field equipment, recording instrumentation, and processing software, and provide both complemental and supplemental outputs.

4.4.1. Field and Processed Data Acquired at the SCI Office in O'Fallon, Illinois (Test Site 1)

SCI acquired both active and Passive MASW data at the SCI office in O'Fallon, Illinois site (Test Site 1; Figures 4.1 and 4.2), using different combinations of the geophone spacings and source offsets. Example Active MASW data are presented as Figures 4.5, 4.6, and 4.7 and Passive MASW data as Figure 4.9.

A representative Active MASW data set, acquired with a 5-foot geophone spacing and a source offset of 20 feet, is presented on Figure 4.8. A representative Passive MASW data set, acquired with a 10-foot geophone spacing, is presented on Figure 4.10.

Data were processed in the SurfSeis software and a 1-D shear wave velocity profiles were generated to a depth of 100 feet for the Active (Figure 4.8C) and for the Passive (Figure 4.10C) MASW data.

A combined Active and Passive Overtone image was then generated, to pick a dispersion curve (Figure 4.11C) and then generate a combined 1-D shear wave velocity profile.

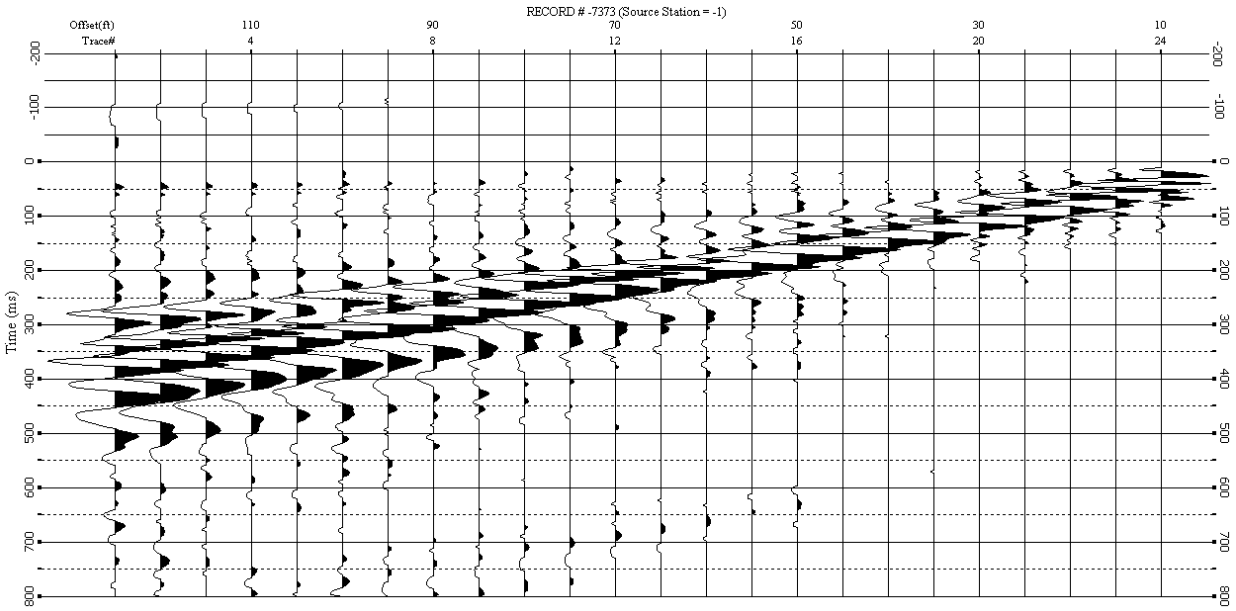

Figure 4.5 Active MASW data acquired along traverse 2 (Figure 4.2) using a 10-foot geophone spacing and a source offset of 30 feet. The vertical axis is in units of time (msec); the horizontal axis is in units of distance (feet).

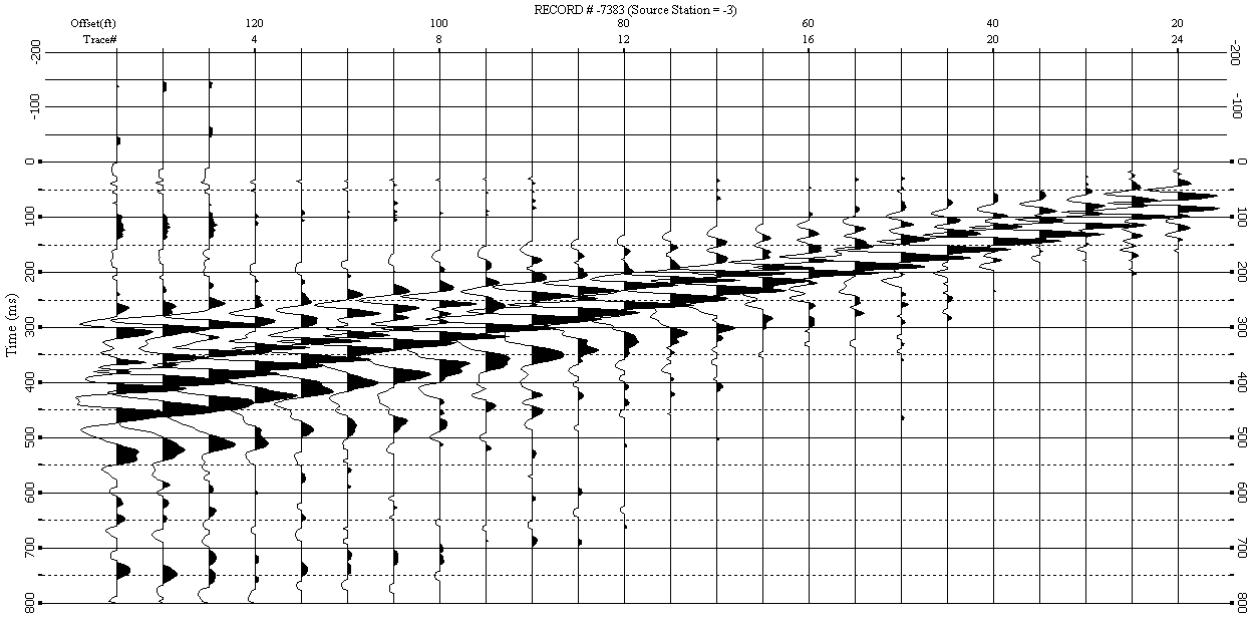

Figure 4.6 Active MASW data acquired along traverse 2 (Figure 4.2) using a 5-foot geophone spacing and a source offset of 20 feet. The vertical axis is in units of time (msec); the horizontal axis is in units of distance (feet).

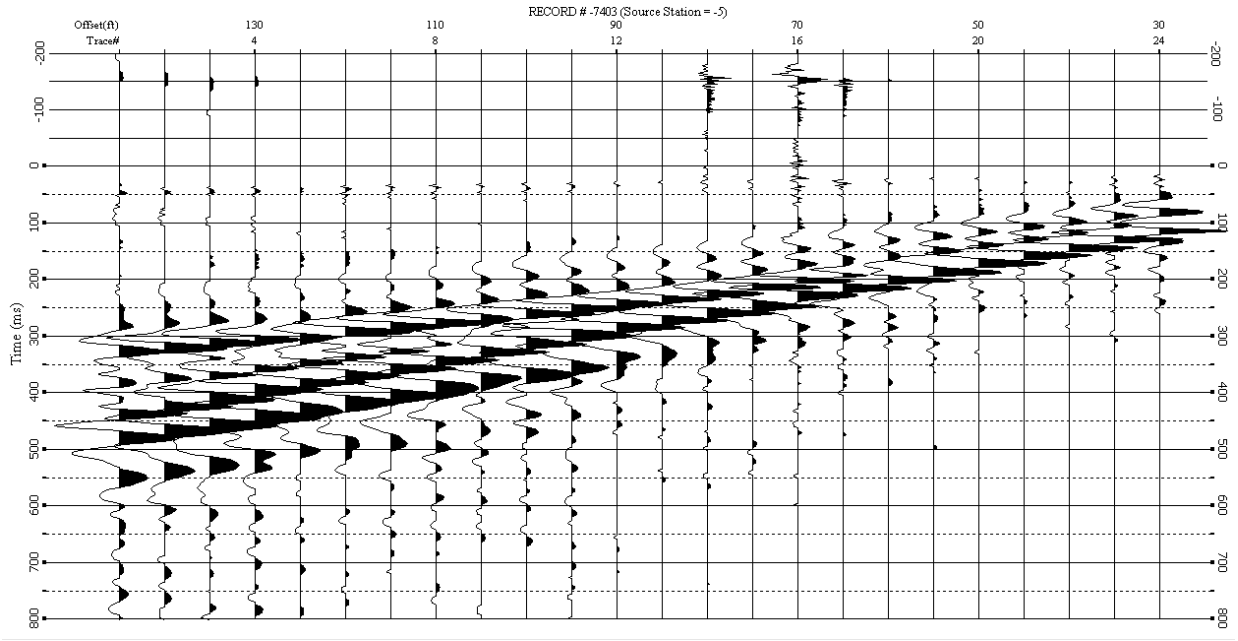

Figure 4.7 Active MASW data acquired along traverse 2 (Figure 4.2) using a 5-foot geophone spacing and a source offset of 30 feet. The vertical axis is in units of time (msec); the horizontal axis is in units of distance (feet).

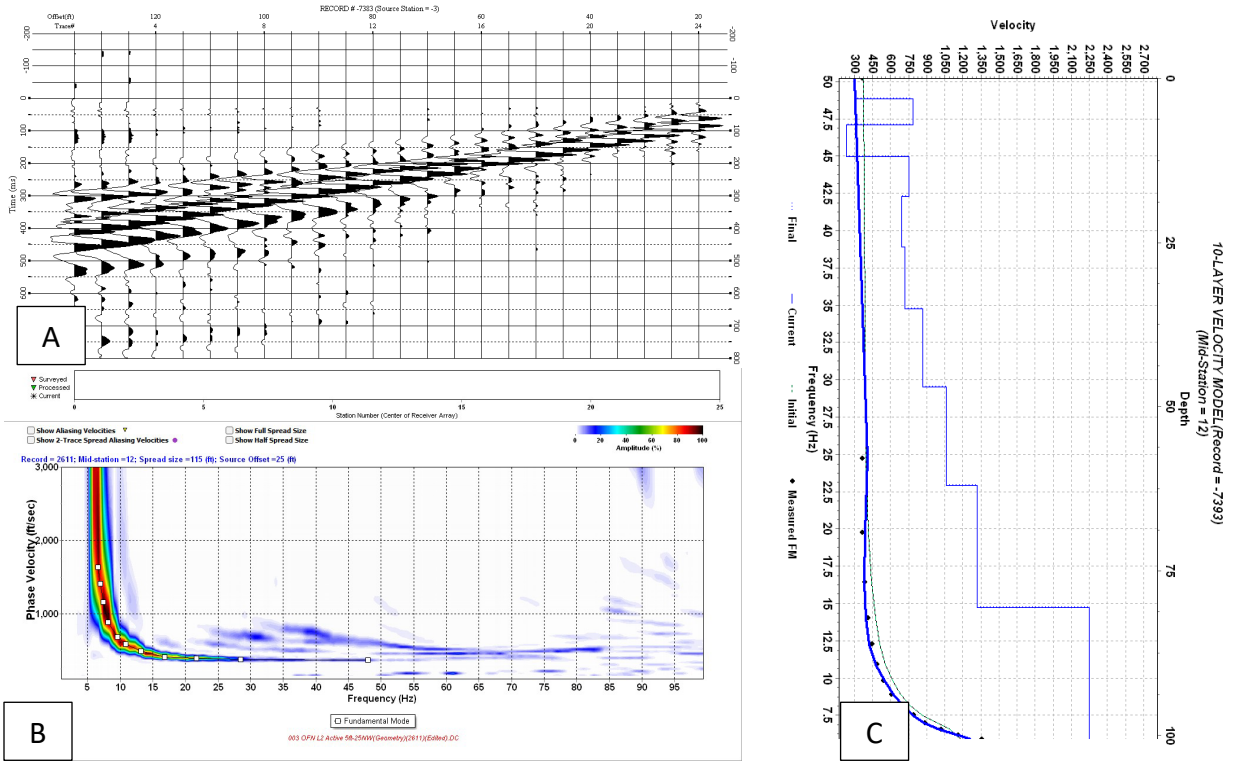

Figure 4.8 Overtone image (B) and output 1-D shear wave velocity profile (C) generated for the active data (A) acquired along traverse 2 (Figure 4.2) using a 5-foot geophone spacing and a source offset of 20 feet. The horizontal axis of the 1-D shear wave velocity profile is depth in units of feet; the vertical axis is shear wave velocity in units of ft/s. The horizontal axis of the overtone image is frequency in units of Hz; the vertical axis is shear wave velocity in units of ft/s.

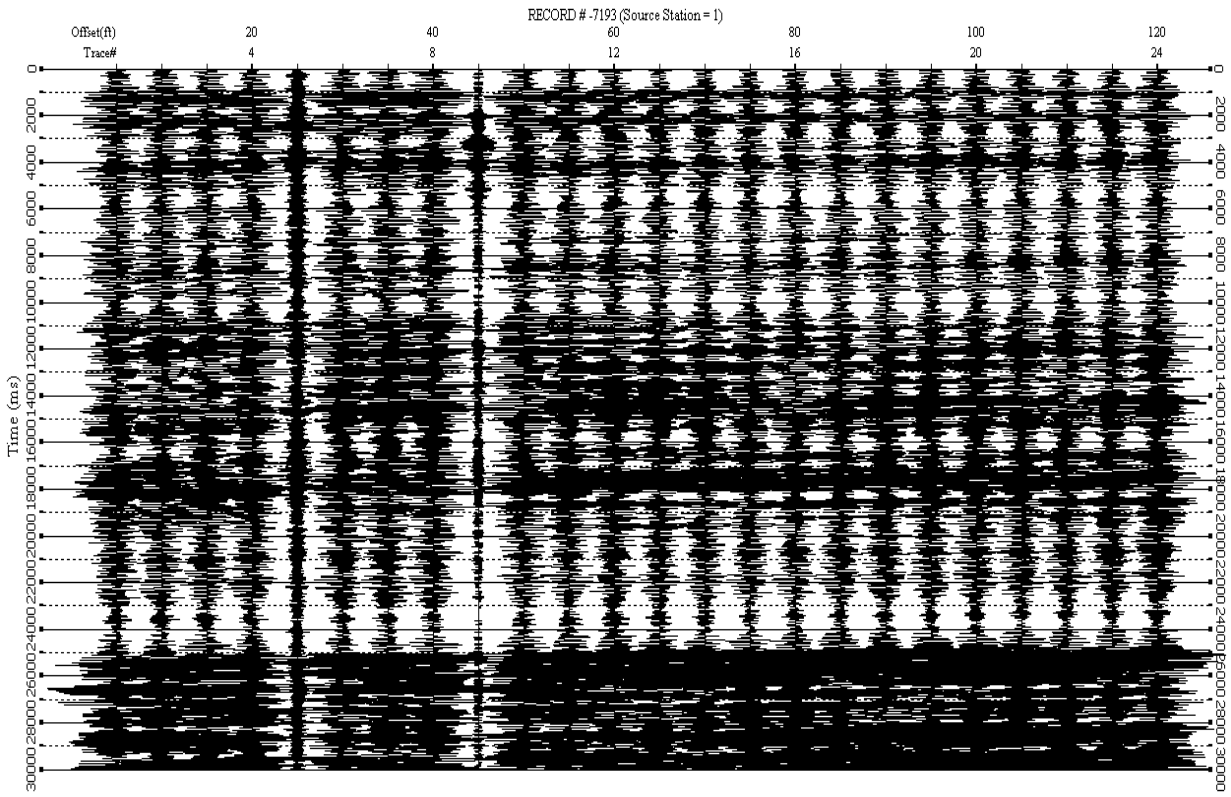

Figure 4.9 Example passive data acquired along traverse 2 (Figure 4.2) using a 10-foot geophone spacing and an ambient source. The vertical axis is in units of time (msec); the horizontal axis is in units of distance (feet).

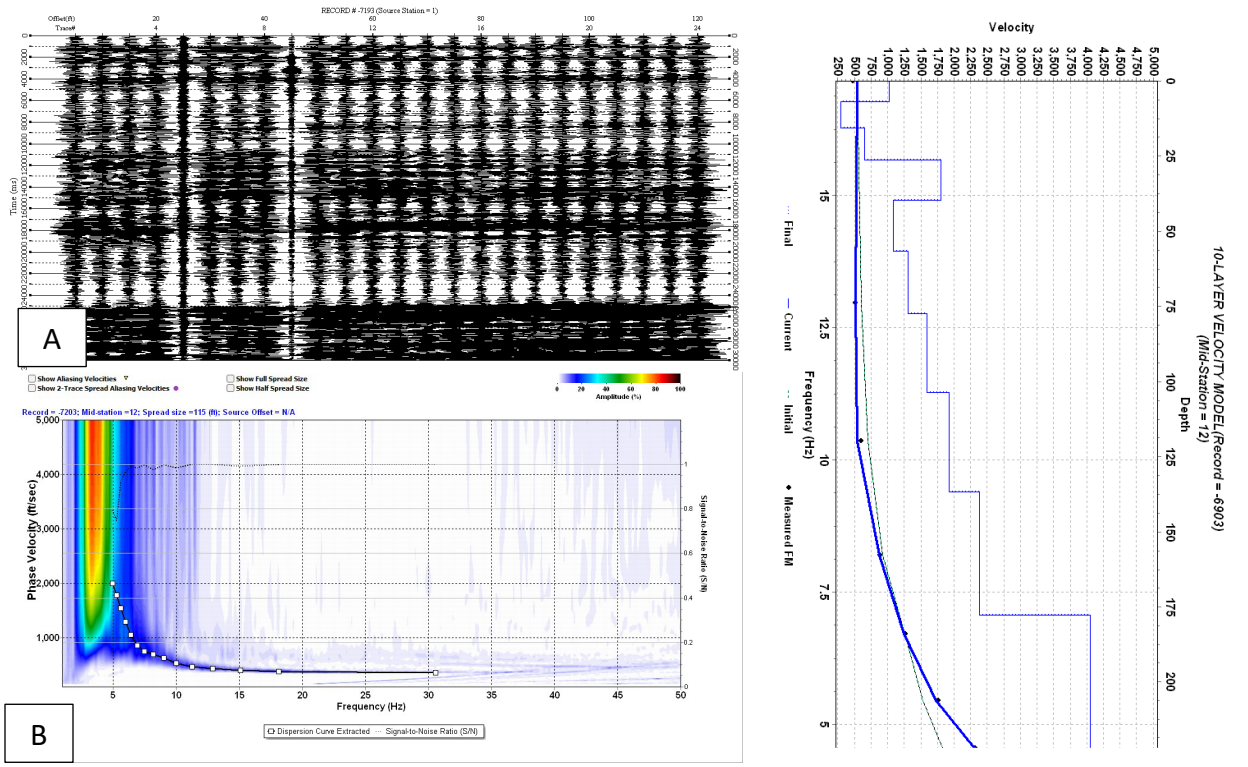

Figure 4.10 Overtone image (B) and output 1-D shear wave velocity profile (C) generated for the passive data (A) acquired along traverse 2 (Figure 4.2) using a 10-foot geophone spacing and an ambient source. The horizontal axis of the 1-D shear wave velocity profile is depth in units of feet; the vertical axis is shear wave velocity in units of ft/s. The horizontal axis of the overtone image is frequency in units of Hz; the vertical axis is shear wave velocity in units of ft/s.

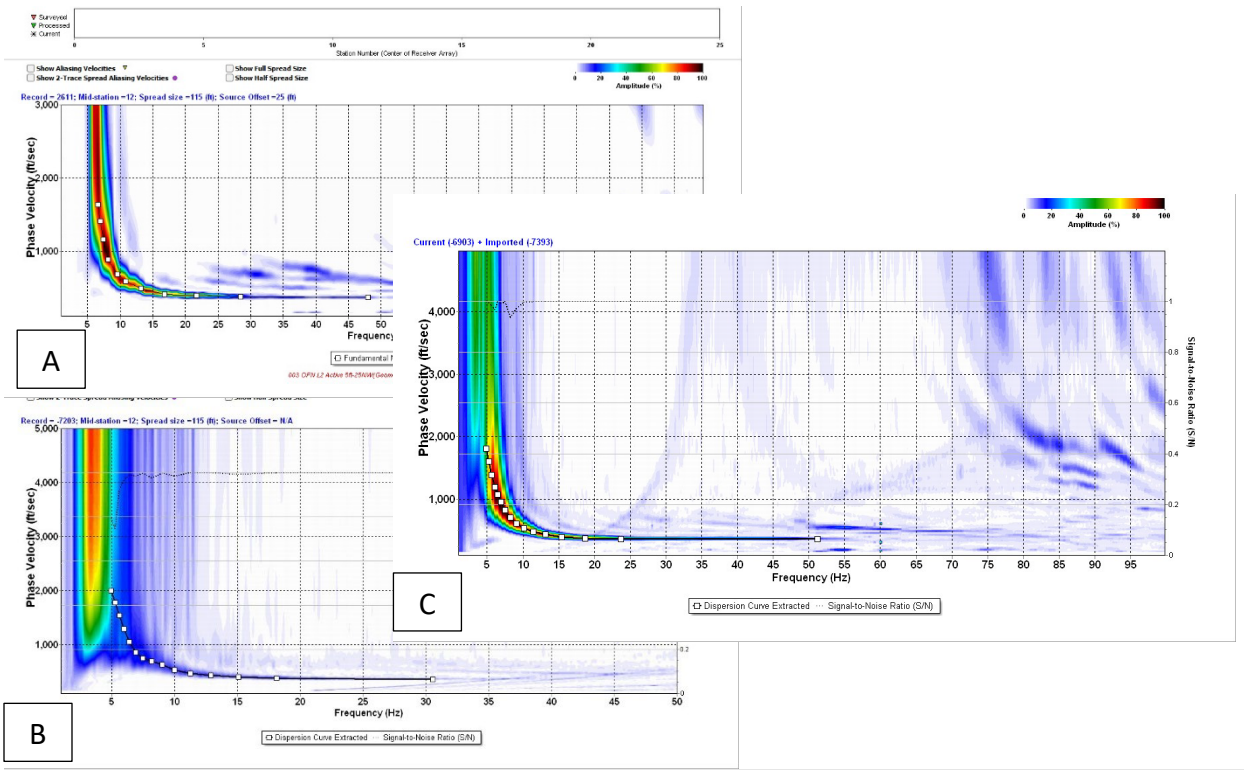

Figure 4.11 In this figure, the overtone images from Figures 4.8 (Active data) and 4.10 (Passive data) have been combined. The combined overtone image (C) has a lower frequency content than the active overtone image (Figure 4.8) and a higher frequency content than the passive overtone image (Figure 4.10). The horizontal axis of the overtone image is frequency in units of Hz; the vertical axis is shear wave velocity in units of ft/s.

Chapter 5 Method, Equipment, and Software Recommendations

Based on the literature search, the field-test results, solicited input from users of the four (4) methods, and discussions with vendors, SCI recommended MoDOT utilize the following two (2) methods: Active MASW and Passive MASW. Although these methods employ different sources, they utilize the same field equipment, recording instrumentation, and processing software, and provide both complemental and supplemental outputs.

SCI determined that the MASW method was superior to the ReMi method for several reasons as noted in the section of Table 3.1 entitled "**Other Considerations**".

1. Active and Passive MASW data can be acquired as readily as ReMi data.
2. The MASW and ReMi methods utilize the same equipment but significantly different processing software.
3. MASW software is more sophisticated and user friendly than ReMi software.
4. MASW software is routinely upgraded by the developers; ReMi software does not appear to be routinely upgraded.
5. Passive MASW data can be acquired using non-linear arrays; Passive ReMi data cannot. This is a significant advantage at test sites where the source of ambient surface wave energy is unknown.
6. Love wave data can be acquired and processed using MASW technology. It cannot be processed using ReMi technology.
7. Higher mode Rayleigh wave data can be processed separately for comparative purposes using the MASW software. Higher mode Rayleigh wave data cannot be processed using the MASW software.

5.1 Hardware

Based on the results of this study, SCI recommends that MoDOT acquire the following equipment and hardware:

Based on the results of this study, SCI recommends that MoDOT acquire the following equipment, hardware, and software:

1. 24-channel Geometrics Geode Exploration Seismograph.
2. SurfSeis software by Kansas Geological Survey (KGS) for processing Active and Passive MASW data.
3. Windows based laptop or tablet.

A Geometrics Geode exploration system (Figure 5.1), including:

1. 24-channel Geometrics Geode exploration seismograph;

2. Geode Laptop Adaptor (with ethernet to USB connector, if necessary);
3. Geode (seismograph) Power Cable;
4. Seismic cable with 24 channel Mueller clip connections and 61-socket connectors;
5. Free standing reel for the seismic cable;
6. Twenty-six (26) (24 connected to the array and 2 spare) vertical 4.5-Hertz geophones; (with spike and Mueller clip connectors),
7. Twenty-six (26) base plates for geophones;
8. Trigger Extension Cable;
9. Hammer Switch (aka Impact sensor, Trigger);
10. Seismic source: 20-pound sledgehammer is recommended;
11. Aluminum (preferred due to lighter weight) or steel strike plate: 6x6x0.75 inches to 10x10x1 inches;
12. Polyethylene strike plate: 10x10x2 inches;
13. Power source: AGM deep cycle or Lithium-Ion 12-V rechargeable battery.

Refer to Appendix B hardware assembly detailed instructions.

Figure 5.1 Equipment and hardware for MASW data acquisition.

5.2 Software

SCI has conducted research on software that can be potentially used for processing MASW (Active and Passive) and ReMi (Active and Passive) data and evaluated seven (7) software package options:

1. SeisOpt ReMi™. Software suite, developed by Optim, was made available commercially in 2004, primarily for ReMi data processing. One of the first commercial software packages for surface wave data processing. The software supported Passive ReMi methods and 1D and 2D shear wave velocity profiles. However, as of 2024 the software was not available for purchase.
2. ZondST2d1. A software package, developed by Zond Software LTD, is used for 1D MASW and ReMi data processing and interpretation. A 2D module is also available for mathematical modeling and joint inversion of MASW and other seismic (i.e., refracted and reflected) data sets. The software developer is registered in Cyprus.
3. Surface Plus. Software, developed by Geogiga Technology Corp, is designed for active and passive surface wave data analysis, including MASW and ReMi methods. The software features 1D and 2D data processing and visualization of shear wave velocity models.
4. ParkSeis. Software, developed by Park Seismic LLC, is used for analyzing MASW data, generating shear wave velocity profiles in 1-D, 2-D, and depth slices. Supports Active and Passive MASW surveys.
5. SurfSeis. Software package, developed by Kansas Geological Survey, process seismic data using the Active and Passive MASW methods. The software features optional additional modules for advanced data processing, such as high-resolution linear radon transform, multi-mode inversion, Love-wave processing, Scholte-wave (i.e., underwater MASW) processing.
6. SeisImager/SW2. Software, developed and supported by Geometrics, designed for the analysis of surface wave data, particularly for MASW. Supports both active and Passive MASW data processing, allowing for the combination of high-frequency data from shallow depths and low-frequency data from deeper layers into one shear wave velocity plot.
7. RadExPro3. A comprehensive software package, developed by RadExPro Seismic Software, designed primarily for processing of seismic reflection and refraction seismic data, but also supports MASW data processing. The software developer is registered in Republic of Georgia.

Below is a summary Table 5.1 on the MASW and ReMi software options with emphasis on ability to process MASW, ReMi or both data sets, type of license (dongle key, hardwire-tied or network), compliance with MoDOT IS (Information Systems) requirements, User Friendly/ Straightforwardness and Approximate cost. Fields marked as N/A indicate that the answers were not available during the research in the fall of 2024, due to the company being out of

business, non-response at the time of the contact and/or inability to evaluate the criteria due to other reasons.

Table 5.1 Evaluated MASW and ReMi software options.

Software	Data Type	License type (dongle, hardwire-tied or network)	Compliance with MoDOT IS requirements	User-Friendly / Straightforwardness	Approximate Cost (Fall 2024)
1. SeisOpt	Passive	Hardwire-tied	-	No	N/A
2. ZondST2d	Active and Passive	USB Dongle	No	No	$1,150 and up, perpetual
3. Surface Plus	Active and Passive	USB Dongle	Yes	N/A	$4,900 perpetual, or $2,900 annual fee
4. ParkSeis	Active and Passive	USB Dongle	N/A	Yes	$4,500 perpetual
5. SurfSeis	Active and passive	USB Dongle	Yes	Yes	$3,900 and up, perpetual, updates for an extra fee
6. SeisImager/SW	Active and passive	Hardwire-tied	No	Yes	$2,200 and up, perpetual
7. RadExPro	Active	USB Dongle	No	N/A	$7,000 and up

Chapter 6 Field Demonstration of the Recommended Method at the Test Site

A MoDOT team consisting of four members traveled to St. Louis, Missouri for the preferred method (MASW) demonstration conducted by SCI at the I-270 Chain of Rocks (COR) Bridge over Mississippi River (Test Site 2a; Coordinates 38.766181°, -90.179479°; Figures 4.1 and Figure 4.3) on December 10, 2024.

The demonstration consisted of field data acquisition at the test site, followed by the presentation on the shear wave velocity measurement methodology, equipment, hardware and software overview, data processing and interpretation. A data set acquired during the demo was processed in the recommended software SurfSeis by Kanas Geological Survey.

Figure 6.1 Photographs taken during the field demonstration beneath the Chain of Rocks Bridge.

For demonstration purposes, Active and Passive MASW field data were acquired at the test location along one traverse oriented approximately east to west, using different geophone spacing and source offsets. The Active MASW data were acquired using linear arrays of twenty four (24) geophones with 4.5 Hz central frequency, spaced at both 5-foot and 10-foot intervals. The active source, consisting of a metal plate and a 20-pound sledgehammer, was discharged at offset distances of 10 feet, 20 feet, 25 feet, and 30 feet.

The Passive MASW data were similarly acquired using a linear array of twenty four (24) geophones with 4.5 Hz central frequency, spaced at both 5-foot and 10-foot intervals. The Passive MASW data were recorded using ambient surface wave energy as the source.

An SCI representative acquired Active MASW data and a generated overtone image for the traverse oriented approximately southeast to northwest during the field demonstration, using a 5-foot geophone spacing and a source offset of 25 feet, located on the southeast, is presented in Figure 6.2. Five (5) 1-second seismic records were recorded and stacked during data processing.

An SCI representative acquired Passive MASW data and a generated overtone image for the same traverse, using a 5-foot geophone spacing is presented in Figure 6.3. Thirty (30) seismic records, each with a 30 second duration, were recorded and stacked during data processing.

Figure 6.4 (A) depicts the combined overtone images from active data and passive data. The combined overtone image has a lower frequency content from the passive data and a higher frequency content from the active data.

It was demonstrated that shear wave data can be successfully acquired using the MASW method to a depth of 100 feet or greater. The MASW method is the most effective method and meets the criteria of 1) limited equipment, source, and personnel requirements for deployment; 2) straightforward data analysis; and 3) ease of interpretation of the results.

The fundamental data acquisition and processing steps for both Active and Passive MASW surveys are outlined in the Appendices A and B. It is important to emphasize that the recommended workflow is based on the test data acquired during this project and may have to be modified to accommodate different site conditions or project requirements. Selecting incorrect data acquisition or processing parameters can potentially lead to misinterpretation of the subsurface conditions. For advanced MASW data processing refer to a KGS SurfSeis software manual.

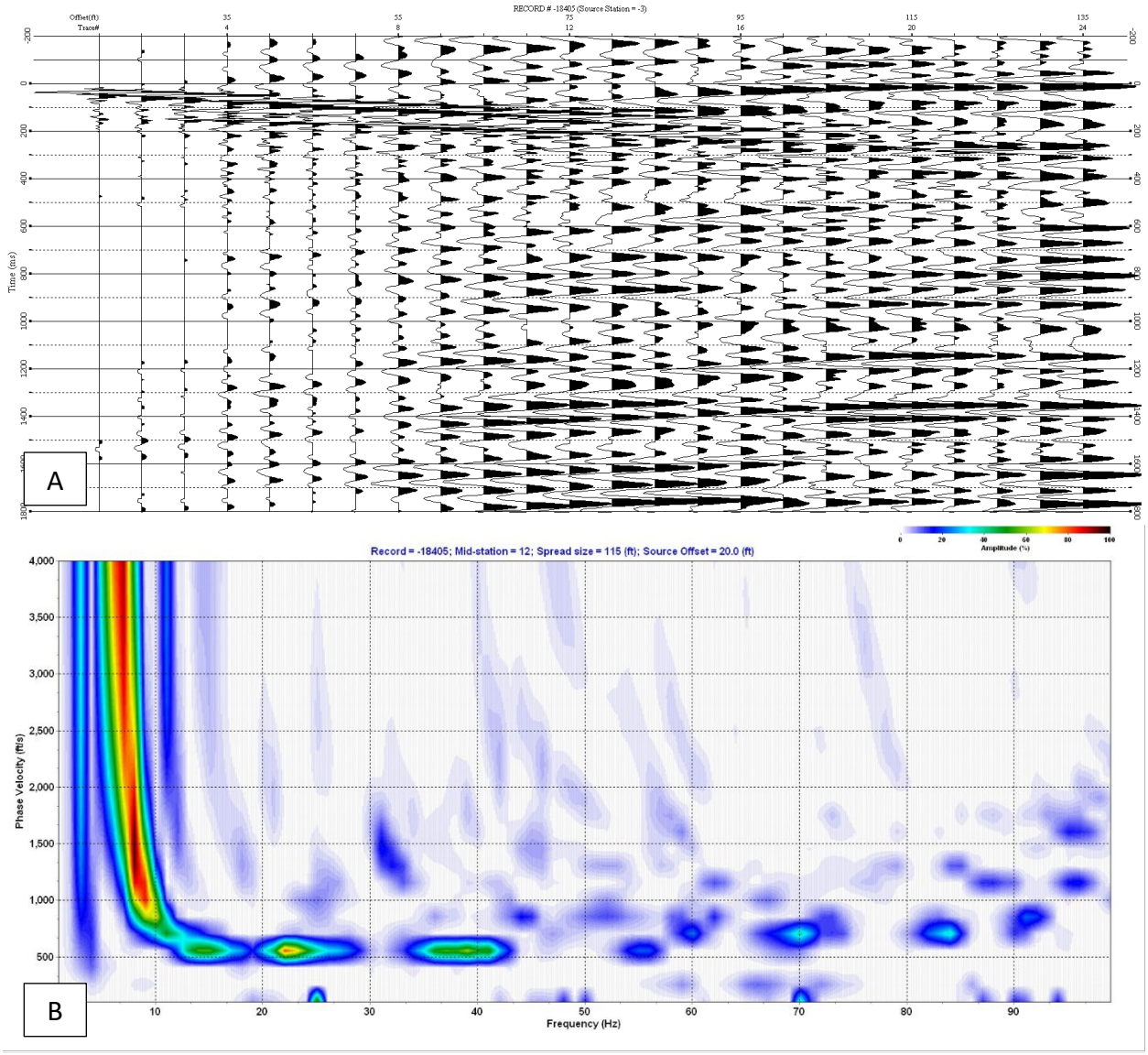

Figure 6.2 Acquired Active MASW data (A) and a generated overtone image (B) for the traverse oriented approximately southeast to northwest during the field demonstration, using a 5-foot geophone spacing and a source offset of 25 feet, located on the southeast. Five (5) 1-second seismic records were recorded and stacked during data processing. The vertical axis is in units of time (msec); the horizontal axis is in units of distance (feet).

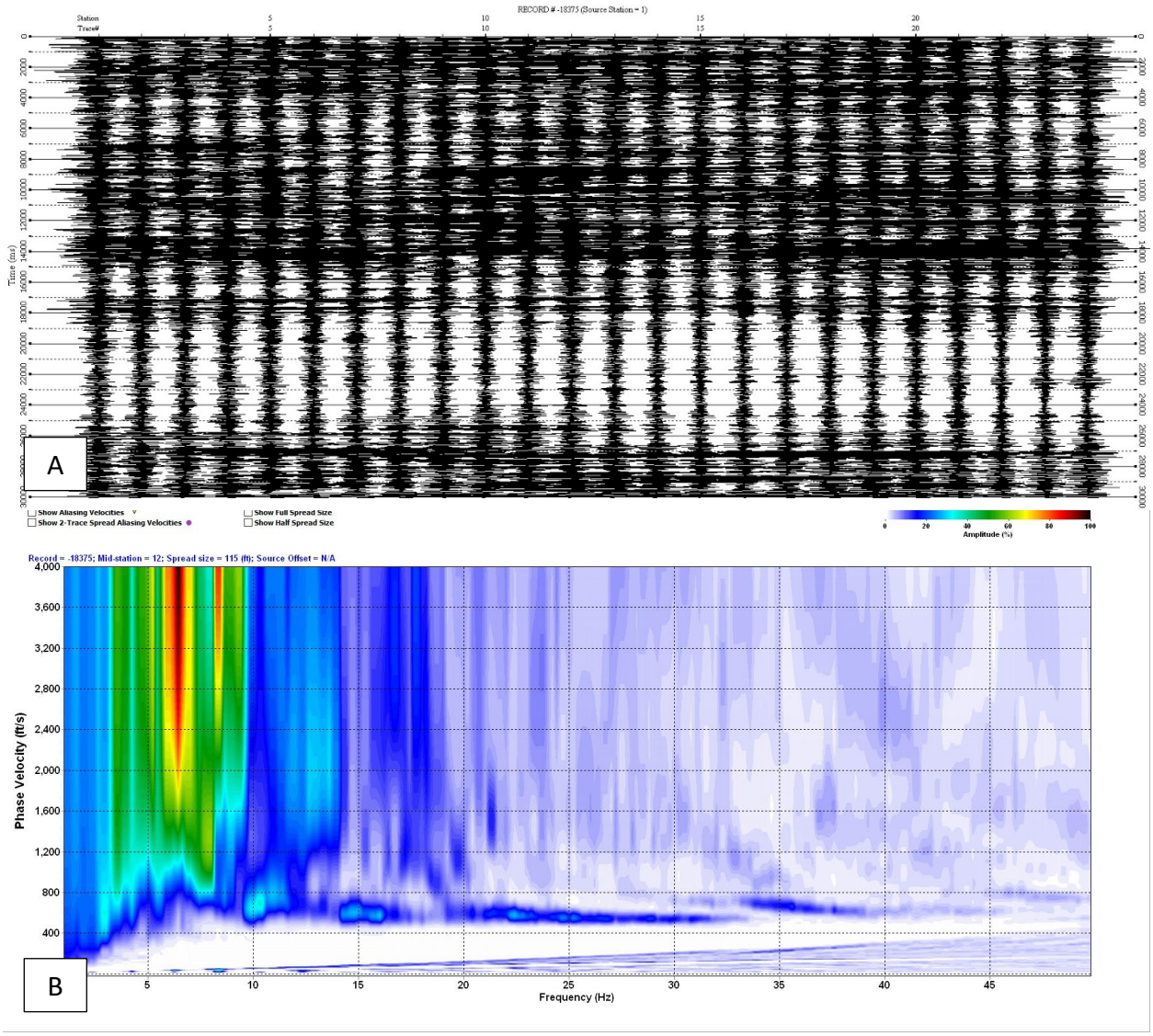

Figure 6.3 Acquired Passive MASW data (A) and a generated overtone image (B) for the traverse oriented approximately southeast to northwest during the field demonstration, using a 5-foot geophone spacing. Thirty (30) 30-second seismic records were recorded and stacked during data processing. The vertical axis is in units of time (msec); the horizontal axis is in units of distance (feet).

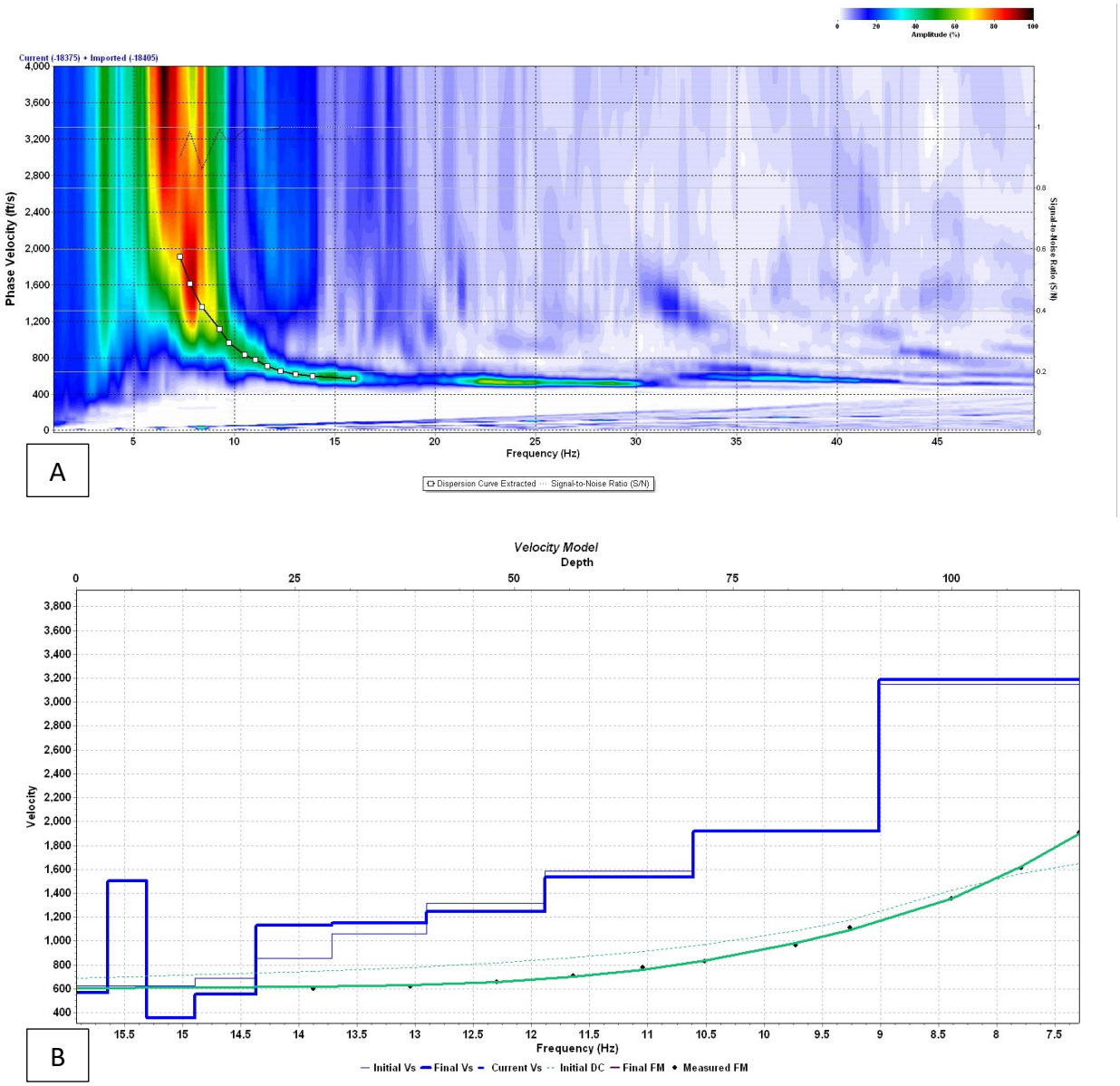

Figure 6.4 Overtone image (A) and output 1-D shear wave velocity profile (B) generated for the combined active data (Figure 6.2) and passive data (Figure 6.3). The combined overtone image (A) has a lower frequency content from the passive data and a higher frequency content from the active data. The horizontal axis of the overtone image is frequency in units of Hz; the vertical axis is shear wave velocity in units of ft/s. The horizontal axis of the 1-D shear wave velocity profile is shear wave velocity in units of ft/s; the vertical axis is depth in units of feet.

References

Abarello D., 2001, Detection of spurious maxima in the site amplification characteristics estimated by the HVSR technique: Bull Seis Soc Am 91(4):718–724.

Aki K., 1957, Space and time spectra of stationary stochastic waves, with special reference to microtremors: Bulletin Earthquake Research Inst. 35:415–456.

Albarello D., Cesi C., Eulilli E., Guerrini F., Lunedei E., Paolucci E., Pileggi D., and Puzzilli L.M., 2011, The contribution of the ambient vibration prospecting in seismic microzoning: an example from the area damaged by the April 6, 2009, L'Aquila (Italy) earthquake: Bolletino Di Geofisica Teorica Ed Applicata 52(3):513–538.

Albarello D., and Lunedei E., 2013, Combining horizontal ambient vibration components for H/V spectral ratio estimates: Geophys J Int 194(2):936–951.

American Society for Testing and Materials (ASTM), 2008, Standard Test Method for Standard Penetration Test (SPT) and Split-Barrel Sampling of Soils: ASTM Standard Method D1586-08a: ASTM, West Conshohocken, PA.

Andrews D.J., 1986, Objective determination of source parameters and similarity of earthquakes of different size, in Earthquake Source Mechanics, S. Das (Editor): American Geophysical Monograph 37:259–267.

Anderson, N., Sneed, L. and Rosenblad, B., 2015, MoDOT pavement preservation research program volume IV, pavement evaluation tools-data collection methods (No. cmr 16-004), Missouri. Dept. of Transportation. Division of Construction and Materials. Report.

Andrus R.D., Piratheepan P., Ellis B., Zhang J., and Juang H., 2004, Comparing liquefaction evaluation methods using penetration VS relationships: Soil Dynamics Earthquake Engineering, Vol. 24, pp. 713–721.

Arai H., and Tokimatsu K., 1998, Evaluation of local site effects based on microtremor H/V spectra: In Proceedings of the 2nd international symposium on the effects of surface geology on seismic motion (Vol. 2, pp. 673-680). Japan: Yokohama.

Arai H., and Tokimatsu K., 2000, Effects of Rayleigh and Love waves on microtremor H/V spectra: In Proceedings of the 12th World Conference on Earthquake Engineering (Vol. 2232, pp. 1-8). Auckland, New Zealand: New Zealand Society for Earthquake Engineering Inc.

Arai H., and Tokimatsu K., 2004, S-wave velocity profiling by inversion of microtremor H/V spectrum: Bull Seis Soc Am 94(1):53–63.

Arai H., and Tokimatsu K., 2005, S-wave velocity profiling by joint inversion of microtremor dispersion curve and horizontal-to-vertical (H/V) spectrum: Bull Seis Soc Am 95(5):1766–1778.

Asten M., Yong A., et al., 2022, Assessment of uncertainties in VS profiles obtained from microtremor observations in the phased 2018 COSMOS blind trials: Journal of Seismology 26, pages 757–780.

Bahavar M., Spica Z.J., Sánchez-Sesma F.J., Trabant C., Zandieh A., and Toro G., 2020, Horizontal-to-vertical spectral ratio (HVSR) IRIS station toolbox: Seis Res Lett 91:3539–3549.

Bard P.Y., Acerra C., Aguacil G., Anastasiadis A., Atakan K., Azzara R., Basili R., Bertrand E., Bettig B., Blarel F., Bonnefoy-Claudet S., Paola B., Borges A., Sørensen M., Bourjot L., Cadet H., Cara F., Caserta A., Chatelain J.L., and Zacharopoulos S., 2008, Guidelines for the implementation of the H/V spectral ratio technique on ambient vibrations measurements, processing and interpretation: Bull Earthq Eng 6(1):1–2

Bard P.Y., 1999, Microtremor measurements: a tool for site effect estimation: In Proceedings of the Effects of Surface Geology on Seismic Motion 3:1251–1279.

Bard P.Y., and Bouchon M., 1985, The two-dimensional resonance of sediment-filled valleys: Bull Seis Soc Am 75(2):519–541.

Bignardi S., Yezzi A.J., Fiussello S., and Comelli A., 2018, Open HVSR-Processing toolkit: enhanced HVSR processing of distributed microtremor measurements and spatial variation of their informative content: Comput Geosci 120:10–20.

Bonilla L.F., Steidl J.H., Lindley G.T., Tumarkin A.G., and Archuleta R.J., 1997, Site amplification in the San Fernando Valley, California: variability of site-effect estimation using the S-wave, coda, and H/V methods.: Bull Seis Soc Am 87(3):710–730.

Bonnefoy-Claudet S., Cotton F., and Bard P., 2006 The nature of noise wavefield and its applications for site effects studies: a literature review: Earth-Sci Rev 79(3–4):205–227,

Bonnefoy-Claudet S., Köhler A., Cornou C., Wathelet M., and Bard P.Y., 2008, Effects of Love waves on microtremor H/V ratio: Bull Seis Soc Am 98(1):288–300.

Bonnefoy-Claudet S., Baize S., Bonilla L.F., Berge-Thierry C., Pasten C., Campos J., Volant P., and Verdugo R., 2009, Site effect evaluation in the basin of Santiago de Chile using ambient noise measurements: Geophys J Int 176(3):925–937.

Borcherdt R.D., 1970, Effects of local geology on ground motion near San Francisco Bay: Bull Seis Soc Am 60(1):29–61.

Bour M., Fouissac D., Dominique P., and Martin C., 1998, On the use of microtremor recordings in seismic microzonation: Soil Dyn and Earthquake Eng 17:465–474.

Brown L.T., Boore D.M., and Stokoe K.H., 2002, Comparison of shear wave slowness profiles at 10 strong motion sites from noninvasive SASW measurements and measurements made in boreholes: Bulletin Seismologic Society America, Vol. 92, pp. 3116–3133.

Cadet H., Bard P.Y., Duval A.M., and Bertrand E., 2012, Site effect assessment using KiK-net data: part 2 – site amplification prediction equation based on f0 and VSZ: Bull Earthquake Eng 10:451–489. https:// doi. org/ 10. 1007/ s10518- 011- 9298-7.

Castellaro S., and Mulargia F., 2009, VS30 estimates using constrained H/V measurements: Bull Seis Soc Am 99(2A):761–773.

Castellaro S., and Mulargia F., 2009, The effect of velocity inversions on H/V: Pure Appl Geophys 166(4):567–592.

Castellaro S., and Mulargia F., 2010, How far from a building does the ground-motion free-field start? The cases of three famous towers and a modern building: Bull Seis Soc Am 100(5A):2080–2094.

Chatelain J.L., and Guillier B., 2013, Reliable fundamental frequencies of soils and buildings down to 0.1 Hz obtained from ambient vibrations recordings with a 4.5-Hz sensor: Seism Res Lett 84(2):199–209. https:// doi. org/ 10. 1785/ 02201 20003.

Chatelain J.L., Guillier B., Cara F., et al., 2008, Evaluation of the influence of experimental conditions on H/V results from ambient noise recordings: Bull Earthq Eng 6(1):33–74.

Cheng T., Hallal M.M., Vantassel J.P., and Cox BR., 2021, Estimating Unbiased Statistics for Fundamental Site Frequency Using Spatially Distributed HVSR Measurements and Voronoi Tessellation: J Geotech Geoenviron, 147(8), 04021068.

Cheng T., Cox B.R., Vantassel J.P., and Manuel L., 2020, A statistical approach to account for azimuthal variability in single-station HVSR measurements: Geophys J Int 223(2):1040–1053.

Chien L.K.; Lin M.C.; and Oh Y.N., 2000, Shear wave velocity and SPT-N values of in-situ reclaimed soil in west Taiwan: Journal Geotechnical Engineering, Vol. 31, pp. 63–77.

Cipta A., Cummins P., Dettmer J., Saygin E., Irsyam M., Rudyanto A., and Murjaya J., 2018, Seismic velocity structure of the Jakarta Basin, Indonesia, using trans-dimensional Bayesian inversion of horizontal-to-vertical spectral ratios: Geophys J Int 215(1):431–449.

Cornou C., Guéguen P., Bard P.Y., and Hagshenas E., 2004, Ambient noise energy bursts observation and modeling: trapping of structure-soil harmonic induced-waves in a topmost sedimentary layer: J Seismolog 8(4):507–524.

Cox B.R., Cheng T., Vantassel J.P., and Manuel L., 2020, A statistical representation and frequency-domain window-rejection algorithm for single-station HVSR measurements: Geophys J Int 221(3):2170–2183. https:// doi. org/ 10. 1093/ gji/ ggaa11 9.

D'Alessandro A., Luzio D., Martorana R., and Capizzi P., Selection of time windows in the horizontal-to-vertical noise spectral ratio by means of cluster analysis: Bull Seis Soc Am 106(2):560–574.

D'Amico V., Picozzi M., Baliva F., and Albarello D., 2008, Ambient noise measurements for preliminary site-effects characterization in the Urban area of Florence, Italy: Bull Seis Soc Am 98:1373–1388.

Dal Moro, G., 2019, Pure and Effective Active and Passive Seismics for the Characterization of Urban and Remote Areas: Four Channels for Seven Objective Functions: Applied Geophysics, 176, pages 1445–1465.

Delgado J., López Casado C., Estévez A., Giner J., Cuenca A., Molina S., 2000, Mapping soft soils in the Segura River valley (SE Spain): a case study of microtremors as an exploration tool: J Appl Geophys 45:19–32.

Di Giacomo D., Gallipoli M.R., Mucciarelli M., Parolai S., and Richwalski S., 2005, Analysis and modeling of HVSR in the presence of a velocity inversion: The case of Venosa: Italy Bull Seis Soc Am 95(6):2364–2372.

Di Giulio G., Savvaidis A., Theodoulidis N., et al., 2010, Inversion of surface wave dispersion at European strong motion sites using a multi-model parameterization and an information-theoretic approach: In Proceedings of the 14th European Conference on Earthquake Engineering, 4595, Ohrid, Macedonia.

Dietiker B., Pugin A.J.M., Crow H.L., Mallozzi S., Brewer K.D., Cartwright T.J., and Hunter J.A., 2018, HVSR measurements in complex sedimentary environment and highly structured resonator topography-Comparisons with seismic reflection profiles and geophysical borehole logs: Society of Exploration Geophysicists and Environment and Engineering Geophysical Society. https://doi. org/10. 4133/sageep. 31-02 5.

Dietiker B., Hunter J.A., and Pugin A.J., 2020, Improved analysis of horizontal-to-vertical spectral ratio measurements for groundwater investigations: Geological Survey of Canada, Open File 8536:159–170.

Dobry R., Oweis I., and Urzúa A., 1976, Simplified procedures for estimating the fundamental period of a soil profile: Bull Seis Soc Am 66(4):1293–1321.

Dunand F., Bard P.Y., and Chatelain J.L., et al., 2002, Damping and frequency from Randomdec method applied to in situ measurements of ambient vibrations. Evidence for effective soil structure interaction: In Proceedings of the 12th European Conference on Earthquake Engineering, London. Paper (Vol. 869).

Dennis R., Hiltunen S.M., and Woods, R.D., 1998, SASW and cross-hole test results compared: In Earthquake Engineering Soil Dynamics II, Recent Advances in Ground Motion Evaluation: Geotechnical Special Publication 20: American Society of Civil Engineers, Park City, UT, pp. 279–289.

Edwards W.N., 2015, Analysis of measured wind turbine seismic noise generated from the Summerside Wind Farm. Prince Edward Island: Geological Survey of Canada, Open File Report 7763:1–66.

Endrun B., 2011, Love wave contribution to the ambient vibration H/V amplitude peak observed with array measurements: J Seismolog 15(3):443–472.

Feigenbaum D.Z., Ivanov J., Miller R.D., Peterie S.L, and Morton S.L.C., 2016, Near-surface Qs estimations using multi-channel analysis of surface waves (MASW) and the effect of non-fundamental mode energy on Q-estimation: An example from Yuma Proving Ground, Arizona: SEG Technical Program Expanded Abstracts 2016, pp. 4971-4976.

Field E., and Jacob K., 1993, The theoretical response of sedimentary layers to ambient seismic noise. Geophys Res Lett 20(24):2925–2928.

Foti S., Hollender F., Garofalo F., et al., 2018, Guidelines for the good practice of surface wave analysis: a product of the InterPACIFIC project: Bull Earthq Eng 16(6):2367–2420.

Fukushima Y., Bonilla L., Scotti O., and Douglas J., 2007, Site classification using horizontal-to-vertical response spectral ratios and its impact when deriving empirical ground-motion prediction equations: J Earthquake Eng 11:712–724.

Fumal T.E., and Tinsley, J.C., 1985, Mapping Shear Wave Velocities of Near Surface Geological Materials: Predicting Aerial Limits of Earthquake Induced Landsliding: U.S. Geologic Survey Professional Paper 1360, pp. 127–150.

García-Jerez A., Piña-Flores J., Sanchez-Sesma F., Luzon F., and Perton M., 2016, A computer code for forward calculation and inversion of the H/V spectral ratio under the diffuse field assumption: Comput Geosci 97:67–78.

Garofalo F., Foti S., Hollender F., Bard P.Y., Cornou C., Cox B.R., Ohrnberger M., Sicilia D., Asten M., Di Giulio G., Forbriger T., Guillier B., Hayashi K., Martin A., Matsushima S., Mercerat D., Poggi V., and Yamanaka H, 2016, InterPACIFIC project: Comparison of invasive and non-invasive methods for seismic site characterization. Part I: Intra-comparison of surface wave methods. Soil Dyn Earthq Eng 82:222–240.

Gorstein M, and Ezersky M., 2015, Combination of HVSR and MASW Methods to Obtain Shear Wave Velocity Model of Subsurface in Israel: International journal of geohazards and environment, DOI:10.15273/ijge.2015.01.004

Gosar A., and Lenart A., 2010, Mapping the thickness of sediments in the Ljubljana Moor basin (Slovenia) using microtremors: Bull Earthq Eng 8:501–518.

Gosselin J.M., Dosso S.E., Askan A., Wathelet M., Savvaidis A., Cassidy J.F., 2022, A review of inverse methods in seismic site characterization: Journal of Seismology 26, pages781–821.

Grippa, A., Bianca, M., Tropeano, M., et al., 2011, Use of the HVSR method to detect buried paleomorphologies (filled incised valleys) below a coastal plain: the case of the Metaponto plain (Basilicata, southern Italy): Bollettino di Geofisica Teorica ed Applicata, 52(2).

Guéguen P., Chatelain J.L., Guillier B., Yepes H., and Egred J., 1998, Site effect and damage distribution in Pujili (Ecuador) after the 28 March 1996 earthquake: Soil Dyn and Earthquake Eng 17:329–334.

Guéguen P., Chatelain J.L., Guillier B., and Yepes H., 2000, An indication of the soil topmost layer response in Quito (Ecuador) using noise H/V spectral ratio: Soil Dyn and Earthquake Eng 19(2):127–133.

Guéguen P., Cornou C., Garambois S., and Banton J., 2007 On the limitation of the H/V spectral ratio using seismic noise as an exploration tool: application to the Grenoble valley (France), a small apex ratio basin: Pure Appl Geophys 164(1):115–134.

Guillier B., Cornou C., Kristek J., Moczo P., Bonnefoy-Claudet S., Bard P.Y., and Fäh D., 2006, Simulation of seismic ambient vibrations: does the H/V provide quantitative information in 2D-3D structures: In Proceedings of the 3rd international symposium on the effects of surface geology on seismic motion, Grenoble, France, 30.

Guillier B., Chatelain J.L., Bonnefoy-Claudet S., and Haghshenas E., 2007, Use of ambient noise: from spectral amplitude variability to H/V stability: J Earthquake Eng 11(6):925–942.

Guillier B., Cornou C., Kristek J., et al., 2006, Simulation of seismic ambient vibrations: does the H/V provide quantitative information in 2D-3D structures: In Proceedings of the 3rd international symposium on the effects of surface geology on seismic motion, Grenoble, France (Vol. 30).

Guillier B., Atakan K., Chatelain J.L., et al., 2008, Influence of instruments on the H/V spectral ratios of ambient vibrations: Bull Earthq Eng 6(1):3–31.

Guillier B., Chatelain J.L., Tavera H., Perfettini H., Zamalloa A., and Herrera B., 2014, Establishing empirical period formula for RC buildings in Lima, Peru: evidence for the impact of both the 1974 Lima earthquake and the application of the Peruvian seismic code on high-rise buildings: Seis Res Lett 85:1308–1315

Haghshenas E., Bard P.Y., Theodulidis N., et al., 2008, Empirical evaluation of microtremor H/V spectral ratio: Bull Earthq Eng 6(1):75–108.

Hallal M.M., and Cox B., 2021., An H/V geostatistical approach for building pseudo-3D Vs models to account for spatial variability in ground response analyses I: model development: Earthq Spectra 37(3):2013–2040.

Haney M.H., and Tsai V.C., 2020, Perturbational and non-perturbational inversion of Love-wave velocities Geophysics, Vol. 85, No. 1 (January-February 2020); P. F19–F26, 6 FIGS. 10.1190/GEO2018-0882.1

Hanumantharao C., and Ramana G.V., 2008, Dynamic soil properties for microzonation of Delhi, India: Journal Earth Science, Vol. 117, No. 2, pp. 719–730.

Harmon J., Hashash Y.M., Stewart J.P., Rathje E.M., Campbell K.W., and Silva W.J., Ilhan O., 2019, Site amplification functions for central and eastern North America–part II: modular simulation-based models.: Earthq Spectra 35(2):815–847

Hassani B., and Atkinson G.M., 2018, Site-effects model for Central and Eastern North America based on peak frequency and average shear wave velocity: Bull Seis Soc Am 108:338– 350. https:// doi. org/ 10. 1785/ 01201 70061.

Hassani B., Yong A., Atkinson G.M., Feng T., and Meng L., 2019, Comparison of site dominant frequency from earthquake and microseismic data in California: Bull Seis Soc Am 109(3):1034–1040.

Hawkins R., 2018, A spectral element method for surface wave dispersion and adjoints: Geophysical Journal International, 215, 267–302, doi: 10.1093/gji/ggy277.

Hobiger M., Bard P.Y., Cornou C., and Le Bihan, N., 2009, Single station determination of Rayleigh wave ellipticity by using the random decrement technique (RayDec): Geophs Res Lett, 36(14).

Hobiger M., Cornou C., Wathelet M., et al., 2013, Ground structure imaging by inversions of Rayleigh wave ellipticity: sensitivity analysis and application to European strong motion sites: Geophys J Int 192(1):207–229.

Horike M., Zhao B., and Kawase H., 2001, Comparison of site response characteristics inferred from microtremors and earthquake shear waves: Bull Seis Soc Am 91:1526–1536.

Herak M., 2008, Model HVSR - a Matlab® tool to model horizontal-to-vertical spectral ratio of ambient noise: Comput Geosci 34:1514–1526.

Hinzen K.G., Weber B., and Scherbaum F., 2004, On the resolution of H/V measurements to determine sediment thickness, a case study across a normal fault in the Lower Rhine embayment: Germany J Earthquake Eng 8(6):909–926.

Hunter J.A., Crow H.L., Brooks G.R., et al., 2010, Seismic site classification and site period mapping in the Ottawa area using geophysical methods: Geological Survey of Canada, Open File 6273:1–80.

Hunter J.A., Crow H.L., Dietiker B., Pugin A., Brewer K., and Cartwright T., 2020, A compilation of microtremor horizontal-to-vertical spectral ratios (HVSRs) and borehole shear wave velocities of unconsolidated sediments in south-central Ontario: Geological Survey of Canada, Open File 8725:1–12

Hunter J.A., Crow H.L., Stephenson W.L., et al., 2022, Seismic site characterization with shear wave (SH) reflection and refraction methods: Journal of Seismology 26, pages 631–652 (2022)

Hutchinson P.J., and Barta L.S., 2003, Imaging your way to a better brownfield site. In RevTech: Cleaning Up Contaminated Properties for Reuse and Revitalization: Effective Technical Approaches and Tools Conference: Environmental Protection Agency, Pittsburgh, PA, 78 p.

Hutchinson P. J., and Beird M. H., 2011, A shear wave velocity comparison—MASW to SPT. In Proceedings of the 24th Symposium of the Application of Geophysics in Engineering and Environmental Problems (abs.): Environmental Engineering Geophysical Society, Charleston, SC.

Hutchinson P.J., and Spieler R., 1998, Characterization of waste disposal facilities through geophysical methods: A case study from Boston, MA. In Ogunro, V. O. (Editor), 4th International Symposium on Environmental Geotechnology and Global Sustainable Development: International Society Environmental Geotechnology, Boston, MA, pp. 1197–1206.

Hutchinson P.J., Teschke, B.J., Zollinger K.M., and Dereume, J.M., 2008, Field applicability of MASWdata. In: Proceedings of the 21st Symposium of the Application of Geophysics in Engineering and Environmental Problems: Environmental Engineering Geophysical Society, Philadelphia, PA, pp. 1226–1231.

Hvorslev M.J., 1949, Subsurface Exploration and Sampling of Soils for Civil Engineering Purposes: U.S. Waterways Experiment Station, Vicksburg, MS, 552 p.

Imai T., and Tonouchi K., 1982, Correlation of N-value with S-wave velocity. In Verruijt, A., Beringen, A.H., and de Leeuw, E.H., (Editors), Proceedings of the 2nd European Symposium on Penetration Testing: International Society Soil Mechanics Foundation, Amsterdam, The Netherlands, pp. 67–72.

Inazaki T., 2006, Relationship between S-wave velocities and geotechnical properties of alluvial sediments. In Proceedings of the 19th Symposium on Application Geophysics Engineering to Environmental Problems: Environmental Engineering Geophysical Society, Seattle, WA, pp. 1075–1085.

Ito E., Nakano K., Nagashima F., Kawase H., 2020, A method to directly estimate S-wave site amplification factor from horizontal-to-vertical spectral ratio of earthquakes (eHVSRs): Bull Seis Soc Am 110:2892–2911.

Ito E., Cornou C., Nagashima F., and Kawase H., 2021, Estimation of velocity structures in the Grenoble Basinusing pseudo earthquake horizontal-to-vertical spectral ratio from microtremor:s Bull Seis Soc Am, 111, https:// doi. org/ 10. 1785/ 01202 00211.

Ivanov, J., 2022, Surface wave methods, in Anna Bondo Medhus and L. Klinkby, eds., Engineering Geophysics (1st ed.): CRC Press.

Ivanov J., Leitner B., Shefchik W.T., Schwenk T.J., and Peterie S.L., 2013a, Evaluating hazards at salt cavern sites using multichannel analysis of surface waves: The Leading Edge, 32, 289-305.

Ivanov J., Miller R.D., Ballard R.F., Dunbar J.B., and Stefanov J., 2004, Interrogating levees using seismic methods in southern Texas: 74th Annual International Meeting, SEG, Technical Program Expanded Abstracts, 23, 1413-1416.

Ivanov J., Miller R.D., Ballard R.F., Dunbar J.B., and Smullen S., 2005, Time-lapse seismic study of levees in southern Texas: 75th Annual International Meeting, SEG, Technical Program Expanded Abstracts, 1121-1124.

Ivanov J., Miller R.D., Dunbar J.B., Lane J.W., and Smullen S., 2007, Interrogating Levees in Texas, New Mexico, and New Orleans Using Various Seismic Methods: Symposium on the Application of Geophysics to Engineering and Environmental Problems, 20, 69-81.

Ivanov J., Miller R.D., Feigenbaum D., Morton S.L., Peterie S.L., and Dunbar J.B., 2017, Revisiting levees in southern Texas using Love-wave multichannel analysis of surface waves with the high-resolution linear Radon transform: Interpretation, Vol. 5, Issue 3 (August 2017).

Ivanov J., Miller R.D., Feigenbaum D.Z., and Schwenk J.T., 2017, Benefits of using the high-resolution linear radon transform (HRLRT) with the multi-channel analysis of surface waves (MASW) method: SEG Technical Program Expanded Abstracts 2017, pp. 2647-2653. (September 2017).

Ivanov J., Miller R.D., Hoch A.M., Peterie S.L., and Morton S., 2019, Surface wave analysis sensitivity to assumptions in a-priori information: SEG Technical Program Expanded Abstracts 2019, pp. 5030-5034 (August 2019).

Ivanov J., Miller R.D., Hoch A.M., Peterie S.L., Morton S., and Borisov D., 2020, A unique approach for estimating surface-wave instability and non-uniqueness, SEG Technical Program Expanded Abstracts 2020, 1835-1839.

Ivanov J., Miller R.D., Lacombe P., Johnson C.D., and Lane J.W., 2006a, Delineating a shallow fault zone and dipping bedrock strata using multi-channel analysis of surface waves with a land streamer: Geophysics, 71, A39-A42.

Ivanov J., Johnson C.D., Lane J.W., Miller R.D., and Clemens D., 2009, Near-surface evaluation of Ball Mountain Dam, Vermont, using multi-channel analysis of surface waves (MASW) and refraction tomography seismic methods on land-streamer data: 79th Annual International Meeting, SEG, Technical Program Expanded Abstracts, 28, 1454-1458.

Ivanov J., Miller R.D., Peterie S.L., Ballard R.F., and Dunbar J.B., 2015, Revisiting levees in southern Texas using Love-wave multi-channel analysis of surface waves (MASW) with the high-resolution linear radon transform (HRLRT): SEG Technical Program Expanded Abstracts 2015, p. 2211-2217.

Ivanov J., Miller R.D., Peterie S., and Dunbar J.B., 2010a, Practical Focusing of Surface-Wave Inversion to Image Levees in Southern New Mexico: Symposium on the Application of Geophysics to Engineering and Environmental Problems, 23, 97-102.

Ivanov J., Miller R.D., Peterie S.L., and Tsoflias G., 2014, Near-surface Qs and Qp estimations from Rayleigh waves using multi-channel analysis of surface waves (MASW) at an Arctic ice-sheet site, SEG Technical Program Expanded Abstracts 2014, 2006-2012.

Ivanov J., Miller R.D., Peterie S., Zeng C., Xia J., and Schwenk T., 2011, Multi-channel analysis of surface waves (MASW) of models with high shear wave velocity contrast: 81st Annual International Meeting, SEG, Technical Program Expanded Abstracts, 30, 1384-1390.

Ivanov J., Miller R.D., Stimac N., Ballard R.F., Dunbar J.B., and Smullen S., 2006b, Time-lapse seismic study of levees in southern New Mexico: 76th Annual International Meeting, SEG, Technical Program Expanded Abstracts, 3255-3259.

Ivanov J., Miller R.D., and Tsoflias G., 2008, Some Practical Aspects of MASW Analysis and Processing: Symposium on the Application of Geophysics to Engineering and Environmental Problems, 21, 1186-1198.

Ivanov J., Miller R.D., Xia J., Dunbar J.B., and Peterie S.L., 2010, Refraction non-uniqueness studies at levee sites using the refraction-tomography and JARS methods; in in R. D. Miller, J. D. Bradford and K. Holliger, eds., Advances in Near-Surface Seismology and Ground-Penetrating Radar: Society of Exploration Geophysicists, 15, 327-338.

Ivanov J., Miller R.D., Xia J., and Peterie S., 2010, Multi-mode inversion of multi-channel analysis of surface waves (MASW) dispersion curves and high-resolution linear radon transform (HRLRT): 80th Annual International Meeting, SEG, Technical Program Expanded Abstracts, 29, 1902-1907.

Ivanov J., Miller R.D., Xia J., Steeples D., and Park C.B., 2006, Joint analysis of refractions with surface waves: An inverse solution to the refraction-travel time problem: Geophysics, 71, R131-R138.

Ivanov J., Park C B., Miller R.D., and Xia J.H., 2005, Analyzing and filtering surface-wave energy by muting shot gathers: Journal of Environmental and Engineering Geophysics, 10, 307-321.

Ivanov J., Park C.B., Miller R.D., and Xia J.H., 2005, Analyzing and filtering surface-wave energy by muting shot gathers: Journal of Environmental and Engineering Geophysics, 10, 307-321.

Ivanov J., Park C., and Xia J., 2008, MASW/SurfSeis2 Workshop: Kansas Geological Survey, Lawrence, KS, 200 p. Jafari, M.K., Shafiee, A., and Razmkhah, A., 2002, Dynamic properties of fine-grained soils in south of Tehran: Journal Seismologic Earthquake Engineering, Vol. 4, No. 1, pp. 25–35.

Ivanov J., Schwenk T.J., Miller R.D., and Peterie S., 2013, Dispersion-curve imaging non-uniqueness studies from multi-channel analysis of surface waves (MASW) using synthetic seismic data: SEG Technical Program Expanded Abstracts 2013, 1794-1800.

Ivanov J., Tsoflias G., Miller R.D., Peterie S., and Morton S., 2016, Impact of density information on Rayleigh surface wave inversion results: Journal of Applied Geophysics.

Ivanov J., Xia, J., and Miller, R.D., 2006, Optimizing Horizontal-Resolution Improvement of the MASW Method. Symposium on the Application of Geophysics to Engineering and Environmental Problems, 19(1), 1128-1134.

Jakica S., 2018, Using passive seismic to estimate the thickness of the Lenora Breakaways, Western Australia: In Proceedings of the 5th Australian Regolith Geoscientists Association Conference, Wallaroo, South Australia, 17–20.

Kanai K., and Tanaka T., 1961, On microtremors VIII: Bull Earthq Res Inst 39:97–114.

Kansas Geological Survey (KGS), 2010, SurfSeis: Seismic processing software, version 3.064: KGS, Lawrence, KS.

Kaufmann R.D., Xia J.H., Benson R.C., Yuhr L.B., Casto D.W., and Park C.B., 2005, Evaluation of MASW data acquired with a hydrophone streamer in a shallow marine environment: Journal of Environmental and Engineering Geophysics, 10, 87-98.

Kayabali K., 1996, Soil liquefaction evaluation using shear wave velocity: Engineering Geology, Vol. 44, pp. 121–127.

Kawase H., Sánchez-Sesma F.J., and Matsushima S., 2011, The optimal use of horizontal-to-vertical spectral ratios of earthquake motions for velocity inversions based on diffuse-field theory for plane waves: Bull Seis Soc Am 101(5):2001–2014.

Kawase H., Matsushima S., Satoh T., and Sánchez-Sesma F.J., 2015, Applicability of theoretical horizontal-to-vertical ratio of microtremors based on the diffuse field concept to previously observed data: Bull Seis Soc Am 105(6):3092–3103.

Kawase H., Mori Y., and Nagashima F., 2018, Difference of horizontal-to-vertical spectral ratios of observed earthquakes and microtremors and its application to S-wave velocity inversion based on the diffuse field concept: Earth, Planets and Space 70(1):1.

Kawase H., Nagashima F., Nakano K., and Mori Y., 2019, Direct evaluation of S-wave amplification factors from microtremor H/V ratios: double empirical corrections to “Nakamura” method: Soil Dynamics and Earthquake Engineering 126:105067.

Koller M.G., Chatelain J.L., Guillier B., Duval A.M., Atakan K., Lacave C., and Bard P.Y., 2004, Practical user guidelines and software for the implementation of the H/V ratio technique: measuring conditions, processing method and results interpretation: In Proceedings of the 13th World Conference on Earthquake Engineering, Vancouver, Canada.

Konno K., and Ohmachi T., 1998, Ground-motion characteristics estimated from spectral ratio between horizontal and vertical components of microtremor: Bull Seis Soc Am 88(1):228–241.

Ktenidou O.J., Chávez-García F.J., Raptakis D., and Pitilakis K.D., 2016, Directional dependence of site-effects observed near a basin edge at Aegion: Greece Bulletin of Earthquake Engineering 14(3):623–645.

Lachet C., and Bard P.Y., 1994, Numerical and theoretical investigations on the possibilities and limitations of Nakamura's technique: J Phys Earth 42(5):377–397.

Ladak S., Molnar S., and Palmer S., 2021, Multi-method site characterization to verify the hard rock (site class A) assumption at 25 seismograph stations across Eastern Canada: Earthq Spectra 37(S1):1487–1515.

Landès M., Hubans F., Shapiro N.M., Paul A., and Campillo M, 2010, Origin of deep ocean microseisms by using teleseismic body waves: J Geophys Res 115: B05302.

Lecocq T., and 75 other authors, 2020, Global quieting of high-frequency seismic noise due to COVID-19 pandemic lockdown measures: Science 369:1338–1343.

Lermo J., and Chávez-García F.J., 1993, Site effect evaluation using spectral ratios with only one station: Bull Seis Soc Am 83(5):1574–1594.

Lermo J., and Chávez-García F.J., 1994a, Are microtremors useful in site response evaluation? Bull Seis Soc Am 84(5):1350–1364.

Lermo J., and Chávez-García F.J., 1994b, Site effect evaluation at Mexico City: dominant period and relative amplification from strong motion and microtremor records: Soil Dyn Earthq Eng 13(6):413–423.

Lontsi A.M., Sánchez-Sesma F.J., Molina-Villegas J.C., Ohrnberger M., and Krüger F., 2015, Full microtremor H/V (z, f) inversion for shallow subsurface characterization: Geophys J Int 202(1):298–312.

Lontsi A.M., García-Jerez A., Molina-Villegas J.C., et al., 2019, A generalized theory for full microtremor horizontal-to-vertical [H/V(z, f)] spectral ratio interpretation in offshore and onshore environments: Geophys J Int 218(2):1276–1297.

Louie J., 2015, Clark County and Reno/Tahoe: Advancing earthquake hazard assessment with physics and geology: Proceedings of the Basin and Range Seismic Hazard Summit III, 12-16 Jan Salt Lake City 10 pp.

Louie J.N., Pancha A., and Kissane B., 2021, Guidelines and pitfalls of refraction microtremor surveys: Journal of Seismology, 26, 567-582.

Lunedei E., and Albarello D., 2010, Theoretical HVSR curves from full wavefield modelling of ambient vibrations in a weakly dissipative layered Earth: Geophys J Int 181(2):1093–1108.

Le Roux O., Cornou C., Jongmans D., and Schwartz S., 2012, 1-D and 2-D resonances in an Alpine valley identified from ambient noise measurements and 3-D modelling: Geophys J Int, 191(2), 579–590.

Lunedei E., and Albarello D., 2015, Horizontal-to-vertical spectral ratios from a full-wavefield model of ambient vibrations generated by a distribution of spatially correlated surface sources: Geophys J Itn 201(2):1142–1155.

Lunedei E., and Malischewsky P., 2015, A review and some new issues on the theory of the H/V technique for ambient vibrations: Geotechnical, Geological and Earthquake Engineering 39:371–394.

Luo Y.H., Xia J.H., Miller, R.D., Xu Y.X., Liu J.P., and Liu Q.S., 2008, Rayleigh-wave dispersive energy imaging using a high-resolution linear Radon transform: Pure and Applied Geophysics, 165, 903-922.

Luzi L., Puglia R., Pacor F., Gallipoli M.R., Bindi D., and Mucciarelli M., 2011, Proposal for a soil classification based on parameters alternative or complementary to VS30: Bull Earthq Eng 9:1877–1898.

Malischewsky P.G., and Scherbaum F., 2004, Love's formula and H/V-ratio (ellipticity) of Rayleigh waves.: Wave Motion 40(1):57–67.

Malischewsky P.G., Scherbaum F., Lomnitz C., Tuan T.T., Wuttke F., and Shamir G., 2008, The domain of existence of prograde Rayleigh-wave particle motion for simple models: Wave Motion 45(4):556–564.

Maranò S., Hobiger M., and Fäh D., 2017, Retrieval of Rayleigh wave ellipticity from ambient vibration recordings.: Geophys J Int 209(1):334–352.

Marcillo O.E., and Carmichael J., 2018, The detection of wind turbine noise in seismic records: Seis Res Lett 89(5):1826–1837.

Matsushima S., Hirokawa T., De Martin F., Kawase H., and SánchezSesma F.J., 2014, The effect of lateral heterogeneity on horizontal-to-vertical spectral ratio of microtremors inferred from observation and synthetics: Bull Seis Soc Am 104(1):381–393.

Matsushima S., Kosaka H., and Kawase H., 2017, Directionally dependent horizontal-to-vertical spectral ratios of microtremors at Onahama, Fukushima, Japan: Earth, Planets and Space 69(1):96.

Meza-Fajardo K.C., Papageorgiou A.S., and Semblat J.F., 2015, Identification and extraction of surface waves from three component seismograms based on the normalized inner product: Bull Seis Soc Am 105(1):210–229.

Mihaylov D., El Naggar M.H., and Dineva S., 2016, Separation of high-and low-level ambient noise for HVSR: application in city conditions for Greater Toronto area: Bull Seis Soc Am 106(5):2177–2184.

Miller R.D., Xia J., Park C.B., and Ivanov, J.M., 2008, Back Page - The history of MASW: The Leading Edge, 27, 568.

Miller R.D., Xia, J., Park, C.B., and Ivanov, J.M., 1999, Multichannel analysis of surface waves to map bedrock: Leading Edge, Vol. 18, No. 12, pp. 97–173.

Miller R.D., Xia, J., Park C.B., and Ivanov, J.M., 2001, Shear wave velocity field to detect anomalies under asphalt. In Lodge, R.G. (Editor), 52nd Highway Geology Symposium: (abs): Maryland Geologic Survey, Baltimore, MD.

Molnar S., and Cassidy J.F., 2006, A comparison of site response techniques using weak-motion earthquakes and microtremors: Earthq Spectra 22(1):169–188.

Molnar S., Ventura C.E., Boroschek R., and Archila M., 2015, Site characterization at Chilean strong-motion stations: comparison of downhole and microtremor shear wave velocity methods: Soil Dyn Earthq Eng 79:22–35.

Molnar S., Cassidy J.F., Castellaro S., et al., 2018, Application of microtremor horizontal-to-vertical spectral ratio (MHVSR) analysis for site characterization: State of the art: Surv Geophys 39(4):613–631.

Molnar S., Assaf J., Sirohey A., and Adhikari S., 2020, Overview of local site effects and seismic microzonation mapping in Metropolitan Vancouver, British Columbia: Canada Eng Geol 270:105568. https:// doi. org/ 10. 1016/j. enggeo. 2020. 105568.

Molnar S., Sirohey A., Assaf J., Bard P.Y., Castellaro S., Cornou C., Cox B., Guillie, B., Hassan, B., Kawase H., Matsushima S., Sánchez-Sesma F.J., and Yong A., 2022, A review of the microtremor horizontal-to-vertical spectral ratio (MHVSR) method: Journal of Seismology 26, 653–685.

Moon S.W., Subramaniam P., Zhang Y., Vinoth G., and Ku T., 2019, Bedrock depth evaluation using microtremor measurement: empirical guidelines at weathered granite formation in Singapore: Journal of Applied Geophysics 171:103866.

Morton S.L., Ivanov J., and Miller R.D., 2019, Selective-window processing for optimized surface wave imaging of passive data: SEG Technical Program Expanded Abstracts 2019, pp. 5035-5039.

Morton S.L., Ivanov J., and Miller R.D., and Parsons, R.L., 2020, Characterizing a physical model of a collapsing void using time-lapse surface-wave analysis, SEG Technical Program Expanded Abstracts 2020, 1935-1939.

Morton S.L., Ivanov J., Peterie S.L., Miller R.D., and Livers-Douglas A.J., 2021, Passive multichannel analysis of surface waves using 1D and 2D receiver arrays: Geophysics, 86, EN63-EN75.

Moscatelli M., Albarello D., Scarascia Mugnozza G., and Dolce M., 2020, The Italian approach to seismic microzonation: Bull Earthq Eng 18:5425–5440.

Motazedian D., Khaheshi Banab K., Hunter J.A., Sivathavalan S., Crow H., and Brooks G., 2011, Comparison of site periods derived from different evaluation methods: Bull Seis Soc Am 101(6):2942–2954.

Mucciarelli M., Gallipoli M.R., and Arcieri M., 2003, The stability of the horizontal-to-vertical spectral ratio of triggered noise and earthquake recordings: Bull Seis Soc Am 93(3):1407–1412.

Mucciarelli, M., and Gallipoli, M.R., 2004, The HVSR technique from microtremor to strong motion: empirical and statistical considerations. In Proceedings of 13th World Conference of Earthquake Engineering, Vancouver, Canada.

Mucciarelli M., Gallipoli M.R., Di Giacomo D., Di Nota F., and Nino E., 2005, The influence of wind on measurements of seismic noise: Geophys J Int 161(2):303–308.

Mucciarelli M., and Gallipoli M.R., 2004, The HVSR technique from microtremor to strong motion: empirical and statistical considerations. In Proceedings of the 13th World Conference on Earthquake Engineering, Vancouver, BC, Canada, Paper (Vol. 45).

Mucciarelli M., Herak M., and Cassidy J.F., 2009, Increasing seismic safety by combining engineering technologies and seismological data: Springer, Dordrecht.

Nakamura Y., 1989, A method for dynamic characteristics estimation of subsurface using microtremor on the ground surface: Quarterly Report of Railway Technical Research 30(1):25–33.

Nakamura Y., 1996, Real-time information systems for seismic hazard mitigation UrEDAS, HERAS and PIC, Q.R. of RTRI, 37–3, 112-127, In Proceedings of the 12th World Conference on Earthquake Engineering, Auckland, New Zealand.

Nakamura, Y., 2008, On the H/V spectrum. In Proceedings of the 14th World Conference on Earthquake Engineering, Beijing, China.

Nakamura, Y., 2014, A modified estimation method for amplification factor of ground and structures using the H/V spectral ratio. In Proceedings of the 2nd Workshop on Dynamic Interaction of Soil and Structure'12, 273–284.

Nakamura Y., 1996, Real-time information systems for seismic hazards mitigation: UrEDAS, HERAS and PIC. Quarterly Report-Rtri, 37(3), 112–127.

Nakamura Y., 2008, On the H/V spectrum. In Proceedings of the 14th World Conference on Earthquake Engineering, Beijing, China.

Nakamura Y., 2000, Clear identification of fundamental idea of Nakamura's technique and its applications. In In Proceedings of the 12th World Conference on Earthquake Engineering (Vol. 2656). New Zealand: Auckland.

Nazarian S., and Stokoe K.H., 1984, In situ shear wave velocities from spectral analysis of surface waves. In Proceedings of the 8th World Conference on Earthquake Engineering: International Association for Earthquake Engineering, San Francisco, CA, pp. 31–38.

Nimiya T., and Tsuji T., 2023, Multimodal Rayleigh and Love Wave Joint Inversion for S-Wave Velocity Structures in Kanto Basin: Japan Journal of Geophysical Research: Solid EarthvVolume 128, Issue 1 e2022JB025017 https://doi.org/10.1029/2022JB025017.

Nogoshi M., and Igarashi T., 1970, On the amplitude characteristics of ambient noise (part 1): J Atmos Oceanic Technol 23:281–303.

Nogoshi M., and Igarashi T., 1971, On the amplitude characteristics of ambient noise (part 2): J Atmos Oceanic Technol 24:26–40.

Novotech Software LTD., 2010, NovoSPT: Proprietary SPT Correlation Computer Software: NovoTech Software, British Columbia, Canada.

Ohsaki, Y., and Iwasaki, R., 1973, Dynamic shear moduli and Poisson's ratio of soil deposits: Soils Foundation, Vol. 13, pp. 61–73.

Ohta Y., and Goto N., 1978, Empirical shear wave velocity equations in terms of characteristic soil indexes: Earthquake Engineering Structural Dynamics, Vol. 6, pp. 167–187.

Okada H., and Suto K., 2003, The microtremor survey method: Society of Exploration Geophysicists DOI 10(1190/1):9781560801740.

Oliveira C.S., and Navarro M., 2010, Fundamental periods of vibration of RC buildings in Portugal from in-situ experimental and numerical techniques: Bull Earthq Eng 8(3):609–642.

Oubaiche E.H., Chatelain J.L., Hellel M., Wathelet M, Machane D., Bensalem R., and Bouguern A., 2016, The relationship between ambient vibration H/V and SH transfer function: Some experimental results: Seis Res Lett 87:1112–1119.

Özalaybey S., Zor E., Ergintav S., and Tapırdamaz M.C., 2011, Investigation of 3-D basin structures in the İzmit Bay area (Turkey) by single-station microtremor and gravimetric methods: Geophys J Int 186(2):883–894

Pancha A., Pullammanappallil S., Louie J., Cashman P.H., and Trexler J.H., 2017, Determination of 3D basin shear wave velocity structure using ambient noise in an urban environment: A case study from Reno, Nevada: Bulletin of the Seismological Society of America, 107, no 6(December):3004–3022. https://doi.org/10.1785/0120170136.

Park C.B., Miller, R.D., and Xia, J., 1999, Multi-channel analysis of surface waves: Geophysics, Vol. 64, No. 3, pp. 800–808.

Park C.B., Miller R.D., Xia J.H., 1998, Imaging dispersion curves of surface waves on multi-channel record: SEG Technical Program Expanded Abstracts 1998, p. 1377-1380.

Park C.B., Miller R.D., and Xia J.H., 1999, Multichannel analysis of surface waves: Geophysics, 64, 800-808.

Park C.B., Miller R.D., Laflen D., Neb C., Ivanov, J., Bennett, B., and Huggins, R., 2004, Imaging dispersion curves of passive surface waves: 74th Annual International Meeting, SEG, Expanded Abstracts, 23, 1357-1360.

Park C.B., Miller R.D., Ryden N., Xia J., and Ivanov, 2005, Combined use of active and passive surface waves: Journal of Environmental and Engineering Geophysics, 10, 323-334.

Park C.B., Miller R.D., Xia J.H., Ivanov, J., Sonnichsen G.V., Hunter J., Goo, R.L., Burn, R.A., and Christian J., 2005, Underwater MASW to evaluate stiffness of water-bottom sediments: The Leading Edge, 24, 724-728.

Park C.B., Miller R.D., Xia J.H., and Ivanov J., 2007, Multichannel analysis of surface waves (MASW) -active and passive methods: The Leading Edge, 26, 60-64.

Parolai S., and Galiana-Merino J.J., 2006, Effect of transient seismic noise on estimates of H/V spectral ratios: Bull Seis Soc Am 96(1):228–236.

Parolai S., Bindi D., and Augliera P., 2000, Application of the generalized inversion technique (GIT) to a microzonation study: numerical simulations and comparison with different site-estimation techniques: Bull Seis Soc Am 90(2):286–297.

Parolai S., Lai C.G., Dreossi OI., Ktenidou O., and Yong A., 2022, A review of near-surface QS estimation methods using active and passive sources: Journal of Seismology 26, pages823–862.

Parolai S., Picozzi M., Richwalski S.M., and Milkereit C., 2005, Joint inversion of phase velocity dispersion and H/V ratio curves from seismic noise recordings using a genetic algorithm, considering higher modes: Geophys Res Lett, 32(1).

Parolai S., Picozzi M., Strollo A., Pilz M., Di Giacomo D., Liss B., and Bindi D., 2009, Are transients carrying useful information for estimating H/V spectral ratios? Increasing Seismic Safety by Combining Engineering Technologies and Seismological Data: Springer, Dordrecht, pp 17–31.

Pastén C., Sáez M., Ruiz S., Leyton F., Salomón J., and Poli P., 2016, Deep characterization of the Santiago Basin using HVSR and cross-correlation of ambient seismic noise: Eng Geol 201:57–66.

Perret D., 2015, Single station H/V technique. In Shear wave velocity measurement guidelines for Canadian seismic site characterization in soil and rock, (ed. J.A. Hunter and H.L. Crow); Natural Resources Canada, Earth Sciences Sector, Information Product 110 (English and French), 78–84; 90–93.

Perton M., Spica Z., and Caudron C., 2017, Inversion of the horizontal to vertical spectral ratio in presence of strong lateral heterogeneity: Geophys J Int 212(2):930–941.

Picozzi M., Parolai S., and Albarello D., 2005, Statistical analysis of noise horizontal-to-vertical spectral ratios (HVSR): Bull Seis Soc Am 95(5):1779–1786.

Pilz M., Parolai S., Leyton F., Campos J., and Zschau J., 2009, A comparison of site response techniques using earthquake data and ambient seismic noise analysis in the large urban areas of Santiago de Chile: Geophys J Int 178(2):713–728.

Pilz M., Parolai S., 2014, Statistical properties of the seismic noise field: influence of soil heterogeneities: Geophys J Int 199(1):430–440.

Piña-Flores J., Perton M., García-Jerez A., et al., 2017, The inversion of spectral ratio H/V in a layered system using the diffuse field assumption (DFA): Geophys J Int 208(1):577–588.

Piña-Flores J., Cárdenas-Soto M., García-Jerez A., et al., 2020, Use of peaks and troughs in the horizontal-to-vertical spectral ratio of ambient noise for Rayleigh-wave dispersion curve picking: J Appl Geophy, 177, 104024.

Piña-Flores J., Cárdenas-Soto M., García-Jerez A., Campillo M., and Sánchez-Sesma F.J., 2021, The search of diffusive properties in ambient seismic noise: Bull Seis Soc Am 111(3):1650–1660.

Pitilakis K., Riga E., and Anastasiadis A., 2013, New code site classification, amplification factors and normalized response spectra based on a worldwide ground-motion database: Bull Earthq Eng, 11(4):925–966.

Pinnegar CR., 2006, Polarization analysis and polarization filtering of three-component signals with the time-Frequency S transform: Geophys J Int 165(2):596–606.

Poggi V., and Fäh D., 2010, Estimating Rayleigh wave particle motion from three-component array analysis of ambient vibrations: Geophys J Int 180(1):251–267.

Poggi V., Fäh D., Burjanek J., and Giardini D., 2012, The use of Rayleigh-wave ellipticity for site-specific hazard assessment and microzonation: application to the city of Lucerne, Switzerland: Geophys J Int 188(3):1154–1172.

Pratt T.L., 2018, Characterizing and imaging sedimentary strata using depth-converted spectral ratios: an example from the Atlantic Coastal Plain of the eastern United States. Bull Seis Soc Am 108(5A):2801–2815.

Puglia R., Albarello D., Gorini A., Luzi L., Marcucci S., and Pacor F., 2011, Extensive characterization of Italian accelerometric stations from single-station ambient-vibration measurements: Bulletin Earthquake Engineering 9:1821–1838.

Qin T., Wang S., Feng X., and Lu L., 2021, A review on microtremor H/V spectral ratio method: Reviews of Geophysics and Planetary Physics, V. 52, No. 6.

Raptakis D., Theodulidis N., and Pitilakis K., 1998, Data analysis of the Euroseistest strong motion array in Volvi (Greece): standard and horizontal-to-vertical spectral ratio techniques: Earthq Spectra 14:203–224.

Raptakis D., Chávez-García, F.J., Makra, K., Pitilakis, K., 2000, Site effects at Euroseistest: 1. Determination of the valley structure and confrontation of observations with 1D analysis: Soil Dyn Earthq Eng 19:1–22.

Rivet D., Campillo M., Sanchez-Sesma F., Shapiro N.M., and Singh S.K., 2015, Identification of surface wave higher modes using a methodology based on seismic noise and coda waves: Geophys J Int 203(2):856–868.

Rollins, K.M., Diehl, N.B., and Weaver, T.J., 1998, Implications of Vs-BPT (N1)60 correlations for liquefaction assessment in gravels. In Dakoulas, P.; Yegian, M.; and Holtz, R.D. (Editors), Geotechnical Earthquake Engineering and Soil Dynamics, Geotechnical Special Publication No. 75: American Society Civil Engineers, Reston, VA, Vol. 1, pp. 506–517.

Rollins, K.M., Evans, M.D., Diehl, N.B., and Daily, W.D., 1998, Shear modulus and damping relationships for gravels: Journal Geotechnical Geoenvironmental Engineering, Vol. 124, No. 5, pp. 396–405.

Rong M., Li H., and Yu Y., 2019, The difference between horizontal lto-vertical spectra ratio and empirical transfer function as revealed by vertical arrays: PLoS One 14(1): e0210852.

Roten D., and Fäh D., 2007, A combined inversion of Rayleigh wave dispersion and 2-D resonance frequencies: Geophys J Int 168(3):1261–1275.

Roten D., Fäh D., Cornou C., and Giardini D., 2006, Two-dimensional resonances in Alpine valleys identified from ambient vibration wavefields: Geophys J Int 165(3):889–905.

Ryden N., and Park C.B., 2004, Surface waves in inversely dispersive media: Near Surface Geophysics, 2, 187-197.

Ryden N., and Park C.B., 2006, Fast simulated annealing inversion of surface waves on pavement using phase-velocity spectra: Geophysics, 71, R49-R58.

Sánchez-Sesma F.J., 2017, Modeling and inversion of the microtremor H/V spectral ratio: physical basis behind the diffuse field approach: Earth, Planets and Space 69(1):92.

Sánchez-Sesma F.J., Rodríguez M., Iturrarán-Viveros U., et al., 2011, A theory for microtremor H/V spectral ratio: application for a layered medium: Int 186(1):221–225.

Sánchez-Sesma F.J., and Yong A., 2022, A review of the microtremor horizontal-to-vertical spectral ratio (MHVSR) method: Journal of seismology, 26:653-685.

Satoh T., Kawase H., and Matsushima S., 2001, Estimation of S-wave velocity structures in and around the Sendai basin, Japan, using array records of microtremors. Bull Seism Soc Am 91:206–21.

Savage M.K., Lin F.C., and Townend J., 2013, Ambient noise cross correlation observations of fundamental and higher mode Rayleigh wave propagation governed by basement resonance: Geophys Res Lett 40(14):3556–3561.

SESAME Project, 2004, Guidelines for the implementation of the H/V spectral ratio technique on ambient vibrations measurements, processing and interpretation: https://sesame.geopsy.org/Delivrables/Del-D23-HV_User_Guidelines.pdf.

Scheib A., Morris P., Murdie R., and Piane C.D., 2016, A passive seismic approach to estimating the thickness of sedimentary cover on the Nullarbor Plain: Western Australia Australian J Earth Sci 63(5):583–598.

Scherbaum F., Hinzen K.G., and Ohrnberger M., 2003, Determination of shallow shear wave velocity profiles in the Cologne, Germany area using ambient vibrations: Geophys J Int 152(3):597–612.

Sgattoni G., and Castellaro S., 2020, Detecting 1-D and 2-D ground resonances with a single-station approach: Geophys J Int 223(1):471–487.

Sloan S.D., Peterie S.L., Miller R.D., Ivanov J., Schwenk J.T., McKenna J.R., 2015, Detecting clandestine tunnels using near-surface seismic techniques: Geophysics, v. 80, no 5, p. EN127-EN135.

Smith N., Reading A., Asten M., and Funk C., 2013, Constraining depth to basement for mineral exploration using microtremor: a demonstration study from remote inland Australia: Geophysics 78: B227–B242.

Socco L.V., and Strobbia C., 2004, Surface-wave method for near surface characterization: a tutorial: Near Surface Geophysics 2(4):165–185.

Spica Z., Caudron C., Perton M., et al., 2015, Velocity models and site effects at Kawah Ijen volcano and Ijen caldera (Indonesia) determined from ambient noise cross correlations and directional energy density spectral ratios: Journal of Vulcanology and Geothermal Research 302:173–189

Spica Z.J., Perton M., Nakata N., Liu X., and Beroza G.C., 2017, Site characterization at Groningen gas field area through joint surface borehole H/V analysis: Geophys J Int 212(1):412–421.

Spica Z.J., Perton M., Nakata N., Liu X., and Beroza G.C., 2018, Shallow vs imaging of the Groningen area from joint inversion of multi-mode surface waves and H/V spectral ratios: Seis Res Lett 89:1720–1729.

Strollo A., Parolai S., Jäckel K.H., Marzorati S., and Bindi D., 2008, Suitability of short-period sensors for retrieving reliable H/V peaks for frequencies less than 1 Hz: Bull Seis Soc Am 98(2):671–681.

Stephenson W., Asten MW., Odum J.K., and Frankel A.D., 2019, Shear wave velocity in the Seattle basin to 2 km depth characterized with the krSPAC microtremor array method: insights for urban basin-scale imaging: Seis Res Lett 90:1230–1242.

Stokoe K.H., Nazarian S., Rix G.J., Sanchez-Saliner, I., Sheu J., and Mok Y., 1988, In situ seismic testing of hard-to-sample soils by surface wave method. In Von Thun, J.L. (Editor), Earthquake Engineering and Soil Dynamics II, Recent Advances in Ground-Motion Evaluation: American Society of Civil Engineers, Park City, UT, pp. 264–278.

Stolte A., Jeong S., and Wotherspoo, L., 2018, Ambient Vibration H/V Spectral Ratio (HVSR) Method Field Testing Guidelines: QuakeCore Centre for Earthquake Resilience.

Schwenk J.T., Miller R.D., Ivanov J., Sloan, S.D., and McKenna, J.R., 2012, Joint Shear wave Analysis Using MASW and Refraction Traveltime Tomography: 82nd Annual International Meeting, SEG, Technical Program Expanded Abstracts.

Schwenk J.T., Sloan S.D., Ivanov J., and Miller R.D., 2016, Surface-wave methods for anomaly detection: Geophysics, 81, EN29-EN42.

Stephenson W.J., Yong A., and Martin A., 2022, Flexible multimethod approach for seismic site characterization: Journal of Seismology 26, pages 687–711.

Sykora D.W., and Koester J.P., 1988, Review of existing correlations between shear wave velocity or shear modulus and standard penetration resistance in soils. In Von Thun, J. L. (Editor), Earthquake Engineering and Soil Dynamics II Conference, Recent Advances in Ground-Motion Evaluation: American Society of Civil Engineers, Park City, UT, pp. 389–404.

Taniguchi E., and Sawada K., 1979, Attenuation with distance of traffic-induced vibrations: Soils Found 19(2):16–28.

Tchawe F.N., Froment B., Campillo M., and Margerin L., 2020, On the use of the coda of seismic noise autocorrelations to compute H/V spectral ratios: Geophys J Int 220(3):1956–1964.

Teague D.P., Cox B.R., and Rathje E.R., 2018, Measured vs. predicted site response at the Garner Valley downhole array considering shear wave velocity uncertainty from borehole and surface wave methods: Soil Dyn and Earthquake Eng 113(10):339–355.

Theodoulidis N., Bard P.Y., Archuleta R., and Bouchon M., 1996, Horizontal-to-vertical spectral ratio and geological conditions: the case of Garner Valley Downhole Array in southern California: Bull Seis Soc Am 86:306–319.

Theodoulidis N., Cultrera G., Cornou C., et al., 2018, Basin effects on ground motion: the case of a high-resolution experiment in Cephalonia. (Greece): Bull Earthq Eng 16(2):529–560.

Theodoulidis N., and Bard P.Y., 1998, Dependence of fmax on site geology: a preliminary study of Greek strong-motion data. In Proceedings of the 11th European Conference on Earthquake Engineering.

Tsai N.C., and Housner G.W., 1970, Calculation of surface motions of a layered half-space: Bull Seis Soc Am 60(5):1625–1651.

Tsoflias G.P., Ivanov, J., Anandakrishnan, S., and Miller, R.D., 2008, Use of Active Source Seismic Surface Waves in Glaciology: Symposium on the Application of Geophysics to Engineering and Environmental Problems, 21, 1240-1243.

Tuan T.T., Scherbaum F., and Malischewsky P.G., 2011, On the relationship of peaks and troughs of the ellipticity (H/V) of Rayleigh waves and the transmission response of single layer over half-space models: Geophys J Int 184(2):793–800.

Tün M., Pekkan E., Özel O., and Guney Y., 2016, An investigation into the bedrock depth in the Eskisehir Quaternary Basin (Turkey) using the microtremor method: Geophys J Int 207:589–607.

Uebayashi H., 2003, Extrapolation of irregular subsurface structures using the horizontal-to-vertical spectral ratio of long-period microtremors: Bull Seis Soc Am 93(2):570–582.

Uebayashi H., Kawabe H., and Kamae K., 2012, Reproduction of microseism H/V spectral features using a three-dimensional complex topographical model of the sediment bedrock interface in the Osaka sedimentary basin: Geophys J Int 189(2):1060–1074.

User's Manual SeisOpt ReMi Version 3.0.

Urzúa A., Dobry R., and Christian J.T., 2017, Is harmonic averaging of shear wave velocity or the simplified Rayleigh method appropriate to estimate the period of a soil profile? Earthq Spectra 33(3):895–915.

Vallianatos F., and Hloupis G., 2009, HVSR technique improvement using redundant wavelet transform. Increasing Seismic Safety by Combining Engineering Technologies and Seismological Data: Springer, Dordrecht, pp 117–137.

van Der Baan M., 2009, The origin of SH-wave resonance frequencies in sedimentary layers. Geophys J Int 178:1587–1596.

Vantassel J., Cox B., Wotherspoon L., and Stolte A., 2018, Mapping depth to bedrock, shear stiffness, and fundamental site period at Centre Port, Wellington, using surface-wave methods: implications for local seismic site amplification: Bull Seis Soc Am 108(3B):1709–1721.

Volant P., Cotton F., and Gabriel J.C., 1998, Estimation of site response using the H/V method. Applicability and limits of this technique on Garner Valley downhole array dataset (California). In Proceedings of the 11th European Conference on Earthquake Engineering.

Volant P., Cotton F., and Gabriel J.C., 1998, Estimation of site response using the H/V method. Applicability and limits of this technique on Garner Valley downhole array dataset (California). In Proceedings of the 11th European Conference on Earthquake Engineering.

Wang, P., 2020, Predictability and repeatability of non-ergodic site response for diverse geological conditions: PhD Thesis, UCLA, Dept. Civil Engineering, 210 p.

Wathelet M., Jongmans D., and Ohrnberger M., 2004, Surface-wave inversion using a direct search algorithm and its application to ambient vibration measurements: Near Surface Geophysics 2(4):211–221.

Wathelet M., Guillier B., Roux P., Cornou C., and Ohrnberger M., 2018, Rayleigh wave three-component beamforming: signed ellipticity assessment from high-resolution frequency-wavenumber processing of ambient vibration arrays: Geophys J Int 215(1):507–523.

Wathelet M., Chatelain J.L., Cornou C., Giulio G.D., Guillier B., Ohrnberger M., and Savvaidis A., 2020, A user-friendly opensource tool set for ambient vibration processing: Seis Res Lett 91(3):1878–1889.

Weaver R.L., and Yoritomo J.Y., 2018, Temporally weighting a time varying noise field to improve Green function retrieval: J Acous Soc Am 143(6):3706–3719. https:// doi. org/ 10. 1121/1. 50434 06.

Wen K.L., Bard P.Y., Sánchez-Sesma F.J., Higashi S., Iwata T., and Maeda T., 2018, Special issue "Effect of surface geology on seismic motion: challenges of applying ground motion simulation to seismology and earthquake engineering.": Earth, Planets and Space 70(1):178.

Wollery WW., and Street R., 2002, 3D near-surface soil response from H/V ambient-noise ratios: Soil Dyn and Earthquake Eng 22(9–12):865–876.

Wotherspoon L.M., Orense R.P., Bradley B.A., Cox B.R., Wood C.M., and Green R.A., 2015, Soil profile characterization of Christchurch central business district strong motion stations: Bull New Zealand Soc Earthquake Eng 48(3):147–157.

Wu H., Masaki K., Irikura K., and Sánchez-Sesma F.J., 2017, Application of a simplified calculation for full waves microtremor H/V based on the diffuse field approximation to identify underground velocity structures: Earth, Planets and Space 69:162.Xia, J., Miller, C.B., and Park, J.A., 1999, Estimation of near surface shear wave velocity by inversion of Rayleigh wave: Geophysics, Vol. 64, pp. 691–700.

Xia JH., Miller R.D., Park C.B., Hunter J.A., and Harris J.B., 1999b, Evaluation of the MASW technique in unconsolidated sediments: SEG Technical Program Expanded Abstracts 1999, p. 437-440.

Xia J., Miller R.D., Park C.B., Hunter J.A., Harris J.B., and Ivanov, J., 2002, Comparing shear wave velocity profiles inverted from multi-channel surface wave with borehole measurements: Soil Dynamics Earthquake Engineering, Vol. 22, pp. 181–190.

Xia JH., Miller R.D., Park, C.B., Hunter JA., and Harris JB., 2000, Comparing shear wave velocity profiles from MASW with borehole measurements in unconsolidated sediments, Fraser River Delta, B.C., Canada: Journal of Environmental and Engineering Geophysics, 1, 1-13.

Xia JH., Miller R.D., Park, C.B., and Tian G., 2002, Determining Q of near-surface materials from Rayleigh waves: Journal of Applied Geophysics, 51, 121-129.

Xia JH., Miller, R.D., Park, C.B., and Tian G., 2003, Inversion of high frequency surface waves with fundamental and higher modes: Journal of Applied Geophysics, 52, 45-57.

Xia J., Miller R.D., Chen C., and Ivanov J., 2004, Increasing horizontal resolution of geophysical models by generalized inversion. In SEG Technical Program Expanded Abstracts 2004 (Vol. 23, pp. 1437-1440).

Xia J., Xu Y., Luo Y., Miller R.D., Cakir R., and Zeng C., 2012, Advantages of using multichannel analysis of love waves (MALW) to estimate near surface shear wave velocity: Surveys in Geophysics, 33, 841–860, doi: 10.1007/s10712-012-9174-2.

Xia J., Xu Y., and Miller, R.D., 2007, Generating an image of dispersive energy by frequency decomposition and slant stacking: Pure and Applied Geophysics, 164, 941-956.

Xia J., Xu Y., Miller R.D., and Ivanov, J., 2012, Estimation of near-surface quality factors by constrained inversion of Rayleigh-wave attenuation coefficients: Journal of Applied Geophysics, 82, 137-144.

Xu R., and Wang L., 2021, The horizontal-to-vertical spectral ratio and its applications: EURASIP Journal on Advances in Signal Processing.

Yamamoto, H., 2000, Estimation of shallow S-wave velocity structures from phase velocities of Love-and Rayleigh waves in microtremors. In Proceedings of the 12th World Conference on Earthquake Engineering. Auckland, New Zealand.

Yamanaka H., Takemura M., Ishida H., and Niwa M., 1994, Characteristics of long period microtremors and their applicability in exploration of deep sedimentary layers: Bull Seis Soc Am 84(6):1831–1841.

Yaniv Darvasi, M., 2021, Shear wave velocity measurements and their uncertainties at six industrial sites: Earthquake Spectra 2021, Vol. 37(3) 2223–2246.

Yin X., Xia J., Shen C., and Xu H., 2014, Comparative analysis on penetrating depth of high-frequency Rayleigh and Love waves, Journal of Applied Geophysics Volume 111.

Yin X., Xu H., Mi B., Hao X., Wang P., and Zhang K., 2020, Joint inversion of Rayleigh and Love wave dispersion curves for improving the accuracy of near-surface S-wave: Elsevier Journal of Applied Geophysics Volume 176, 103939.

Yong A., Martin A., Stokoe K., and Diehl J., 2013, ARRA-funded VS30 measurements using multi-technique approach at strong-motion stations in California and Central-Eastern United States: U.S. Geological Survey, Open File Report 2013–1102:1–60.

Zhao J.X., Irikura K., Zhang J., et al., 2006, An empirical site classification method for strong-motion stations in Japan using H/V response spectral ratio: Bull Seis Soc Am 96(3):914–925.

Zhu C., Pilz M., and Cotton F., 2020, Evaluation of a novel application of earthquake HVSR in site-specific amplification estimation: Soil Dyn and Earthquake Eng 139:106301.